REPORT DOCUMENTATION PA[redacted]

AFRL-SR-BL-TR-98-

0846

1. AGENCY USE ONLY *(Leave blank)*	2. REPORT DATE	3. REPORT TYPE AND DATES COVERED
	Mar 23 ,1998	Final Technical Report 1 Sep 94 to 31 Dec 97

4. TITLE AND SUBTITLE
The Optimal Desighn of Structures Incorporating "Smart Materials"

5. FUNDING NUMBERS
F49620-94-1-0442

6. AUTHOR(S)
Professor P. D. Washabaugh, Professor J. E. Taylor, Professor A. M. Waas

7. PERFORMING ORGANIZATION NAME(S) AND ADDRESS(ES)
University of Michigan
1320 Beal Street
Ann Arbor, MI

8. PERFORMING ORGANIZATION REPORT NUMBER

9. SPONSORING/MONITORING AGENCY NAME(S) AND ADDRESS(ES)
AFOSR/NA
801 N. Randolph Street, Room 732
Arlington, VA 22203-1977

10. SPONSORING/MONITORING AGENCY REPORT NUMBER
F49620-94-1-0442

11. SUPPLEMENTARY NOTES

12a. DISTRIBUTION AVAILABILITY STATEMENT
APPROVED FOR PUBLIC RELEASE; DISTRIBUTION UNLIMITED.

12b. DISTRIBUTION CODE

13. ABSTRACT *(Maximum 200 words)*

The purpose of this project was to develop a rigorous theoretical foundation of the design of structures incorporating general 'smart' materials, and to explore, extend and develope the use of sensors and actuators that employ 'finite length' paths. It is anticipated that this project will fundamentally impact the practice of designing passive and active materials, and structural topologies. There were three main tasks to be performed under this grant. These tasks are listed below along with some of the details of our current approach and status. Even though this grant has ended, some of this work (as described below) is continuing with support from various other sources.

19981215 139

14. SUBJECT TERMS

15. NUMBER OF PAGES

16. PRICE CODE

17. SECURITY CLASSIFICATION OF REPORT	18. SECURITY CLASSIFICATION OF THIS PAGE	19. SECURITY CLASSIFICATION OF ABSTRACT	20. LIMITATION OF ABSTRACT
UNCLASSIFIED	UNCLASSIFIED	UNCLASSIFIED	UL

The Optimal Design of Structures Incorporating 'Smart Materials'

Final Progress Report

ARPA/AFOSR # F49620-94-1-0442

Technical Monitor: Spencer Wu

Total Program Duration: September 30, 1994 through September 29, 1997
(zero cost extension to Jan 1, 1998)

Principal Investigator:
Professor P. D. Washabaugh
1320 Beal St.
University of Michigan,
Ann Arbor, MI
phone: 734-763-1328
fax: 734-763-0578
e-mail: pete@umich.edu

Collaborating Investigators:
Professor J.E. Taylor
University of Michigan, Ann Arbor, MI

Professor A. M. Waas
University of Michigan, Ann Arbor, MI

Program Costs to Sponsor:
During This Last Period: $150,00.00
Total: $428,00.00

Revised March 23, 1998

Table of Contents

1.0 Current Objectives

The purpose of this project was to develop a rigorous theoretical foundation of the design of structures incorporating general 'smart' materials, and to explore, extend and develope the use of sensors and actuators that employ 'finite length' paths. It is anticipated that this project will fundamentally impact the practice of designing passive and active materials, and structural topologies.

There were three main tasks to be performed under this grant. These tasks are listed below along with some of the details of our current approach and status. Even though this grant has ended, some of this work (as described below) is continuing with support from various other sources.

These objectives are identical to those that were listed in the proposal and the last progress report with one exception: an additional task, 'practical implementation of the optimization procedure for large scale problems' has been appended. As will be briefly discussed below and borne out through most of the references, in some cases the objectives have been achieved and in others we have at least made substantial progress. That is, at a minimum we have been able to create simple problem formulations that take into account each of the tasks (e.g. General Design Objectives, General Local Design, General Tensor Design, ect.).

1.1 Optimal Design

The purpose of this main task is to develop a rigorous theoretical foundation to design structures incorporating 'smart' materials. The aspects to be explored include:

1.1.1 General Design Objectives

Rather than be restricted to designing for 'minimum compliance', other objectives such as 'maximum strength', or 'maximum life' within the context of a combined loading environment will be examined.

1.1.2 General Local Design Constraint

The current formulation has very limited means to restrict local type of material being optimized. Here, a formulation that allows the local material to be restricted in some manner (e.g. isotropic or to be 'manufacturable') will be developed.

1.1.3 General Tensor Fields

The present analysis 'designs' the constitutive tensor of a generally linear anisotropic material. Here other tensor fields, such as those associated with 'smart' materials, will be incorporated into the design.

1.1.4 Nonlinear Materials

Many of the above elements to be incorporated will lead to certain non-linearities in the design process. Here the aim is to investigate the design of materials that have constitutive non-linearities.

1.1.5 Nonlinear Kinematics

Many current 'solutions' to aerospace problems that employ smart materials, are mechanisms. It is possible to incorporate nonlinear kinematics and potentially 'contact' mechanics into the optimal design formulation.

1.1.6 Practical Implementation

How the numerical implementation of these optimization routines scale to larger more practical problems is not obvious. In fact it appears that to solve problems of any type of substantial size may require alot of computation effort (e.g. parallel processing machines) or some imaginative solution procedures. This is being listed as a separate task because this difficulty spans all the above optimization tasks.

1.2 Distributed Sensing and Actuation

The goal here is to further extend and explore aspects of sensors and actuators that employ 'finite-length' paths.

1.2.1 Theoretical Investigation

The current isotropic analysis is to be used to explore bounds on the feasibility of using these types of sensors. The analysis is to be extended to include an explicit measure of structural integrity sensing. It is also to be extended to more general materials (e.g. the anisotropic material of a composite torque tube) and configurations (e.g. a rotor blade).

1.2.2 Prototype Construction and Testing

In cooperation with Boeing Helicopter, a prototype torque tube is to be constructed and bench tested. The ability of the system to measure torque, and structural integrity will be examined.

1.2.3 Practical Implementation

The current means to 'design' distributed sensors involves knowing an analytical model of the system. A goal of this aspect of the investigation is to 'design' distributed sensors and actuators (using the approach of the 'optimal design' above) on more practical structures.

1.2.4 Performance of an Electroactive Hydraulic Actuator

Certain electroactive materials (Re. Shoko Yoshikawa) show a substantial volume change under an applied magnetic field. Under certain limiting conditions similar to those proposed by other members of the Smart Structures Rotorcraft Consortium these materials can potentially achieve a 1% change in volume. This is an effect that is huge (almost an order of magnitude) greater than the intrinsic effects being proposed for other actuator designs. The purpose here it to construct a small prototype pump that will allow feasibility of using the volumetric effect of certain electroactive materials in hydraulic systems.

1.3 Interaction with Other Program Participants

We will cooperate with other participants so as to be in a position to disseminate results, incorporate their objectives and constraints into this study.

2.0 Status of Effort

Substantial progress has again been made toward fulfilling all the objectives. As alluded to in the last report we have extremum principles that now work for all of the tasks listed above. Listed below is a description of the status in each of the areas. In some cases there is reference to publish documents or the papers appended at the end of this report.

2.1 Optimal Design

In general we have addressed or solved at some level every topic here. However, in some cases these issues will remain as research topics for the foreseeable future. The topics being explored or that have been solved include:

2.1.1 General Design Objectives

Designing for 'minimum compliance' is still used as a baseline objective. However other objectives, especially at the urging of some of the industrial contacts (e.g. ALCOA), such as 'minimum cost' or 'minimum life-cycle cost' are also being explored. To see example of these please refer to the documents [1, 5, 6]. There remains much work to be done here. For instance the 'maximum strength' objective has been explored - some simple sample problems (and still yet to be published) have been solved.

2.1.2 General Local Design Constraint

The original formulation had very limited means to restrict the local type of material being optimized. The original formulation used purely 4-tensor invariants. Thus, any arbitrarily rotation of the material coordinate frame could never result in a cost. While this approach has appeal from an academic perspective, it fundamentally ignores basic manufacturing issues. In addition, certain manufacturing costs that involve orientation dependance can also be incorporated. We can now restrict the material to be anything from isotropic to generally anisotropic. Please refer to the document [6, 8, 12]. We can now local restrict material properties in multiple ways. This task is essentially solved for our current purposes.

2.1.3 General Tensor Fields

Optimization formulations that include distributed temperature and electrical fields have been formulated. Here we have a formulation that incorporates an elastic field and another field that is linearly coupled. The interesting feature here is that the solution drastically changes character. For instance for a simple bar rather than having simple 'diffusion equations' (and for example simple polynomial solutions) you get equations that are analogous to 'wave equations' (and for example transcendental solutions). This represent the interplay or exchange of energy between the two fields. We have some simple analytical solutions here, as well has an extremum principle! However, we are currently working on designing parameters (e.g. the mixture of passive and active materials) in this two field system. Much of this these simple examples have yet to be published however, the method to separate the 'active' and 'passive' phases appears in [14, 16].

2.1.4 Nonlinear Materials

It is a relatively straightforward matter to incorporate nonlinear constitutive properties into the typification formulation. In fact, it is perfectly allowable to design the nonlinear portions of the constitutive equation. This task is essentially completed for lots of examples. Please refer to the documents [2, 3, 6, 9, 12]

2.1.5 Nonlinear Kinematics

In much the same manner that nonlinear constitutive properties can be incorporated, nonlinear kinematics can also be used. This task is essentially complete. Please refer to the documents [9, 11]

2.2 Distributed Sensing and Actuation

We've essentially completed all that can be done here except the last, self-imposed task.

2.2.1 Theoretical Investigation

A structural integrity sensor was analyzed and shown to exist for a prismatic homogeneous isotropic structure with arbitrary cross-section. Current efforts are still to extend this analysis to a structure that uses an anisotropic material. Refer to document [4, 7]

2.2.2 Prototype Construction and Testing

We've constructed several prototypes which substantiate this approach. That is, it works!. Refer to document [10].

2.2.3 Practical Implementation

Since the approach is technically sound we are trying to locate an application that requires the increase in range and stiffness of the transducer. There have been no real buyers here. We have written a proposal NASA-JPL to make use of this technique to measure boom deformations/loads in a space interferometer experiment.

2.2.4 Performance of an Electroactive Hydraulic Actuator

(This task was not actually in the original proposal)

We've purchased the necessary equipment to test this device. However, we have not had the resources to finish this task.

2.3 Interaction with Other Program Participants

During the course of this grant there were discussions held with many organizations. These included:

- SSRC: (Boeing/MIT/Penn State Consortium)
- Aluminum Company of America (Alcoa)
- Ford Scientific Research (Dearborn)
- Michigan Scientific Company:
- Smiths Industries

In addition numerous government agencies were contacted along with many discussions at PI meetings at conferences. The most notable result of all this is that we now have an active program with Ford Research and they have incorporated some of our work into their research and production design codes (e.g. see [16]).

Also, in an attempt to interact with the helicopter community we've specifically addressed design problems that involve inertial loads (e.g. see [13,15]). We anticipate that these will be of interest to Boeing Helicopter.

3.0 Accomplishments/New Findings

During this period there were several significant accomplishments. They are:

1) We've shown how to include a body force (for the specific helicopter rotor problem) into the formulation, and that significant applications can be solved [13, 15]

2) We can now incorporate an arbitrary number of materials (either passive or active) into the formulation. Refer to documents [14, 16].

3) A three-dimensional version of the optimal design code has been implemented and appears to be sufficient to handle problems of significant scale. Refer to document [15].

4.0 Personnel most recently Supported

Professor Peter D. Washabaugh (1 Summer Month)

Professor John E. Taylor (1 Summer Month)

Dr. Sergio Turteltaub (9 Months - Post Doc)

5.0 Past Report Publications

1) "Analysis and Design of Trussed Structures Made of Elastic/Stiffening Materials", J.E. Taylor and P.D. Washabaugh, *Structural Optimization*, **8** 1-8, 1994

2) "Applications of a Generalized Complementary Energy Principle for the Equilibrium Analysis of Softening Material", Plaxton, S., Taylor, J.E., *Comp. Meth. Appl. Mech. Engng*, 117, pp 91-103, 1994

3) "A Global Extremum Principle in Mixed Form for Equilibrium Analysis with Elastic/Stiffening Materials: A Generalized Minimum Potential Energy Principle", Taylor, J.E., *Journal of Applied Mechanics*, Vol 61-No. 4, pp 914-918.

4) "Elastic Transducers Incorporating Finite Length Optical Paths", K. J. Peters and P.D. Washabaugh, *Applied Optics*, **3**, No. 22, 4993-5002, 1995

5) "Optimal Design of Material Properties and Material Distribution for Multiple Loading Conditions", Bendsoe, M.P., Diaz, A., Lipton, R., Taylor, J.E., *Int. J. Num. Meth. Engng.* 1996

6) "Generalized Potential Formulations for Kinematically Linear Elastostatics of Constitutively Nonlinear Structures, Taylor, J.E., *Int. J. Solids and Structures*, 1996.

7) "A Technique for Monitoring In-Situ the Structural Integrity of Prismatic Structures Under General Loading", K.J. Peters and P.D. Washabaugh, *AIAA Journal, Vol 35, No. 4, 1997*

8) "On Structural optimization Formulations with Generalized Cost Constraints", Taylor, J.E. and Washabaugh, P.D., *Proceedings PACAM V Meeting Puerto Rico*, 1996.

9) "Generalized Potential Formulations for Elastostatics of Constitutively Nonlinear Structures Under General Loading", Taylor, J.E., *International Journal of Mechanical Sciences*, Vol 61-No. 4, pp 914-918.

10) "Application of Finite-Length Displacement Sensors to Precision Torque Measurements of a Tail Rotor Transmission Tube" K.J. Peters and P.D. Washabaugh, *Proceedings of SPIE Smart Structures and Materials meeting,* San Diego Ca, 1996

11) "Finite Strain Elastostatic with Stiffening Materials a Constrained Minimization Model", Hollister, S.J., Taylor, J.E., Washabaugh, P. D., *Journal of Applied Mechanics, Vol 63, No. 2, 1997*

12) "A Formulation for Generalized Hyperelasticity using a Composition of Potentials", Guedes, J.M., Taylor, J.E., to appear *Journal of Applied Mechanics.* 1997

6.0 Most Recent Publications

13) "Optimal distribution of material properties for an elastic continuum with structure-dependent body force", Sergio Turteltaub and Peter Washabaugh., *To appear in the International Journal of Solids and Structures*, 1998.

14) "Prediction of Optimal Material Layout (Topology) and Properties for an Elastic Continuum Structure using Weighted Resource Constraint", J. Pawlicki, J.E. Taylor, S. Turteltaub and P.D. Washabaugh., *Submitted to Structural Optimization*, 1998.

15) "Three-dimensional optimal design of structural topology, shape and material properties with design-dependent field force", Sergio Turteltaub, Jakub Pawlicki, John E. Taylor, and Peter Washabaugh., *Submitted to the International Journal of Solids and Structures*, 1998.

16) "A Design Model to Predict Optimal Two-Material Composite Structures", H. Rodrigues, Ciro A. Soto. and. John E. Taylor, *in preparation*, 1998.

The current versions of these papers are appended at the end of this report.

7.0 Interactions/Transitions

Please refer to the section 2.3 for interactions with other program participants and the above publication list. The most notable transition of this information to industry has come from an unexpected source. In the past year and a half we have been collaborating with Ford Research Laboratories. As evident by the last publication above [16], the work on Optimal Topology Design has made it into some of the design codes at Ford. They are continuing to support this work.

8.0 New Discoveries, Inventions, Patent Disclosures

No new patent disclosures.

9.0 Honors and Awards

None.

Optimal distribution of material properties for an elastic continuum with structure-dependent body force.

Sergio Turteltaub and Peter Washabaugh

Department of Aerospace Engineering
The University of Michigan
Ann Arbor, MI 48109

Abstract

The simultaneous optimization of material properties and structural layout for an elastic continuum is formulated and analyzed. The objective is to obtain the maximum structural stiffness for prescribed surface loads and displacements, taking into account a body force that depends on the structural layout. Optimization with an account of self-weight or centrifugal forces are examples of these type of problems. Arbitrary elasticity tensor fields are considered as the problem's variable and necessary conditions satisfied by the solution are established. The use of a spectral decomposition of the elasticity tensor is emphasized since it provides a simple geometrical interpretation. Typical examples which illustrate the effects of the structure-dependent body force are analyzed. It is found that a commonly used isoperimetric restriction (known as the resource constraint) is not necessarily active and that the optimal structure is locally stiffer in areas where the body force and the displacement field have opposite directions and locally weaker otherwise. This, interestingly, leads to a non-symmetrical distribution of material properties even for prismatic bodies under anti-symmetric surface loads.

1 Introduction.

The problem of characterizing the maximum structural stiffness of a linearly elastic continuum structure has been extensively analyzed using different techniques. It has been recognized that it is possible to find simultaneously the optimal material properties and structural layout. One way to achieve this is simply by enlarging the space of variables in order to include all possible structures, i.e., by considering completely general elasticity tensor fields. This approach is known as the free-material optimization method and it relies on the use of elasticity tensor fields which, a priori, correspond to *anisotropic* and *inhomogeneous* materials (see Bendsøe et al. (1994)). Other methods consider a special class of anisotropic materials, namely composites obtained by combining two distinct homogeneous materials, although the problem requires relaxation in order to include optimal composites. In that case, usually assuming the existence of some type of periodic microgeometry, homogenization theory is used to compute the effective properties at a macroscopic level. Parameters related to the microgeometry are used as variables (see, e.g., Bendsøe (1995) for a comprehensive review of both methods). The advantage of the free-material optimization method is that issues related to homogenization do not need to be taken into account. Once the optimal material properties have been identified (at a macroscopic level) one can solve, if desired, an inverse problem in order to obtain at each point a microgeometry that provides the best match to the optimal properties as shown by Sigmund (1994) (see also Milton and Cherkaev (1995)). The purpose of the present analysis is to include, within the free-material formulation, a body force that depends on the optimization variable (i.e., on the elasticity tensor). The motivation for this extension is to analyze cases where a non-negligible inertial force acts on the structure. Typical examples are structural elements rotating at a relatively large angular speed or large structures whose own weight becomes a relevant factor in the analysis. Early work on problems with a structure-dependent body force include applications where the objective is to distribute a given amount of material in an elastic structure in order to match a desired natural frequency (see, e.g., Prager (1974) and the references therein). A more recent review on the subject was given by Olhoff (1987). Here, however, the objective is to maximize the structural stiffness taking into account a variable body force but no restrictions are placed upon natural frequencies.

The use of a formulation based on a spectral decomposition of the elas-

ticity tensor is emphasized since it provides a simple geometrical interpretation of the results in a fourth-order tensor space. It will be shown that the optimized material has two main components: a term which provides the optimal stiffness and a term which provides the required stability against possible perturbations of the prescribed loads. In this analysis, it is assumed that the magnitude of the elastic moduli and the material's mass density are correlated. Even though in general there is no a priori relation between these quantities, some models used for cellular solids exhibit a functional relation between the elastic moduli (see, e.g., Gibson and Ashby (1997)). From a different point of view, a relation between mass density and elastic properties can be assumed if one has in mind using, a posteriori, a method like the one proposed by Sigmund (1994). In that case, a microgeometry composed of weak (essentially void) and strong materials is used to match given effective properties. Bearing in mind that the strong material is fixed (and so is its mass density), the resulting volume fraction of the strong material is directly related to the mass density of the composite material. Thus, in this restricted sense, one can establish a relation between elastic moduli and mass density and it is assumed that this relation is strictly monotonic.

The outline of the paper is as follows: in Section 2, the optimization problem is formulated and under some specific assumptions a simplified version of it is derived by analyzing the restrictions imposed at a local level (for a continuum) by the global structural requirements. Optimality conditions for the problem are developed in Section 3 and specific examples with an inertial body force are treated in Section 4. A discussion and concluding remarks follow in the last section.

2 Formulation of the problem.

2.1 Notation.

As a general scheme of notation, scalar quantities are represented by italicized normal-face letters, vectors and points in a three-dimensional Euclidean space by bold-face lower case letters (except for the stress tensor σ and strain tensor ε), second order tensors by bold-face upper case letters and fourth order tensors by bold-face upper case italicized letters. Throughout this analysis, coordinate-free notation is employed. To ease the transition to indicial notation, the following definitions are referred to a three-dimensional

Cartesian basis (indices range in $\{1,2,3\}$, δ_{ij} is Kronecker's delta and the summation convention is used):

$$\begin{aligned}
&\mathrm{a}\cdot\mathrm{b} = a_i b_i \ , && \mathrm{A}\cdot\mathrm{B} = A_{ij}B_{ij} \ , && C\cdot D = C_{ijkl}D_{ijkl} \ ,\\
& && \|\mathrm{A}\| = \sqrt{\mathrm{A}\cdot\mathrm{A}} \ , && \|C\| = \sqrt{C\cdot C} \ ,\\
&(\mathrm{Ab})_i = A_{ij}b_j \ , && (\mathrm{AB})_{ij} = A_{ik}B_{kj} \ , && (C\mathrm{A})_{ij} = C_{ijkl}A_{kl} \ ,\\
& && (\mathrm{a}\otimes\mathrm{b})_{ij} = a_i b_j \ , && (\mathrm{A}\otimes\mathrm{B})_{ijkl} = A_{ij}B_{kl} \ ,\\
& && (\mathrm{I})_{ij} = \delta_{ij} \ , && (I)_{ijkl} = \tfrac{1}{2}(\delta_{ik}\delta_{jl} + \delta_{il}\delta_{jk}) \ .
\end{aligned}$$

In general, when the meaning is clear by the context, a scalar, vector or tensor field defined in a domain Ω and its value at a point x will be denoted by the same letter, e.g., $\mathrm{A} = \mathrm{A}(\mathrm{x})$. Similarly, a scalar, vector or tensor function of a scalar, vector or tensor field will be denoted by the same symbols, e.g., $\varphi = \varphi(\mathrm{A}) = \varphi(\mathrm{A}(\mathrm{x}))$, when it is clear by the context that φ is not, for example, a functional.

2.2 Preliminaries.

Consider a linearly elastic body that occupies a given domain Ω. Suppose that the prescribed tractions t and displacements u are

$$\left.\begin{aligned}
&\mathrm{t}(\mathrm{x}) = \hat{\mathrm{t}}(\mathrm{x}) && \mathrm{x}\in\partial\Omega_t\\
&\mathrm{u}(\mathrm{x}) = 0 && \mathrm{x}\in\partial\Omega_u
\end{aligned}\right\} \qquad (1)$$

where $\partial\Omega_t \cup \partial\Omega_u = \partial\Omega$ is the boundary of Ω. Only mixed boundary conditions of the form (1) are considered here. Let ε be the strain tensor field which, viewed as a function of $\mathrm{u}(\mathrm{x})$, is given by

$$\varepsilon = \varepsilon(\mathrm{u}) = \varepsilon(\mathrm{u}(\mathrm{x})) = \tfrac{1}{2}\left(\nabla\mathrm{u}(\mathrm{x}) + \nabla\mathrm{u}(\mathrm{x})^T\right) \ , \qquad \forall \mathrm{x}\in\Omega \ .$$

Let C be a (fourth-order) elasticity tensor field. The stress tensor field σ is related to the strain tensor via the constitutive law

$$\sigma(\mathrm{x}) = C(\mathrm{x})\varepsilon(\mathrm{x}) \ .$$

As a matter of terminology, the word "structure" should be understood in the present analysis to refer to a *distribution of material properties* over the given domain Ω, i.e., to the field $C(\mathrm{x})$, $\mathrm{x}\in\Omega$. By "optimal distribution" it

is meant that a specific structure (i.e., distribution of $C(\mathrm{x})$) is sought based on maximization of the overall stiffness of the structure. A formal statement of this problem is given in Section 2.4.

To obtain the optimal distribution of material properties, the basic idea is to let the elasticity tensor field be variable. It is worth noting that one can accomplish two seemingly distinct objectives with this approach. Firstly, the minimizing field C_0 provides information on the mechanical properties of a material at each point (i.e., the material optimization). Secondly, since points where the material properties are "small" are interpreted as holes (in a sense to be defined later), then C_0 also provides the shape of the structure within the domain Ω by specifying the location of holes. Hence, the shape optimization (structural layout) is obtained as a by-product of the material optimization. This ability to perform simultaneously optimization of material properties and structural layout is one of the main benefits of the free-material optimization method and its simplicity (compared to homogenization techniques) provides an additional advantage.

2.3 Body force and space of admissible variables.

The space of admissible optimization variables is, in this case, a subspace of fourth-order tensor fields defined in Ω. For practical reasons, both physical and mathematical, some additional restrictions on the space of optimization variables are required. To introduce these restrictions it is convenient to use a spectral decomposition of the elasticity tensor. Since the admissible elasticity tensors are symmetric (major symmetry), they can be represented at each point x in terms of their real eigenvalues α_μ ($\mu = 1, \ldots, 6$) and unit eigentensors A_μ (2-tensors), i.e., the spectral decomposition is given by

$$C = \sum_{\mu=1}^{6} \alpha_\mu \mathrm{A}_\mu \otimes \mathrm{A}_\mu \,, \tag{2}$$

where $\alpha_\mu > 0$ and $\{\mathrm{A}_\mu\}_{\mu=1}^{6}$ forms an orthonormal basis for the space of symmetric 2-tensors. Recall that for a general (anisotropic) material, the eigentensors contain information about the material behavior (via "angles" in a tensor space) but the "true" stiffness information is provided by the six principal values of the elastic moduli (i.e., eigenvalues α_μ). For example, for an isotropic material there are two distinct eigenvalues: 3κ (multiplicity one) and 2μ (multiplicity five), where κ is the bulk modulus and μ is the shear

modulus (see, e.g., Knowles (1995)). It is also important to note that the result of this decomposition is that the design variables are now explicitly the eigenvalues and eigenvectors.

The fact that the eigenvalues are strictly positive means that C is positive definite. To satisfy this requirement, it is assumed that all eigenvalues are bounded below by the same *constant* α_m. Additionally, an upper bound α_M is imposed on each α_μ (same constant α_M for all α_μ). Since $\{\alpha_\mu\}_{\mu=1}^6$ are the principal stiffnesses, the upper bound is seen as a limitation of real materials: the elastic moduli cannot exceed the values of the stiffest material known in nature (or, in fact, of a predetermined material that would be used to reinforce the structure). Finally, a global upper bound on the eigenvalues (known as a *resource constraint*) is also imposed. To this end, consider a positive-valued scalar function $\bar{\varphi}$ of C which is referred to as the *resource constraint density*. In the work of Bendsøe et al. (1994), a resource constraint density equal to the trace of C was used, i.e., $\bar{\varphi}(C) = \sum_{\mu=1}^6 \alpha_\mu$. Following a similar approach, the resource constraint density considered here is assumed to be independent of the orientation of the principal directions of the elasticity tensor and dependent on the eigenvalues of C via their maximum only, i.e.,

$$\bar{\varphi}(C) = \alpha \,, \tag{3}$$

where α is the maximum principal stiffness, i.e.,

$$\alpha = \alpha(\mathrm{x}) = \max_{1\le\mu\le 6}\{\alpha_\mu(\mathrm{x})\} \tag{4}$$

Observe that (3) is not the only choice since $\bar{\varphi}$ could depend on A_μ (the orientation of material properties) which could be interpreted, e.g., as a constraint imposed by manufacturing requirements. In terms of α, the resource constraint is expressed by the following isoperimetric inequality:

$$\int_\Omega \alpha(\mathrm{x})\mathrm{d}v \le R \,,$$

where the left hand side is the total resource and the given positive constant R represents an upper bound on the resource. The main role of the resource constraint is to rule out some trivial solutions. A typical trivial case occurs when the body force b is *zero* and the isoperimetric inequality is *not*

enforced: the stiffest structure is obtained when the optimization variable coincides with the local upper bound, i.e., it coincides with the stiffest material properties everywhere.

For future use, all the requirements on the space of admissible optimization variables can be collected via the following sets:

$$\mathcal{S}_{\alpha_\mu} = \left\{ \{\alpha_\mu\}_{\mu=1}^{6} \mid \alpha_m \leq \alpha_\mu(\mathrm{x}) \leq \alpha_M \, , \, \int_\Omega \alpha \mathrm{d}v \leq R \, , \, \forall \mathrm{x} \in \Omega \right\} \, ,$$

and

$$\mathcal{S}_{\mathrm{A}_\mu} = \left\{ \{\mathrm{A}_\mu\}_{\mu=1}^{6} \mid \mathrm{A}_\mu \cdot \mathrm{A}_\nu = \delta_{\mu\nu} \, , \, \mathrm{A}_\mu = \mathrm{A}_\mu^T \, , \, \textstyle\sum_{\mu=1}^{6} \mathrm{A}_\mu \otimes \mathrm{A}_\mu = I \right\} \, ,$$

where α is defined by (4) and $\delta_{\mu\nu}$ is Kronecker's delta. The symmetry of each A_μ reflects the minor symmetries of C. Now, it is assumed that there exist functional relations between the principal elastic moduli (eigenvalues α_μ) and the mass density ρ, i.e., $\alpha_\mu = \bar{\alpha}_\mu(\rho)$. To motivate this assumption from a physical point of view, one could refer, for example, to models used for cellular solids (see Gibson and Ashby (1997)). In that context, it has been found experimentally that, in the linearly elastic range, the material properties scale with some power of the mass density (e.g., the shear modulus for elastomeric foams is $\mu \sim \rho^2$, etc.). Similar relations are sometimes used in some simple models for composite materials where the material properties depend on the volume fraction of each component (hence they depend on the relative mass densities). Furthermore, assuming that these relations can be inverted, then the mass density could be expressed as a function of one of the eigenvalues of C; in particular, $\rho = \bar{\rho}(\alpha)$, where α is the maximum principal stiffness. Thus, assuming the existence of such a model, an (inertial) body force can be viewed as a function of α, i.e.,

$$\mathrm{b} = \hat{\mathrm{b}}(\bar{\rho}(\alpha)) = \bar{\mathrm{b}}(\alpha) \, . \tag{5}$$

With this interpretation, the resource constraint can also be seen as a restriction on the total mass of the structure. However, it is important to mention that the present analysis is limited to cases where a relation such as (5) can be identified.

Let W be the work done by the external forces, i.e.,

$$W[\mathrm{u}, \bar{\mathrm{b}}(\alpha)] = \int_\Omega \bar{\mathrm{b}}(\alpha(\mathrm{x})) \cdot \mathrm{u}(\mathrm{x}) \mathrm{d}v + \int_{\partial\Omega_t} \hat{\mathrm{t}}(\mathrm{x}) \cdot \mathrm{u}(\mathrm{x}) \mathrm{d}a \, . \tag{6}$$

Let $\mathcal{V}$ be a suitably chosen space of kinematically admissible displacement fields. For given boundary conditions (1) and for a specific (i.e., "frozen") elasticity tensor field C, the displacement field u that satisfies the equilibrium equation is the (unique) element of the set $\mathcal{E}_C$ defined as follows:

$$\mathcal{E}_C = \left\{ \mathrm{u} \in \mathcal{V} \mid \int_\Omega \epsilon(\mathrm{u}) \cdot C\epsilon(\mathrm{v}) dv = W[\mathrm{v}, \bar{\mathrm{b}}(\alpha)] \quad \forall \mathrm{v} \in \mathcal{V} \right\}. \tag{7}$$

The work W given by (6) is viewed as a global measure of the stiffness of a structure and takes into account the prescribed domain Ω and boundary conditions. The stiffest structure corresponds to the one which minimizes W for *fixed* boundary conditions (1) when the elasticity tensor field C is taken as variable.

2.4 Optimization problem: maximum structural stiffness.

The optimization problem is stated as: for a linearly elastic material occupying a given domain Ω and for boundary conditions given by (1), find the minimizer $C = \sum_{\mu=1}^{6} \alpha_\mu \mathrm{A}_\mu \otimes \mathrm{A}_\mu$ of the following expression:

$$\min_{\{\alpha_\mu\} \in S_{\alpha_\mu}} \min_{\{\mathrm{A}_\mu\} \in S_{\mathrm{A}_\mu}} W[\mathrm{u}, \bar{\mathrm{b}}(\alpha)] \tag{P1}$$

where $\mathrm{u} \in \mathcal{E}_C$ (hence the admissible field u is the equilibrium solution for a given field C) and α is given by (4). The two minimization parts reflect a decomposition of the optimization problem in terms of two sets of variables (eigenvalues $\{\alpha_\mu\}$ and eigentensors $\{\mathrm{A}_\mu\}$ of C). The sets S_{α_μ} and S_{A_μ} correspond to the constraints on the optimization variables. For the *solution* u of the elastostatic problem (i.e., $\mathrm{u} \in \mathcal{E}_C$), the dependence of W on C, as given by (6), is two-fold: u depends implicitly on the constitutive law and, by assumption, the body force depends explicitly on the maximum eigenvalue of C. Formally, W also depends on Ω and the prescribed boundary conditions, but these are considered *fixed*.

The problem (P1) can be simplified considerably by virtue of a saddle point theorem as proved in Bendsøe et al. (1994) (see also Jog et al. (1993) and Lipton (1994)). This is an established result in the optimization of structures. Nonetheless, in order to illustrate the explicit role played by

the eigenvalues and eigentensors of C introduced in (2) and to show that the saddle point theorem remains unaffected by a structure-dependent body force of the form (5), it is useful to revisit this result. More significantly, the analysis presented here provides an interpretation of the solution of the optimization problem in terms of a positive definite material, as opposed to previous solutions which were given in terms of semi-definite materials. To this end, the admissible displacement fields in (P1) are characterized as minimizers of the potential energy (instead of enforcing the equilibrium equations). The potential energy is given by $\Pi = U - W$, where $U = \frac{1}{2}\int_\Omega \varepsilon \cdot C\varepsilon dv$ is the total strain energy. The minimum value of the potential energy is $\Pi_* = -\frac{1}{2}W_*$, hence, reversing the sign of the objective functional, the problem (P1) can be expressed alternatively as: find the maximizing eigenvalue fields, eigentensor fields and minimizing displacement field of the following expression:

$$\max_{\{\alpha_\mu\}\in S_{\alpha_\mu}} \max_{\{\mathbf{A}_\mu\}\in S_{\mathbf{A}_\mu}} \min_{\mathbf{v}\in\mathcal{V}} \Pi[\alpha_\mu, \mathbf{A}_\mu; \mathbf{v}] \,, \tag{P2}$$

where, since $\varepsilon \cdot C\varepsilon = \sum_{\mu=1}^{6} \alpha_\mu (\varepsilon \cdot \mathbf{A}_\mu)^2$, the potential energy is

$$\Pi[\alpha_\mu, \mathbf{A}_\mu; \mathbf{v}] = \sum_{\mu=1}^{6} \int_\Omega \tfrac{1}{2}\alpha_\mu (\varepsilon(\mathbf{v}) \cdot \mathbf{A}_\mu)^2 dv - W[\mathbf{v}, \bar{\mathbf{b}}(\alpha)] \,. \tag{8}$$

The minimization part in (P2) corresponds to the elastostatic problem for a given elasticity tensor field. In view of the saddle point theorem mentioned above, the two inner problems in (P2) can be interchanged (the theorem can be applied because it is assumed that $\bar{\mathbf{b}}$ is not a function of $\mathbf{A}_\mu$). It is worth noting that the outermost maximization problem cannot be interchanged with the innermost minimization problem since they provide different solutions. After interchanging the two inner problems in (P2), the innermost problem becomes, for given $\mathbf{v}$ and $\{\alpha_\mu\}_{\mu=1}^6$, a *local algebraic* problem, i.e., find the maximizers, at each point $\mathbf{x} \in \Omega$, in the following expression:

$$\max_{\{\mathbf{A}_\mu\}\in S_{\mathbf{A}_\mu}} \sum_{\mu=1}^{6} \tfrac{1}{2}\alpha_\mu (\varepsilon(\mathbf{v}) \cdot \mathbf{A}_\mu)^2 \,. \tag{9}$$

To provide a "geometrical" interpretation of the problem notice that, since $\varepsilon \cdot C\varepsilon = (\varepsilon \otimes \varepsilon) \cdot C$, then (9) is equivalent to

$$\max_{\{\mathrm{A}_\mu \otimes \mathrm{A}_\mu\}} \left[\tfrac{1}{2}(\varepsilon(\mathrm{v}) \otimes \varepsilon(\mathrm{v})) \cdot \sum_{\mu=1}^{6} \alpha_\mu (\mathrm{A}_\mu \otimes \mathrm{A}_\mu) \right] , \tag{10}$$

where the maximization is carried out for six 4-tensors of the form $\mathrm{A}_\mu \otimes \mathrm{A}_\mu$ and the problem is *linear* since the goal is to maximize the scalar product of "vectors" in a 4-tensor space, where both $\{\alpha_\mu\}_{\mu=1}^{6}$ and $\varepsilon \otimes \varepsilon$ are fixed. The objective function in the inner problem (10) (or (9)) admits the following trivial bound:

$$\tfrac{1}{2}(\varepsilon \otimes \varepsilon) \cdot \sum_{\mu=1}^{6} \alpha_\mu (\mathrm{A}_\mu \otimes \mathrm{A}_\mu) \leq \tfrac{1}{2} \max_{1 \leq \mu \leq 6} \{\alpha_\mu\} \|\varepsilon \otimes \varepsilon\| = \tfrac{1}{2} \alpha \varepsilon \cdot \varepsilon \ . \tag{11}$$

This upper bound is independent of $\{\mathrm{A}_\mu\}$ and depends on the local values of $\{\alpha_\mu\}$ only via their maximum α. To reach this bound, one could choose the eigentensor corresponding to the maximum eigenvalue as

$$\mathrm{A} = \hat{\varepsilon} = \frac{\varepsilon}{\|\varepsilon\|} \ ,$$

while the other eigentensors can be chosen arbitrarily as long as they form an orthonormal basis. This choice can be made regardless of the multiplicity of the maximum eigenvalue (i.e., one of the eigentensors corresponding to α can be defined as above). With this specific choice the upper bound is *reached*, thus providing an optimal solution for the set $\{\mathrm{A}_\mu\}$, valid for any point $\mathrm{x} \in \Omega$, in terms of the (kinematically admissible) displacement field v. An explicit expression for the eigentensors different than $\hat{\varepsilon}$ is not required for the present purposes. From (8), (11) and the definition of S_{α_μ}, one can see that if the upper bound is reached, then the problem (P2) depends only on the maximum eigenvalue α. In that case, the eigenvalues smaller than α can be chosen arbitrarily as long as they belong to S_{α_μ}. This problem has no unique solution, however a convenient choice is to set these eigenvalues to the lower bound α_m in order to guarantee that α is the maximum. If the multiplicity of α is greater than one, then the above choice corresponds to reducing its multiplicity to one. The essential point is that any admissible choice provides the same final result (i.e., upper bound). The optimal material can now be

expressed as

$$C_0 = C_0(\alpha, \mathrm{v}) = (\alpha - \alpha_m)\frac{\varepsilon(\mathrm{v}) \otimes \varepsilon(\mathrm{v})}{\|\varepsilon(\mathrm{v})\|^2} + \alpha_m I \ . \tag{12}$$

The coupling between the optimization and elastostatic problems is reflected in the fact that the elasticity tensor depends on the strain field. It is noted in passing that C_0 is an orthotropic material with symmetry directions aligned (locally) with the principal directions of the strain tensor: to see this, suppose that Q is a proper orthogonal second order transformation that commutes with ε, hence Q and ε have the same principal directions in an Euclidean space. Since C_0 transforms as $\sum_{\mu=1}^{6} \alpha_\mu \mathrm{Q}\mathrm{A}_\mu\mathrm{Q}^T \otimes \mathrm{Q}\mathrm{A}_\mu\mathrm{Q}^T$ and since $\mathrm{Q}\varepsilon\mathrm{Q}^T = \varepsilon$ then it follows from (12) that Q belongs to the material symmetry group of C_0. The orthotropy of the optimal material is, in fact, a well-known result (see, e.g., Pedersen (1989), Cowin (1994)). However, the specific form (12) has a new ingredient compared to the one proposed by Bendsøe et al. (1994), i.e., the term $\alpha_m I$, which provides the required stability of the material. Recently, Taylor (1997) proposed a general framework where, among other things, terms such as $\alpha_m I$ can be easily introduced. The essential term in the material (12) is a 4-tensor perpendicular projection onto the 2-tensor space spanned by the strain tensor (which can be interpreted as an optimal "reinforcement," characterized by the maximum principal stiffness α). For illustration purposes, the material properties of the orthotropic material can also be expressed in terms of the (three) Young moduli E_i, the (three independent) Poisson's ratios ν_{ij} and (three) shear moduli G_{ij}. Let $\hat{\varepsilon}_i$, $i = 1, 2, 3$, be the principal values of the (unit) strain tensor $\hat{\varepsilon} = \varepsilon/\|\varepsilon\|$; for an *arbitrary* strain tensor γ, the corresponding stress is, from (12), $\sigma = C_0\gamma = (\alpha - \alpha_m)(\hat{\varepsilon} \cdot \gamma)\hat{\varepsilon} + \alpha_m\gamma$. Hence, the elastic moduli referred to a Cartesian basis aligned locally with the principal directions of $\varepsilon(\mathrm{v})$ are given by

$$E_i = \frac{\alpha\alpha_m}{\alpha_m + (1 - \hat{\varepsilon}_i^2)\alpha} \ , \quad \nu_{ij} = \frac{(\alpha - \alpha_m)\hat{\varepsilon}_i\hat{\varepsilon}_j}{\alpha_m + (1 - \hat{\varepsilon}_i^2)\alpha} \ , \quad G_{ij} = \tfrac{1}{2}\alpha_m \ .$$

Moreover, the stress field associated with the *optimal* strain field $\varepsilon(\mathrm{v})$ takes the following simple form:

$$\sigma = C_0\varepsilon = \alpha\varepsilon \ . \tag{13}$$

By optimal strain field it is meant that ε is the strain field in the elastostatic problem after the material C has been optimized analytically with respect to

the set $\{A_\mu\}$. Although the elasticity tensor given by (12) is anisotropic, its *restriction* to the optimal strain field, given by (13), corresponds *formally* to an isotropic material with material coefficients $3\kappa = 2\mu = \alpha$ or, equivalently, to $\nu = 0$ and $E = \alpha$ where ν is Poisson's ratio and E is Young's modulus. This formal interpretation is valid since the optimization and elastostatic problems are being solved simultaneously, hence the optimal material properties are coupled to the optimal displacement field (this is referred to as a self-adaptive material, although it is a mathematical rather than a physical property).

In view of (12), the problem (P1) can be simplified in terms of the scalar field α (maximum principal stiffness), i.e., find the minimizer α of

$$\min_{\alpha \in \mathcal{S}_\alpha} W[\mathrm{u}, \bar{\mathrm{b}}(\alpha)] \,, \tag{P3}$$

where $\mathrm{u} \in \mathcal{E}_\alpha$,

$$\mathcal{E}_\alpha = \left\{ \mathrm{u} \in \mathcal{V} \,|\, \int_\Omega \alpha \varepsilon(\mathrm{u}) \cdot \varepsilon(\mathrm{v}) dv = W[\mathrm{v}, \bar{\mathrm{b}}(\alpha)] \quad \forall \mathrm{v} \in \mathcal{V} \right\} \tag{14}$$

and

$$\mathcal{S}_\alpha = \left\{ \alpha |\, \alpha_m \leq \alpha(\mathrm{x}) \leq \alpha_M \,,\, \int_\Omega \alpha dv \leq R \,,\, \forall \mathrm{x} \in \Omega \right\}$$

At points where the maximum principal stiffness α is equal to its lower bound α_m, the interpretation is that no reinforcement is required. The formulation (P3) provides a significant simplification from (P1) since the minimization is carried out for a single scalar field as opposed to a tensor field. For given α, the local form of the elastostatic problem for the *optimal* strain ε at points where α and ε are smooth is, from (14),

$$\left.\begin{aligned} \mathrm{div}(\alpha\varepsilon) + \bar{\mathrm{b}}(\alpha) = 0 \quad & \text{in } \Omega \,, \\ \sigma \mathrm{n} = \alpha \varepsilon \mathrm{n} = \hat{\mathrm{t}} \quad & \text{on } \partial\Omega_t \,, \\ \mathrm{u} = 0 \quad & \text{on } \partial\Omega_u \,, \end{aligned}\right\} \tag{15}$$

where n is the outward unit normal vector to the boundary $\partial\Omega$. Observe that the for shape optimization, "holes" are identified via a limit process when $\alpha_m/\alpha_M \to 0$, for which uniqueness is preserved. However, in the limit, the material becomes semi-definite, which is in fact one of the limitations of the "true" single-loading shape optimization problem. Hence, after the

solution to (P3) has been identified (optimal structure) and is considered to be fixed, α_m needs to be bounded away from zero by an amount comparable to possible perturbations on the surface loads in order to have a "robust" structure.

3 Optimality conditions.

The optimality conditions correspond to a set of necessary relations satisfied locally by the minimizer of (P3) and can be used for numerical methods or to solve some simple problems in closed form as will be shown in Section 4. To obtain these conditions, consider the Lagrangian L given by

$$L[\alpha;\lambda_m,\lambda_M,\Lambda] = W_0[\mathrm{u},\bar{\mathrm{b}}(\alpha)] + \int_\Omega [\lambda_m(\alpha_m-\alpha) - \lambda_M(\alpha-\alpha_M)]\,\mathrm{d}v + \Lambda\left\{\int_\Omega \alpha \mathrm{d}v - R\right\}, \tag{16}$$

where $\lambda_m = \lambda_m(\mathrm{x}), \lambda_M = \lambda_M(\mathrm{x})$ are Lagrange multipliers associated with the upper and lower bound constraints respectively and Λ is the (constant) multiplier corresponding to the resource constraint. As mentioned before, the displacement field u is viewed as a function of α since it can be obtained from (14). Hence, in terms of the Lagrangian L, the problem (P3) can be expressed as: find the maximizers $\lambda_m, \lambda_M, \Lambda$ and minimizer α in the following expression:

$$\max_{\lambda_m\geq 0,\ \lambda_M\geq 0,\ \Lambda\geq 0} \min_{\alpha} L[\alpha;\lambda_m,\lambda_M,\Lambda]\ .$$

The gradient of L with respect to α can be computed as follows: consider a variation $\delta\alpha$ which induces variations $\delta\mathrm{u}$ and $\delta\bar{\mathrm{b}}$. Let L' be the gradient of L, therefore, from (5), (6), (12) and (16), it follows that

$$\delta L[\delta\alpha] = \int_\Omega L'\delta\alpha \mathrm{d}v = \int_\Omega \left(\delta\bar{\mathrm{b}}\cdot\mathrm{u} + \bar{\mathrm{b}}\cdot\delta\mathrm{u}\right)\mathrm{d}v + \int_{\partial\Omega_t} \hat{\mathrm{t}}\cdot\delta\mathrm{u}\mathrm{d}a - \int_\Omega (\lambda_m - \lambda_M - \Lambda)\,\delta\alpha \mathrm{d}v\ . \tag{17}$$

To complete the calculation, one can take variations in (14), then integrate by parts, choose $\mathbf{v} = \mathbf{u}$, and use (15) and (17) to get

$$\int_\Omega L'\delta\alpha dv = \int_\Omega 2\delta\bar{\mathrm{b}} \cdot \mathrm{u} dv - \int_\Omega \delta\alpha \left(\varepsilon(\mathrm{u}) \cdot \varepsilon(\mathrm{u}) + \lambda_m - \lambda_M - \Lambda\right) \mathrm{d}v \ .$$

Since $\delta\bar{\mathrm{b}} = \bar{\mathrm{b}}'\delta\alpha$, where $\bar{\mathrm{b}}'$ is the gradient of $\bar{\mathrm{b}}$ with respect to α, then, assuming enough differentiability, the local form of the gradient is

$$L' = 2\bar{\mathrm{b}}' \cdot \mathrm{u} - \varepsilon(\mathrm{u}) \cdot \varepsilon(\mathrm{u}) - \lambda_m + \lambda_M + \Lambda \ . \tag{18}$$

Therefore, the optimality conditions (Karush-Kuhn-Tucker conditions) are, $\forall \mathrm{x} \in \Omega$,

$$\left.\begin{aligned} L' &= 0 \ , & & \\ \lambda_m(\alpha_m - \alpha) &= 0 \ , & \lambda_m &\geq 0 \ , \\ \lambda_M(\alpha - \alpha_M) &= 0 \ , & \lambda_M &\geq 0 \ , \\ \Lambda\left\{\textstyle\int_\Omega \alpha dv - R\right\} &= 0 \ , & \Lambda &\geq 0 \ . \end{aligned}\right\} \tag{19}$$

To interpret the optimality conditions one can use the following domains:

$$\begin{aligned} \Omega_m &= \{\mathrm{x} \in \Omega \mid \alpha(\mathrm{x}) = \alpha_m\} \ , \\ \Omega_M &= \{\mathrm{x} \in \Omega \mid \alpha(\mathrm{x}) = \alpha_M\} \ , \\ \Omega_i &= \{\mathrm{x} \in \Omega \mid \alpha_m < \alpha(\mathrm{x}) < \alpha_M\} \ . \end{aligned} \tag{20}$$

Hence, since $\lambda_m = 0$ for $\mathrm{x} \in \Omega_M$, $\lambda_M = 0$ for $\mathrm{x} \in \Omega_m$ and $\lambda_m = \lambda_M = 0$ for $\mathrm{x} \in \Omega_i$, the optimality conditions (19) become

$$\left.\begin{aligned} \Lambda &= \varepsilon(\mathrm{u}) \cdot \varepsilon(\mathrm{u}) - 2\bar{\mathrm{b}}' \cdot \mathrm{u} \ , & & & \mathrm{x} &\in \Omega_i \ , \\ \Lambda - \lambda_m &= \varepsilon(\mathrm{u}) \cdot \varepsilon(\mathrm{u}) - 2\bar{\mathrm{b}}' \cdot \mathrm{u} \ , & \lambda_m &> 0 \ , & \mathrm{x} &\in \overset{\circ}{\Omega}_m \ , \\ \Lambda + \lambda_M &= \varepsilon(\mathrm{u}) \cdot \varepsilon(\mathrm{u}) - 2\bar{\mathrm{b}}' \cdot \mathrm{u} \ , & \lambda_M &> 0 \ , & \mathrm{x} &\in \overset{\circ}{\Omega}_M \ , \\ \Lambda\left\{\textstyle\int_\Omega \alpha dv - R\right\} &= 0 \ , & \Lambda &\geq 0 \ , & \mathrm{x} &\in \Omega \ . \end{aligned}\right\} \tag{21}$$

If $\bar{\mathrm{b}} = \bar{\mathrm{b}}' = 0$ then one can prove that $\Lambda > 0$ (and hence that the resource constraint is active (i.e., satisfied as an equality; see Bendsøe et al. (1994)). Clearly, to have a non-trivial solution in the case when the resource constraint is active, the upper bound R in the resource constraint has to satisfy $\alpha_m|\Omega| < R < \alpha_M|\Omega|$. However, if $\bar{\mathrm{b}}' \not\equiv 0$, it is possible that $\Lambda = 0$ and the problem (P3) has a non-trivial solution. This case will be illustrated by an example in

Section 4. Furthermore, recall that it was assumed that $\bar{\mathbf{b}}$ is a monotonically increasing function of α hence, in view of (18), if $\bar{\mathbf{b}} \cdot \mathbf{u} > 0$, the local effect of the term $2\bar{\mathbf{b}}' \cdot \mathbf{u}$ is to increase the value of the gradient of the Lagrangian L. Conversely, if $\bar{\mathbf{b}} \cdot \mathbf{u} < 0$ (hence $\bar{\mathbf{b}}' \cdot \mathbf{u} < 0$), the local effect of the term $2\bar{\mathbf{b}}' \cdot \mathbf{u}$ is to decrease L'. Therefore, compared to the case when the body force zero, the optimal structure is locally *weaker* (*smaller* maximum principal stiffness α) if $\bar{\mathbf{b}} \cdot \mathbf{u} > 0$ and locally *stiffer* (greater α) otherwise. This effect will be illustrated by a three-dimensional example in next section.

4 Example: the optimal rotating structure.

As an example of a structure-dependent body force, consider the problem of finding the stiffest structure occupying a domain Ω and rotating at a constant angular velocity ω. Let $\{\mathbf{e}_r, \mathbf{e}_\theta, \mathbf{e}_z\}$ be a cylindrical orthonormal basis where $\mathbf{e}_z$ is aligned with the axis of rotation and $\mathbf{e}_r, \mathbf{e}_\theta$ are fixed with respect to Ω ($\mathbf{e}_r$ points in the outward radial direction). For illustration purposes, suppose that the optimization is carried out with a material for which the mass density ρ is related to the maximum principal stiffness α linearly, i.e.,

$$\rho = \kappa\alpha \ ,$$

where κ is a positive constant. It is worth noting that for nonlinear functions ρ the corresponding problem is nonlinear and might not have a solution. The inertial force can be modeled in the elastostatic problem as the body force

$$\bar{\mathbf{b}}(\alpha) = \omega^2 r \rho \mathbf{e}_r = \omega^2 r \kappa \alpha \mathbf{e}_r \ , \tag{22}$$

where r is the orthogonal distance from a given point in Ω to the axis of rotation. To obtain some insight in the problem, it is possible to solve analytically a one-dimensional example. To this end, consider a prismatic region Ω of length l and cross-sectional area a. Suppose that the displacement field and the maximum principal stiffness α depend on r only, $r \in [0, l]$. As an ansatz, assume that the domains defined by (20) are such that $\Omega_M = [0, r_1]$, $\Omega_i = [r_1, r_2]$, $\Omega_m = [r_2, l]$ and that the resource constraint is not active (i.e., $\Lambda = 0$). It will be shown a posteriori that these assumptions are appropriate to characterize solutions with boundary conditions $u(0) = 0$ and $\sigma = \alpha(l)u'(l) = \sigma_0 > 0$, where $u(r)$ is the radial displacement. The optimality

conditions (21) become

$$\begin{array}{lll} \lambda_M(\tau) = (u'(\tau))^2 - 2\kappa\omega^2\tau u(\tau) \quad \lambda_M(\tau) \geq 0 & 0 \leq \tau \leq \tau_1 \\ (u'(\tau))^2 - 2\kappa\omega^2\tau u(\tau) = 0 & \tau_1 \leq \tau \leq \tau_2 \\ \lambda_m(\tau) = -(u'(\tau))^2 + 2\kappa\omega^2\tau u(\tau) \quad \lambda_m(\tau) \geq 0 & \tau_2 \leq \tau \leq l \end{array} \tag{23}$$

and the balance of linear momentum is, from $(15)_1$,

$$(\alpha u')' + \kappa\omega^2\tau\alpha = 0 \qquad 0 \leq \tau \leq l\,. \tag{24}$$

Observe that, since $\alpha = \alpha_M > 0$ in Ω_M and $\alpha = \alpha_m > 0$ in Ω_m, then (24) becomes

$$u''(\tau) + \kappa\omega^2\tau = 0\,, \qquad \forall\tau \in \Omega_M \cup \Omega_m\,.$$

The displacement field can be determined in Ω_M and Ω_m up to a constant (say, c_M and c_m) by solving the above equation and using the boundary conditions. This, in turn, provides an expression for $\lambda_M(\tau)$ and $\lambda_m(\tau)$ from $(23)_{1,3}$. Furthermore, solving $(23)_2$ gives the displacement field in Ω_i up to a constant (say, c_1). With this displacement field one can solve (24) in Ω_i and determine $\alpha(\tau)$ up to a constant (say, c_2). The solution is displayed more conveniently in nondimensional form. Define

$$\bar{u} = \frac{u}{l\gamma}\,, \quad \bar{\tau} = \frac{\tau}{l}\,, \quad \bar{\alpha} = \frac{\alpha}{\alpha_M}\,, \quad \text{where } \gamma = \kappa\omega^2 l^2\,,$$

and the following nondimensional parameters:

$$f = \frac{2\sigma_0}{\alpha_M\kappa\omega^2 l^2}\,, \quad \beta = \frac{\alpha_m}{\alpha_M}\,. \tag{25}$$

The parameter f, referred to as the *loading parameter*, includes the applied loads, the upper bound of the material properties and a term related to the body force, so it can be interpreted as the ratio of surface to body forces. The parameter β, referred to as the *moduli parameter*, corresponds to the nondimensional ratio of the lower and upper bounds of the reinforcement or, equivalently, to the nondimensional modulus of the term $\alpha_m I$ of the optimal material C_0. The displacement field and the maximum principal stiffness (reinforcement) are given by

$$\bar{u}(\bar{\tau}) = \begin{cases} \frac{1}{6}\bar{\tau}\left(c_M - \bar{\tau}^2\right) & \bar{\tau} \in \Omega_M = [0, \bar{\tau}_1]\,, \\ \frac{1}{18}\left(3c_1 + 2\bar{\tau}^{\frac{3}{2}}\right)^2 & \bar{\tau} \in \Omega_i = [\bar{\tau}_1, \bar{\tau}_2]\,, \\ \frac{1}{6}\left[c_m + \bar{\tau}(3c_0^2 - \bar{\tau}^2)\right] & \bar{\tau} \in \Omega_m = [\bar{\tau}_2, 1]\,, \end{cases} \tag{26}$$

and

$$\bar{\alpha}(\bar{r}) = \begin{cases} 1 & \bar{r} \in \Omega_M = [0, \bar{r}_1] \ , \\ \dfrac{c_2}{\sqrt{\bar{r}}\left(3c_1 + 2\bar{r}^{\frac{3}{2}}\right)^2} & \bar{r} \in \Omega_i = [\bar{r}_1, \bar{r}_2] \ , \\ \beta & \bar{r} \in \Omega_m = [\bar{r}_2, 1] \ , \end{cases} \tag{27}$$

where the constant c_0 in $(26)_3$ is $c_0 = \sqrt{1 + f/\beta}$. Two relevant nondimensional quantities can be identified in this solution: the loading and moduli parameters f and β defined in (25) which can be used to characterize the different loading cases. The constants $c_m, c_M, c_1, c_2, \bar{r}_1$ and $\bar{r}_2$ are determined as follows: since $\bar{r}_1$ and $\bar{r}_2$ represent the location of the boundaries between Ω_M, Ω_i and Ω_i, Ω_m respectively, then, for an admissible solution, it is required that $\lambda_M(\bar{r}_1) = \lambda_m(\bar{r}_2) = 0$. These conditions can be satisfied by choosing c_M and c_m as follows:

$$c_M = (9 + 2\sqrt{15})\bar{r}_1^2 \ , \quad c_m = \frac{1}{4\bar{r}_2}\left(3c_0^4 - 18c_0^2\bar{r}_2^2 + 7\bar{r}_2^4\right) \ .$$

Furthermore, two additional relations can be obtained from the continuity of $\bar{u}$ at $\bar{r} = \bar{r}_1$ and $\bar{r} = \bar{r}_2$, i.e.,

$$c_1 = \frac{1}{3}\left(1 + \sqrt{15}\right)\bar{r}_1^{3/2} = \frac{1}{6\sqrt{\bar{r}_2}}\left(3c_0^2 - 7\bar{r}_2^2\right) \ .$$

There are other possible values for c_M and c_1 (c_m is unique), but these can be discarded a posteriori based on the requirements that the solution should not be singular and that the multipliers λ_m and λ_M should be positive in $[0, \bar{r}_1)$ and $(\bar{r}_2, 1]$ respectively. Finally, the value of c_2 and an additional relation between $\bar{r}_1$ and $\bar{r}_2$ can be obtained by enforcing the continuity of $\bar{\alpha}$ at $\bar{r} = \bar{r}_1$ and $\bar{r} = \bar{r}_2$ which gives

$$c_2 = 6(4 + \sqrt{15})\bar{r}_1^{7/2} = \beta\sqrt{\bar{r}_2}\left[(1 + \sqrt{15})\bar{r}_1^{3/2} - 2\bar{r}_2^{3/2}\right]^2 \ .$$

The values of $\bar{r}_1$ and $\bar{r}_2$ can be computed numerically from the above relations. As f increases, so do $\bar{r}_1$ and $\bar{r}_2$. For some values of f, $\bar{r}_2 \geq 1$, then the solution needs to be modified since $\Omega_m = \emptyset$ (i.e., the solution never reaches its lower bound β). In that case the solution depends on the loading parameter f

but not on β. The value of $\bar{r}_1$ can be obtained from the boundary condition $\alpha(l)u'(l) = \sigma_0$, which can be expressed as

$$4(4+\sqrt{15})\bar{r}_1^{\frac{7}{2}} = f(2+(1+\sqrt{15})\bar{r}_1^{\frac{3}{2}}) \ . \tag{28}$$

Finally, for f large enough, $\bar{r}_1 \geq 1$, hence the solution is trivial: $\bar{\alpha} \equiv 1$ and the boundary condition is satisfied with $c_M = 3(f+1)$. From (27) one can obtain the total resource, $R_t = a\int_0^l \alpha d\tau$, where a is the cross-sectional area. Since $\bar{\alpha}(\bar{r})$ is a monotonically decreasing function from 1 to β as $\bar{r}$ ranges from 0 to 1, then $0 < \beta < \bar{R}_t < 1$ where $\bar{R}_t = R_t/(\alpha_M a l)$. Therefore, one can always choose an upper bound $\bar{R} = R/(\alpha_M a l)$ on the resource such that $\bar{R}_t < \bar{R} < 1$, i.e., such that the resource constraint is not active but $\bar{R}_t \neq 0$. This confirms the assumption that there are non-trivial solutions with $\Lambda = 0$. Clearly, if the prescribed $\bar{R}$ is such that $\bar{R}_t > \bar{R}$, then (26)-(27) would not be an admissible solution since the resource constraint would be violated. However, an analytical expression for the solution when the resource constraint is active is not available.

Figure 1 represents the total resource $\bar{R}_t$ for different values of the moduli parameter β and loading parameter f. Observe that for values of f large enough, the solution does not depend on β anymore and all curves merge into a common envelope which can be thought of as the limit case $\beta \to 0$ for all values of f (see insert in Figure 1). If, for a given pair β, f, the prescribed upper bound on the resource constraint $\bar{R}$ is above the corresponding curve for $\bar{R}_t$, then the resource constraint is not active. The maximum principal stiffness $\bar{\alpha}(\bar{r})$ is shown in Figure 2 for different values of β and a common loading parameter $f = 0.1$. The solid curve represents the case for which the solution does not depend on β for the given f (i.e., from Figure 1, β is below some critical value β_*). In the first part of each curve, $\bar{\alpha}$ is at its upper bound then it decreases monotonically to its lower bound β (except for $\beta < \beta_*$). The corresponding minimum values of the objective functional are $\bar{W}_*(\beta = 0.3) = 5.11 \cdot 10^{-2}$, $\bar{W}_*(\beta = 0.2) = 4.07 \cdot 10^{-2}$ and $\bar{W}_* = 3.30 \cdot 10^{-2}$ for $\beta < \beta_*$. Although β is viewed as a fixed parameter, the optimal solution is reached for values of $\beta < \beta_*$. However, as mentioned before, β needs to be bounded away from zero in order to have a stable structure. Figure 3 corresponds to the displacement field as a function of $\bar{r}$ for different values of β. Observe that at $\bar{r} = 1$ the displacement of the solution that does not depend on β (solid line) is greater than for the other curves, however, the energy norm which measures structural stiffness is smaller. Similarly,

as shown in Figure 4, the stress distribution is also smaller for $\beta < \beta_*$, which corresponds to the stress-based notion of optimal structure. Figure 5 shows, for different values of β, the (negative) unconstrained gradient of the Lagrangian L as defined in (16) (i.e., $-(L' + \lambda_m - \lambda_M)/\gamma^2 = \dot{\bar{u}}^2 - 2\bar{r}\bar{u}$, where the dot represents differentiation with respect to $\bar{r}$). For each curve, the value of the function in the first interval $\Omega_M = [0, \bar{r}_1)$ (where the local upper bound is active ($\bar{\alpha} = 1$) and where $L' = \lambda_M = 0$) corresponds to $\lambda_M/\gamma^2 > 0$; in the second interval $\Omega_i = [\bar{r}_1, \bar{r}_2]$ (where no local bounds are active) to $L' = \lambda_M = \lambda_m = 0$ and in the third interval $\Omega_m = (\bar{r}_2, 1]$ (where the local lower bound is active ($\bar{\alpha} = \beta$) and where $L' = \lambda_m = 0$) to $-\lambda_m/\gamma^2 < 0$. Observe that for $\beta < \beta_*$ (solid curve), there is no third interval since $\Omega_m = \emptyset$.

To illustrate that this procedure can be used in a more general setting, a three-dimensional example was solved using a finite element program. Consider again the case of the optimal distribution of material properties in order to obtain maximum structural stiffness of a rotating prismatic structure of length l and square cross-sectional area h^2. The side attached to the axis of rotation is modeled as a clamped end. The remaining sides of the structure are subjected to the following loads:

Case 1: shearing load:

$$\hat{\mathrm{t}} = \begin{cases} \tau_0 \mathrm{e}_z & \text{for } r = l \quad \text{(Uniform shear stress)} \\ 0 & \text{otherwise} \end{cases}$$

Case 2: torsional load:

$$\hat{\mathrm{t}} = \begin{cases} -\tau_0 \mathrm{e}_z & \text{for } r = l\ ,\ x \in [-h, -h + \epsilon]\ , \\ \tau_0 \mathrm{e}_z & \text{for } r = l\ ,\ x \in [h - \epsilon, h]\ , \\ 0 & \text{otherwise} \end{cases}$$

where ϵ is a small number, the origin of coordinates is in the mid-section and x is measured in the e_θ direction. The numerical values used here, for illustration purposes, are as follows: $l = 1$ m, $h = 0.1$ m, $\alpha_M = 10^{10}$ Pa, $\alpha_m = 10^8$ Pa, $\kappa = 10^{-7}$ s$^2 \cdot$ m^{-2} and $\omega = 500$ RPM. In Case 1, $\tau_0 = 10^6$ Pa and in Case 2, $\tau_0 = 1.5 \cdot 10^6$ Pa, $\epsilon = 0.01$ m. In both cases the resource constraint is active with $R = 0.5lh^2\alpha_M = 0.5 \cdot 10^8$ Pa$\cdot$m^3. The maximum principal stiffness $\bar{\alpha} = \alpha/\alpha_M$ is shown for the loading Case 1 (shearing load) in Figures 6 (without a body force) and 7 (with a body force). Figure 8 represents contour plots of $\bar{\alpha}$ at the cross-section $\bar{r} = 0.75$ for the load Case

1; the section on the left corresponds to the case when the body force is absent and the right one when it is included. Observe that, in the latter cross-section, the top of the structure is in compression, thus $\bar{b} \cdot u < 0$, which results in a greater reinforcement than the bottom which is in tension (see end of Section 3). In contrast, when the body force is absent, the solution is symmetric with respect to the r, θ mid-plane, as shown in the left cross-section in Figure 8 (compare also Figures 6 and 7). The heuristic interpretation is as follows: first, observe that in this example the body force always creates tension at any point of the structure. Now, consider a point of the structure which is in compression *because of the applied shear load.* If the material is locally stiffer (hence, the local mass density is higher), then the body force that tends to oppose compression would be higher resulting in an overall smaller displacement. The opposite effect occurs at points which, because of the applied shear load, are in tension.

For the loading Case 2 (torsional load), Figure 9 shows the maximum principal stiffness when the body force is not present and Figure 10 when it is. In Figure 11, two cross-sections at $\bar{r} = 0.75$ are shown; the left one corresponds to the case without the body force and the right one when the body force is taken into account. The procedure reproduces the well-known optimal "circular" layout (within the limitations of the mesh and the effect of the boundary conditions at $r = 0$ and $r = l$). The center of the cross-section is at the lower bound (hence, it can interpreted as a "weak" region, i.e., as a "hole"). This illustrates the ability of the method to obtain the optimal *shape* as a by-product of the material optimization. The effect of the body force is reflected in the gradual decrease of reinforcement from $r = 0$ to $r = l$, as shown by the cross-sections in Figure 11 (compare also Figures 9 and 10).

5 Discussion and conclusions.

The method presented here identifies a positive-definite optimal material that maximizes the structural stiffness when a structure-dependent body force is taken into account. Two interesting aspects arise due to the presence of the body force: as opposed to problems with zero body force, the resource constraint might not be active yet it is possible to have a non-trivial solution where $\int_\Omega \varphi(\alpha) dv = R_* \neq 0$. This suggests that there is a "natural" upper limit R_* on the amount of reinforcement material that needs to be used (i.e., trying to specify from the onset a greater amount will not affect the optimal solution). Also, it is not necessarily true that the presence of the

body force will result in a local increase of the material properties in order to stiffen the structure. In fact, as shown by (21), this depends on whether the scalar product of the body force and the displacement is negative (local stiffening) or positive (local weakening). It is usually assumed that at points on the surface where the loads are applied, the optimal layout would consist of some type of reinforcing structure to support those loads. However, this is not the case if the structure itself turns out to increase substantially the work done by the body force. Clearly, as shown by the optimality conditions, there is a compromise between these two opposite effects and the outcome can be quantified based on a characteristic magnitude of the surface loads, the upper bound on material properties, a characteristic magnitude of the body force and whether the resource constraint is active or not. If the inertial forces are small compared to the applied loads (i.e., large loading parameter f) then, as expected, the procedure converges to a solution similar to the case without body force. However, if the inertial forces are large (small f), then the procedure might fail to develop a suitable structure to support the loads and large displacement gradients could occur at those points. Nevertheless, a layout which includes a supporting structure for the loads can always be obtained by selecting an appropriately large value for the lower bound α_m. Finally, it is worth noting that the numerical implementation of this method for three-dimensional problems can be achieved with relative ease by combining (existing) finite element programs and customized optimizing codes.

Acknowledgments.

The authors are pleased to acknowledge John Taylor, Jakub Pawlicki and Helder Rodrigues for many valuable discussions and recommendations. This work was supported in part by the Ford Motor Company (Ford Research) under project No. 95-106R and in part by the Defense Advanced Research Projects Agency (DARPA) through the AFOSR grant No. F49620-94-1-0472.

References

Bendsøe, M. P. (1995), *Optimization of Structural Topology, Shape and Material*, Springer.

Bendsøe, M. P., Guedes, J. M., Haber, R. B., Pedersen, P. and Taylor, J. E. (1994), 'An analytical model to predict optimal properties in the context of optimal structural design', *Journal of Applied Mechanics* 61, 930–937.

Cowin, S. C. (1994), 'Optimization of the strain energy density in linear anisotropic elasticity', *Journal of Elasticity* 34, 45–68.

Gibson, L. J. and Ashby, M. F. (1997), *Cellular solids: Structure and properties*, Cambridge University Press.

Jog, C. S., Haber, R. B. and Bendsøe, M. P. (1993), A displacement-based topology design method with self-adaptive layered materials, *in* M. P. Bendsøe and C. A. Mota Soares, eds, 'Topology Design of Structures', Vol. 227, NATO ASI series, Kluwer, pp. 219–238.

Knowles, J. K. (1995), 'On the representation of the elasticity tensor for isotropic materials', *Journal of Elasticity* .

Lipton, R. (1994), 'A saddle-point theorem with application to structural optimization', *Journal of Optimization Theory and Applications* 81(3), 549–568.

Milton, G. and Cherkaev, A. V. (1995), 'Which elasticity tensors are realizable?', *Journal of Engineering Materials and Technology* 117, 483–493.

Olhoff, N. (1987), Structural optimization by variational method, *in* C. A. Mota Soares, ed., 'Computer Aided Optimal Design: Structural and Mechanical Systems', Springer-Verlag, pp. 87–179.

Pedersen, P. (1989), 'On optimal orientation of orthotropic materials', *Structural Optimization* 1, 101–106.

Prager, W. (1974), *Introduction to Structural Optimization*, Springer-Verlag.

Sigmund, O. (1994), 'Materials with prescribed constitutive parameters: an inverse homogenization problem', *International Journal of Solids and Structures* 31(17), 2313–2329.

Taylor, J. E. (1997), An energy method for the optimal design of linear continuum structures. Publication pending.

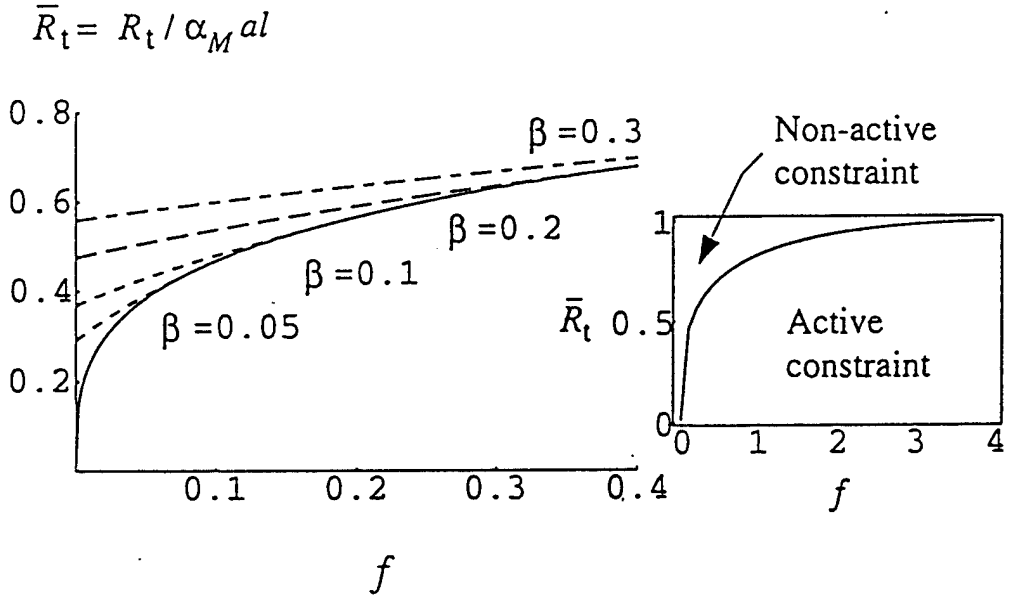

Figure 1: One-dimensional case: normalized total resource $\bar{R}_t = R_t/(\alpha_M al)$ for different values of the loading and moduli parameters f and β. The insert corresponds to the limit case $\beta \to 0$ and shows the full range $0 \leq \bar{R}_t \leq 1$. For prescribed values of f and β, the resource constraint is not active if the prescribed $\bar{R}$ is above the corresponding $\bar{R}_t$ and active otherwise.

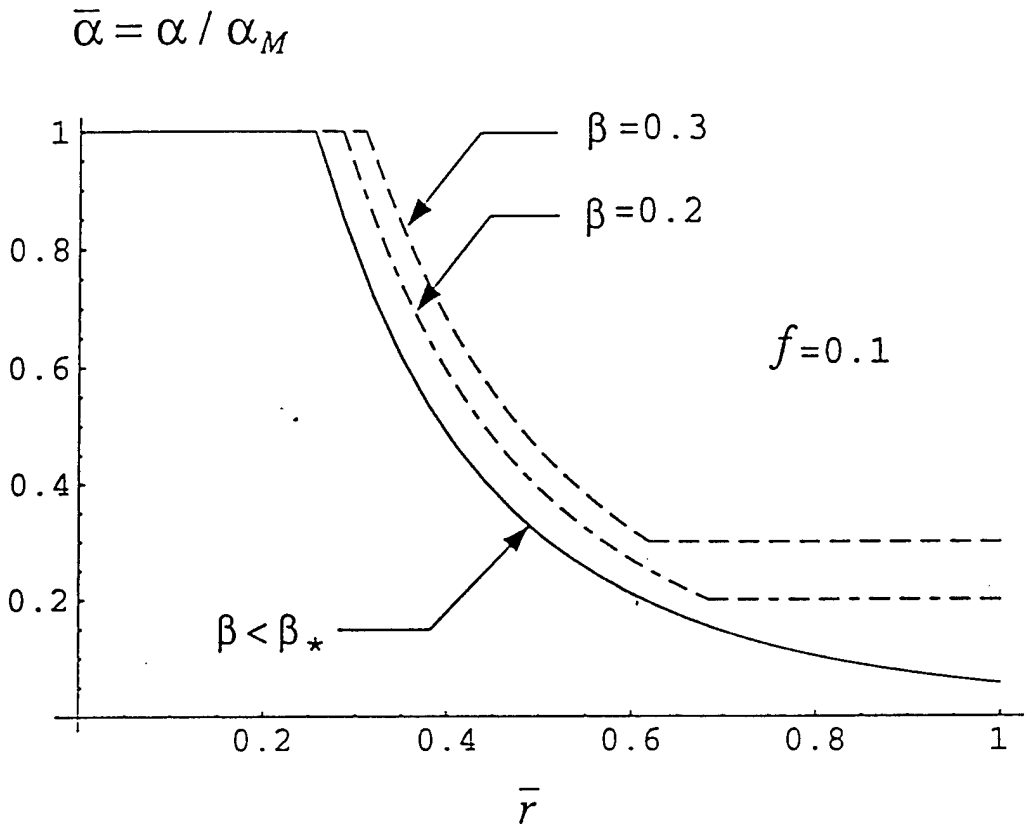

Figure 2: One-dimensional case: value of the maximum principal stiffness $\bar{\alpha}$ (reinforcement) in the radial direction for various values of the moduli parameter β and a common loading parameter $f = 0.1$. The solid curve represents the limit case for which the solution does not depend on β.

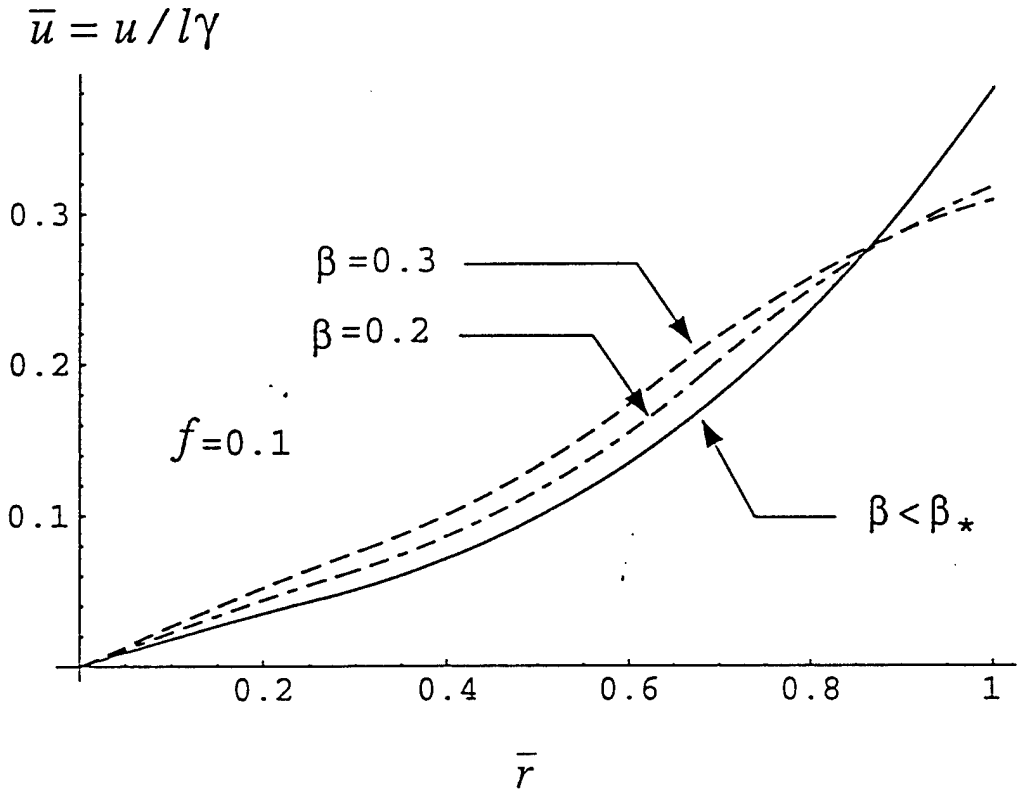

Figure 3: One-dimensional case: radial displacement $\bar{u}(\bar{r})$ for various values of the moduli parameter β and a common loading parameter $f = 0.1$. The solid curve represents the limit case for which the solution does not depend on β.

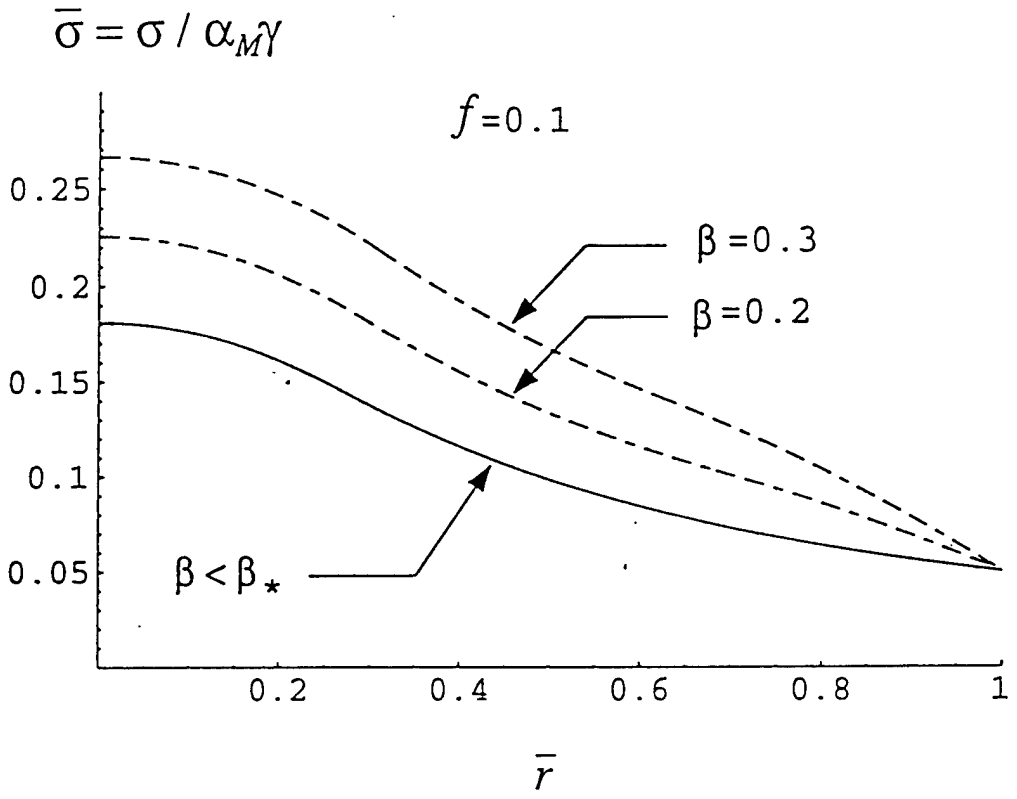

Figure 4: One-dimensional case: stress distribution as a function of radial position for various values of the moduli parameter β and a common loading parameter $f = 0.1$ (i.e., the boundary condition is $\bar{\sigma}(1) = f/2$).

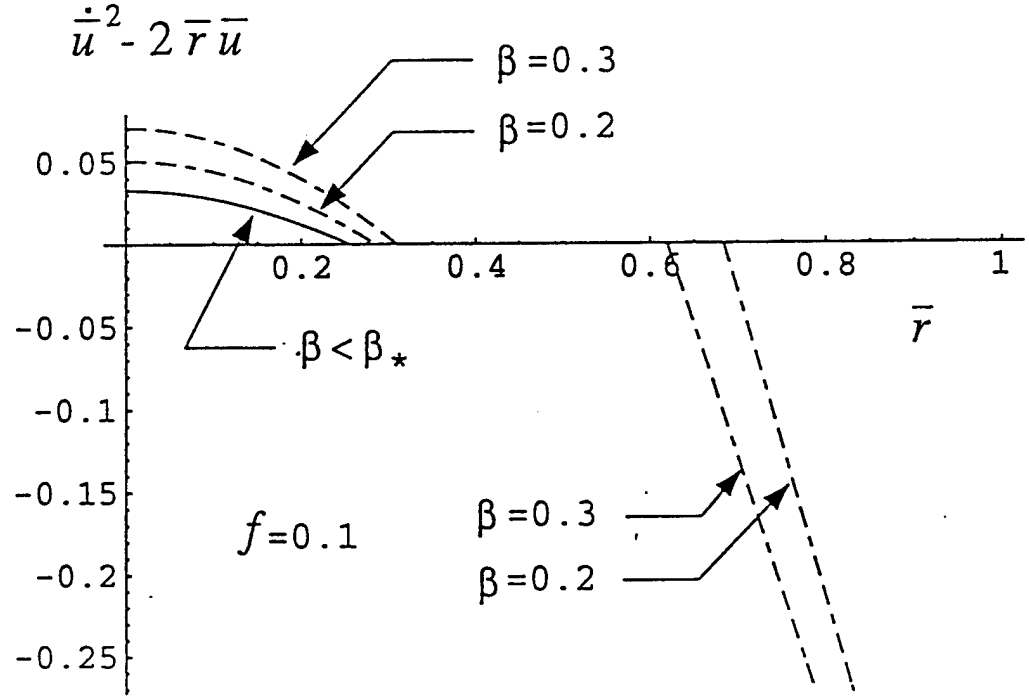

Figure 5: One-dimensional case: (negative) unconstrained gradient of the Lagrangian ($= \dot{\bar{u}}^2 - 2\bar{r}\bar{u}$) for various values of the moduli parameter β and a common loading parameter $f = 0.1$. The solid curve represents the limit case for which the solution does not depend on β. See text for detailed explanation.

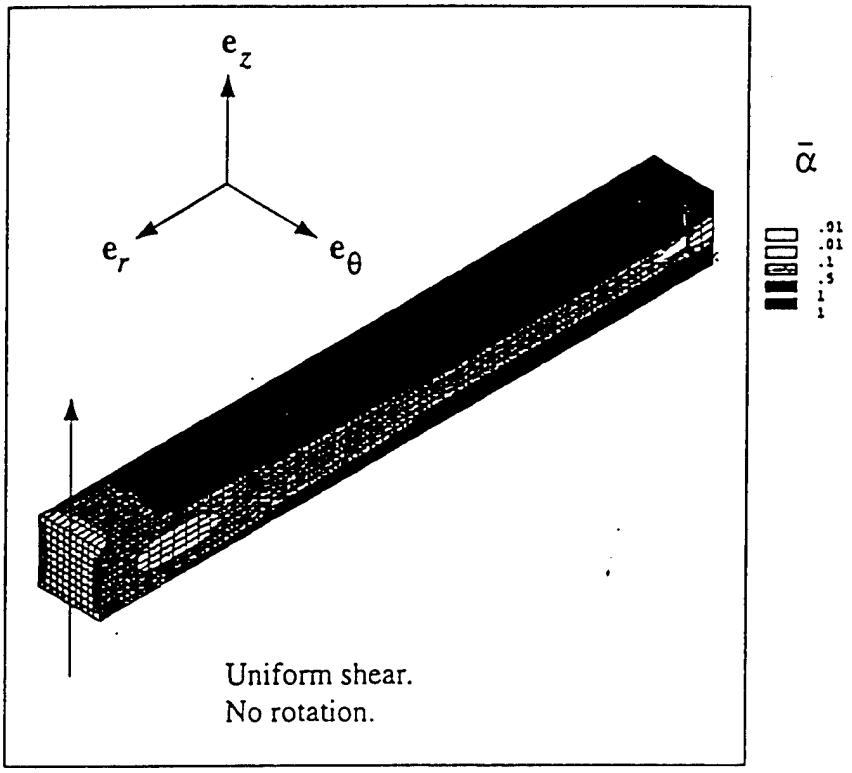

Figure 6: Loading Case 1 (shearing load): contour plot of the maximum principal stiffness (reinforcement) *without* a body force. Observe the symmetry of the solution with respect to the e_r, e_θ mid-plane.

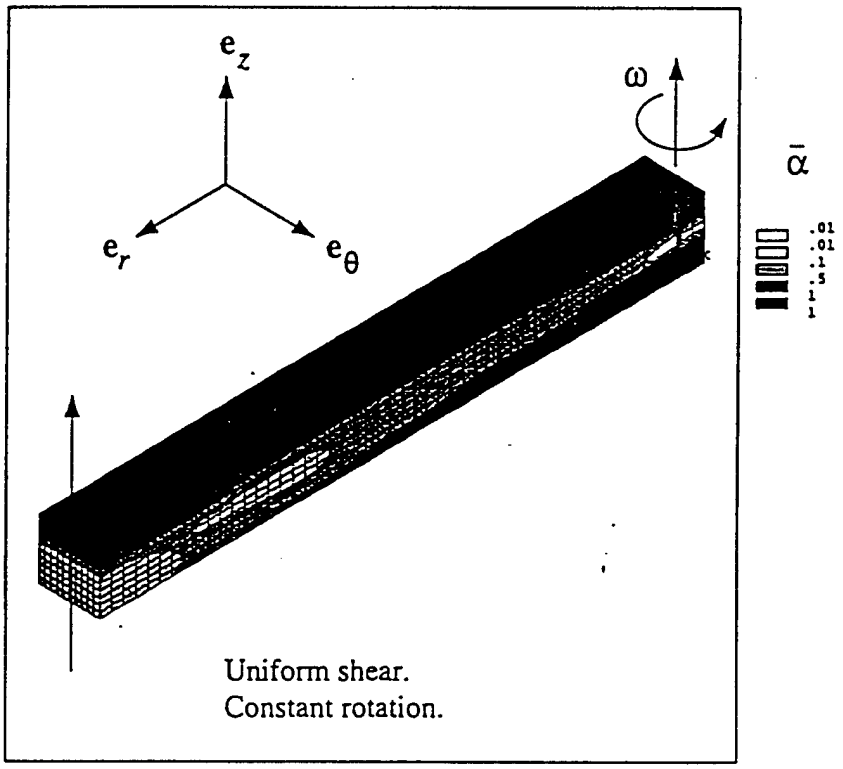

Figure 7: Loading Case 1 (shearing load): contour plot of the maximum principal stiffness (reinforcement) *with* a body force. The upper section has a greater reinforcement than the lower section.

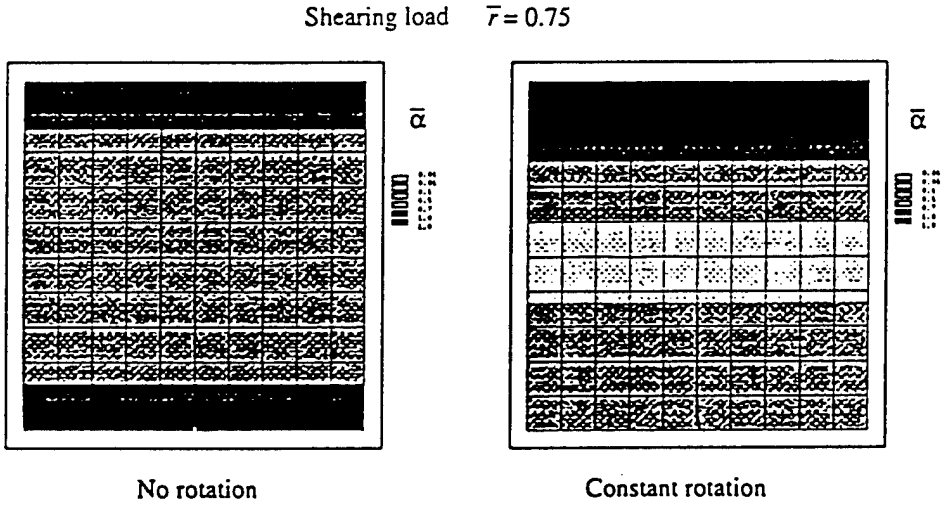

Figure 8: Loading Case 1 (shearing load): cross-sectional contour plot of the maximum principal stiffness (reinforcement) at $\bar{r} = 0.75$; the left plot corresponds to the case without a body force (symmetric solution) and the right one to the case with body force (greater reinforcement in upper section which is in compression, lesser reinforcement in lower section which is in tension).

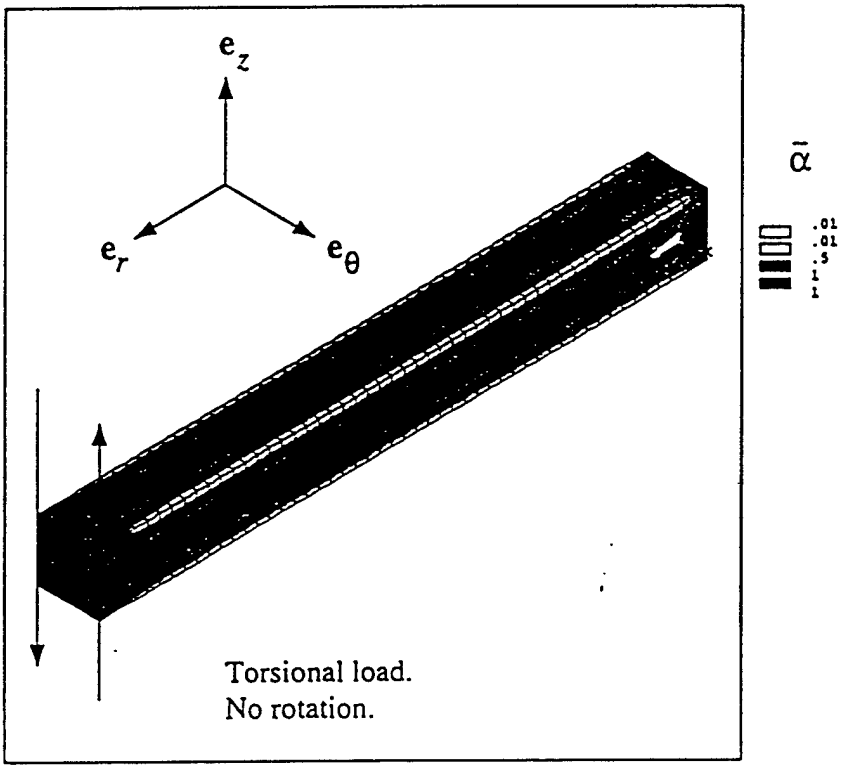

Figure 9: Loading Case 2 (torsional load): contour plot of the maximum principal stiffness (reinforced material) *without* a body force. Observe that the distribution of reinforcement is prismatic, except close to $\bar{r} = 0$ and $\bar{r} = 1$ due to the boundary conditions.

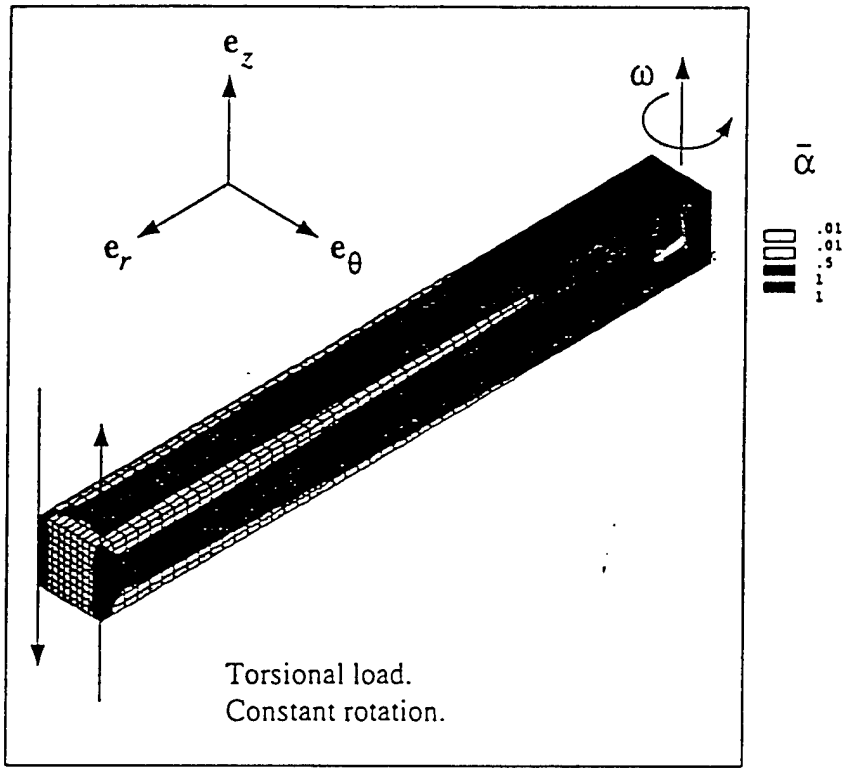

Figure 10: Loading Case 2 (torsional load): contour plot of the maximum principal stiffness (reinforced material) *with* a body force. Observe the gradual decrease in reinforcement from $\bar{r} = 0$ to $\bar{r} = 1$

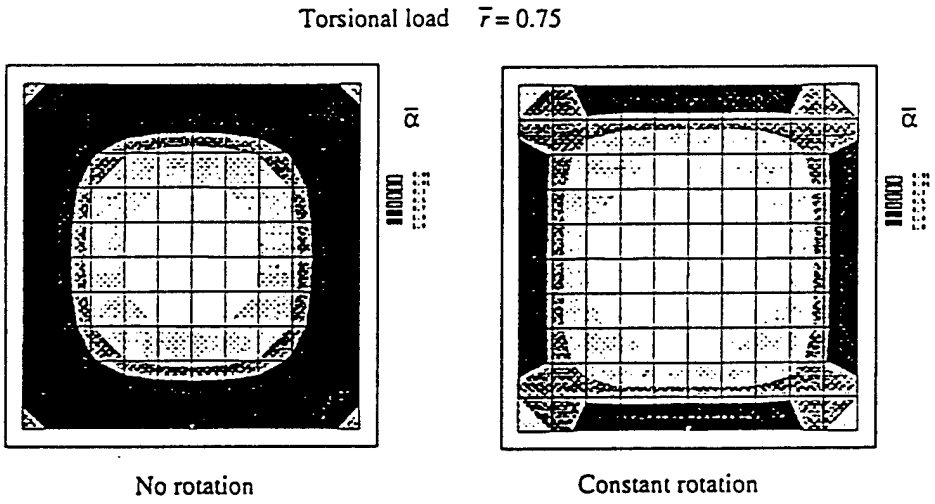

Figure 11: Loading Case 2 (torsional load): cross-sectional contour plot of the maximum principal stiffness (reinforcement) at $\bar{r} = 0.75$; the left plot corresponds to the case without a body force and the right one to the case with body force.

Prediction of Optimal Material Layout (Topology) and Properties for an Elastic Continuum Structure using Weighted Resource Constraint.

J. Pawlicki

Institute of Aeronautics and Applied Mechanics
Warsaw University of Technology
Warsaw, Poland

and

J. E. Taylor, S. Turteltaub, P. D. Washabaugh

Department of Aerospace Engineering
The University of Michigan
Ann Arbor, MI 48109, USA

Abstract

An effective procedure for the solution of the optimal layout and properties of an elastic material is presented. Design of 2D and 3D structures is considered for minimum compliance under a single load condition with a constraint on the amount of material and bounds on material properties. The method is based on an already established formulation for continuum design with the elasticity tensor being the design variable. The optimization with respect to local dependence of the tensor on orientation may be separated from the variation of material properties density (represented by an invariant of the tensor) over the field and solved analytically. A weighting function is introduced to measure the cost of the material properties density. An optimal layout composed of either zero or full material properties density (optimal topology) is predicted out of a sequence of solutions to material properties design sub-problems, each corresponding to a different

weighting function. As a first step, the optimal distribution of continuously varying material properties density is predicted for *uniform* weighting function. For each subsequent sub-problem, the weighting function is systematically adjusted and applied to the optimal material distribution obtained in the previous step. This sequence results in a segregation of the material properties density to either its lower or upper bound. The final design can be identified as topology design, where the lower bound value is small enough—on the order of 10^{-5} in the examples—compared to the value for the upper bound (full material). Thus, this technique consists in a gradual transition from the initial optimal *continuous* elastic structure to one having *sharply defined* topology by the use of a weighted total resource constraint. The method was successfully implemented using a commercial finite element analysis package to solve several example problems in 2D and 3D.

1. Introduction

This study centers on the development of a procedure for the prediction of the optimal material distribution and properties of two- and three-dimensional linear elastic continuum structures using finite element discretization. The goal is to find the least compliant design subject to a constraint on the total amount of available material. The material layout of the continuum structure design is described by a density field that assigns value to a pointwise measure of the material properties. Restricting the material properties density function to take one of two discrete values makes it possible to treat the topology optimization problem. The upper bound of the material density is identified as the fully concentrated measure of the structural material, while the lower bound represents extremely weak material—essentially a lack of structure. Thus the contour of the concentrated material properties density describes the topology of the optimized structure.

Most of the well-established characterizations for the topology design within structural optimization are based on the assumption that the material properties are

represented by a composite composed of two isotropic elastic components. Material layout and properties optimization as well as topology optimization problems have been treated using such formulations. It follows from the requirement of well-posedness and numerical tractability that models of this type have to be relaxed, since the optimal design is often composed of an infinitely fine composite microstructure. Choosing the procedure to represent *effective* elastic moduli of possible material microstructures is the usual way to achieve relaxation. In some schemes all possible arrangements are present (see e.g. Díaz & Lipton (1997)), while in others only a subclass of microstructures is allowed as a consequence of specific composite microgeometry parametrization. Regardless of possible microstructure restrictions, relaxation is usually achieved using a homogenization technique. More details on the procedures and models for topology design related to the two-material composite approach can be found in Bendsøe's treatise (1995) and in the proceedings Bendsøe and Mota Soares (1993).

In this paper we use the formulation of structural optimization where the design is represented by the unrestricted elastic properties tensor field. There is no restriction on the elasticity tensor except for those required to represent stable physical materials and to provide existence of elastostatics problem solutions. This formulation was originally presented in Bendsøe *et al.* (1994) for linear materials and subsequently extended for multiobjective optimization problems (Bendsøe *et al.* (1995)), nonlinear materials (Bendsøe *et al.* (1996)) and optimal design of a structure with design-dependent field force (Turteltaub and Washabaugh (1998)). It is noteworthy that optimization of the material tensor orientation forms the local problem and may be separated from the determination of the material properties density distribution over the structure. The local problem has an analytical solution (Bendsøe *et al.* (1994)). Thus the original problem is effectively reduced to one of finding the optimal field of an invariant of the elasticity tensor (the trace of the elasticity tensor is used here for this purpose). The resulting material density distribution is continuous in the design domain and non-uniform except for those regions where local bounds are reached. Note that subregions bounded by adjacent contours on a plot of results for the density, where each contour corresponds to a level of density, represent a form of design topology. This property is exploited for prediction of optimal structural topology in the form of a sharp (black/white) image

(Guedes and Taylor (1997)). There, the usual form for the total resource constraint is replaced by a generalized form, having a weighting function introduced to measure the local cost of material properties density (trace) of the elasticity tensor. (A generalized formulation of unit cost fields is described in Taylor and Washabaugh (1995) and (1997).) Applying stepwise adjustment of the weighting leads to a reduction in regions having intermediate density levels in redesign results for optimal material density. Only two values of material properties density remain in the refined topology final design. One, identified by black, corresponds to full measure of the material while the other (white) has the trace measure at the lower bound and symbolizes lack of material.

The free material tensor design problem is well posed and does not require relaxation as is needed in formulations based on two-material composite models. The simplicity of the material tensor approach in the optimal material properties field problem is preserved for the generalized formulation with weighted resource constraint as used for sharp image (black/white) design. Consequently the usual steps required in existing procedures for topology design, such as imposition of additional constraints on the design space, or penalization techniques for design variable, are avoided here.

In this paper we deal with the sharp image design using the characterization which closely follows that described by Guedes and Taylor (1997). A computational procedure based on the elastic free material tensor approach for prediction of optimal material layout (topology) was implemented using a commercial finite element analysis package and tested on 2D and 3D examples. Topology design results for several problems are presented in this paper. Several objectives represent the core of the present work: it is shown that the method for predicting optimal topology can be extended to a three-dimensional setting with virtually no modifications. Furthermore, the examples included in the present paper illustrate situations where the weighted resource constraint method can be effectively applied in order to satisfy geometrical requirements of a design (e.g., formation of holes in predetermined regions). Of practical relevance, it is also shown that the method can be easily implemented using available finite element programs.

2. Problem statement

The analytical model for the optimal design of linear structures with an isoperimetric (cost) constraint presented here closely follows the formulation given by Bendsøe, *et al.* (1994) and subsequently elaborated to predict optimal topology by Guedes and Taylor (1997). It differs however, from the original by means of how the specified unit cost field is defined. Here the unit cost is required to belong to the set of functions such that the product of a function and material properties density is normalized to the total material resource. With this restriction, the original total resource constraint is automatically satisfied whenever the constraint of total design cost is satisfied.

We consider a linear elastic continuum structure occupying a domain Ω, subjected to the single set of body forces $\tilde{f}$, boundary traction $\tilde{t}$ (on part of the boundary $\partial\Omega_t$) and zero displacement on $\partial\Omega_u$. The design variables are the local elastic properties, which are described by the material modulus tensor E. An invariant measure (the trace ρ of the modulus tensor, i.e., $\rho = E_{ijij}$) is subject to local and global constraints (see (1c,d) below). We seek to predict the structure (in terms of its material properties distribution) that satisfies equilibrium and minimizes the total work of external forces at this state (i.e., minimum compliance design). This problem can be expressed as

[P1]
$$\min_{E}\left\{ l(u) \equiv \int_{\Omega} \tilde{f}_i u_i \mathrm{d}\Omega + \int_{\partial\Omega_t} \tilde{t}_i u_i \mathrm{d}S \right\} \tag{1}$$

subject to:

$$\int_{\Omega} \varepsilon_{ij}(u) E_{ijkl} \varepsilon_{kl}(v) \mathrm{d}\Omega = l(v) \qquad \forall\, v \in U\,, \tag{1a}$$

$$E \geq 0\,, \tag{1b}$$

$$\int_{\Omega} w\rho \mathrm{d}\Omega - R \leq 0\,, \tag{1c}$$

$$\underline{\rho} \leq \rho \leq \overline{\rho}\,. \tag{1d}$$

Here u, v represent displacement fields belonging to a set U of kinematically admissible fields, E or E_{ijkl} symbolizes the fourth-order symmetric positive semi-definite elasticity

tensor field and $\varepsilon_{ij}(u) = \frac{1}{2}(u_{i,j} + u_{j,i})$ stands for the strain tensor (associated with either u or v). In the third and fourth constraints (1c,d), $w = w(x) > 0$ is a given function—referred to as the *weight function*—whereas $\underline{\rho}$ and $\overline{\rho}$ are specified local bounds on the trace ρ. The global cost of the design is limited by a specified value R.

Optimal material properties.

The equilibrium state described by equation (1a) in weak form can be expressed alternatively as the minimum of the potential energy with respect to admissible displacement fields u. Furthermore, minimization of the total work of external forces stated in (1) might be exchanged by maximization of the potential energy because the total work of external forces at equilibrium equals the negative of twice the potential energy. Thus the original problem [P1] can be reformulated as

$$\max_{E} \min_{u \in U} \Pi(E,u) \tag{2}$$

subject to

$$E \geq 0, \tag{2a}$$

$$\int_{\Omega} w\rho \mathrm{d}\Omega - R \leq 0, \tag{2b}$$

$$\underline{\rho} \leq \rho \leq \overline{\rho}, \tag{2c}$$

where the potential energy is given by

$$\Pi(E,u) = \tfrac{1}{2}\int_{\Omega} \varepsilon_{ij}(u)\, E_{ijkl}\, \varepsilon_{kl}(u)\, \mathrm{d}\Omega \; - l(u). \tag{3}$$

(See also Bendsøe *et al.* (1994).) The maximization with respect to the design variable (i.e., the elasticity tensor E) can be separated into two sets of parameters: one that corresponds to the local material properties orientation and another which refers to the variation over the field. The latter, representing the cost of the material, is taken to be the first invariant ρ of the elasticity tensor as in the global cost constraint (2b).

After this separation of the design maximization into two parts, our problem takes the form

$$\max_{\rho} \quad \max_{E} \quad \min_{u \in U} \quad \Pi(\rho, E, u). \tag{4}$$

$$\text{subject to: } \underline{\rho} \le \rho \le \overline{\rho} \qquad \text{subject to: } E \ge 0$$

$$\int_{\Omega} w\rho \, d\Omega - R \le 0 \qquad E_{ijij} = \rho$$

Interchanging the inner max and min problems (which is valid since it is a saddle point as proved in Bendsøe *et al.* (1994)) makes it possible to recognize the optimal local material properties in the form

$$E_{ijkl} = \rho \frac{\varepsilon_{ij}\varepsilon_{kl}}{\varepsilon_{mn}\varepsilon_{mn}} . \tag{5}$$

This corresponds to an orthotropic material having axes of orthotropy co-aligned with the principal strain directions. According to (5), the strain energy stored in the optimized material is given by

$$U = \tfrac{1}{2} E_{ijkl}\varepsilon_{ij}\varepsilon_{kl} = \tfrac{1}{2}\rho\varepsilon_{ij}\varepsilon_{ij} . \tag{6}$$

Thus the optimal material has the same *effective* energy of an isotropic linear elastic material with zero Poisson ratio and Young modulus equal to ρ. This feature is a consequence of the specific orthotropy orientation (i.e., it is related to the coupling between the elastic properties and the strain field at equilibrium). However, the cost measured by the trace of the elastic moduli tensor of the optimal material is six times lower than for the isotropic one (i.e., the trace of $\rho(\delta_{ik}\delta_{jl} + \delta_{il}\delta_{jk})$ is 6ρ)

The analytical result for the local optimal material properties (5), (6) can be incorporated into the problem statement (4). The number of design variables is then reduced to only one, which is the distribution of the trace of the elasticity tensor ρ. Thus the problem statement may be expressed as

[P2] $$\max_{\rho} \min_{u \in U} \left\{ \frac{1}{2} \int_{\Omega} \rho \varepsilon_{ij} \varepsilon_{ij} \mathrm{d}\Omega - \int_{\Omega} \tilde{f}_i \, u_i \mathrm{d}\Omega - \int_{\partial\Omega_t} \tilde{t}_i \, u_i \mathrm{d}S \right\} \tag{7}$$

subject to:

$$\rho - \overline{\rho} \leq 0, \tag{7a}$$

$$\underline{\rho} - \rho \leq 0, \tag{7b}$$

$$\int_{\Omega} w\rho \mathrm{d}\Omega - R \leq 0. \tag{7c}$$

According to (7), the original problem for the prediction of the optimal material properties field consists of obtaining the optimal distribution of the trace of the elasticity tensor and the corresponding strain field. Applying the analytical solution (5) of the local problem gives the pointwise optimal orientation of the elasticity tensor. We note again that the original problem (see Bendsøe *et al.* (1994)) can be obtained from the present formulation simply by setting $w(x) \equiv 1$.

Optimality conditions.

The Lagrangian corresponding to the constrained design problem (P2) is given by

$$\begin{aligned} L = \frac{1}{2} \int_{\Omega} \rho \varepsilon_{ij} \varepsilon_{ij} \mathrm{d}\Omega - l(u) - \int_{\Omega} \overline{\lambda} (\rho - \overline{\rho}) \mathrm{d}\Omega - \int_{\Omega} \underline{\lambda} (\underline{\rho} - \rho) \mathrm{d}\Omega \\ - \Lambda \left(\int_{\Omega} w\rho \mathrm{d}\Omega - R \right) \end{aligned} \tag{8}$$

and the optimality condition for the distribution of elastic material properties ρ may be stated as

$$\frac{1}{2} \varepsilon_{ij} \varepsilon_{ij} - \overline{\lambda} + \underline{\lambda} - \Lambda w = 0. \tag{9}$$

The solution also satisfies

$$\bar{\lambda} \geq 0 \qquad \bar{\lambda}(\rho - \bar{\rho}) = 0, \tag{10}$$
$$\underline{\lambda} \geq 0 \qquad \underline{\lambda}(\underline{\rho} - \rho) = 0.$$

The resource constraint is satisfied as an equality (see Bendsøe *et al.* (1994)) and the corresponding multiplier is positive, i.e.,

$$\Lambda > 0 \quad \text{and} \quad \int_{\Omega} w\rho \mathrm{d}\Omega - R = 0. \tag{11}$$

Weighting function.

Henceforth, we consider a specific stepwise constant weighting function, defined as follows:

$$w(x) = (\bar{w} - \underline{w})\, I(\rho(x), \rho_{th}) + \underline{w} \tag{12}$$

where $I(\rho(x), \rho_{th})$ is the unit Heaviside function, i.e.,

$$I(\rho(x), \rho_{th}) = \begin{cases} 0 & \text{for} \quad \rho(x) \leq \rho_{th} \\ \\ 1 & \text{for} \quad \rho(x) > \rho_{th} \end{cases} \tag{13}$$

and ρ_{th} is a designated *cutoff* value between $\underline{\rho}$ and $\bar{\rho}$. From (9) and (10), the optimality condition in the subdomain where $\underline{\rho} < \rho(x) < \bar{\rho}$ becomes

$$\tfrac{1}{2}\varepsilon_{ij}\varepsilon_{ij} = \Lambda w \quad \forall x \in \Omega \ \text{ s.t. } \rho(x) \in (\underline{\rho}, \bar{\rho}) \ , \tag{14}$$

hence $\frac{1}{2\underline{w}}\varepsilon_{ij}\varepsilon_{ij} = \Lambda$ for $\underline{\rho} < \rho < \rho_{th}$ and $\frac{1}{2\overline{w}}\varepsilon_{ij}\varepsilon_{ij} = \Lambda$ for $\rho_{th} < \rho < \overline{\rho}$. This condition states that the weighted unit strain energy for the optimal material configuration should be uniform in the design domain Ω except possibly for intervals or points in Ω where ρ equals $\underline{\rho}$ or $\overline{\rho}$. The strain energy is to be taken at the equilibrium state (inner max in P2). A jump of the unit strain energy $\frac{1}{2}\varepsilon_{ij}\varepsilon_{ij}$ occurs at the boundary between low and high weighted regions as the consequence of the discontinuous specific weighting function (12).

3. Computational procedure

The optimal material properties design problem (P2) was implemented and solved for 2D and 3D examples using a finite element approximation for a discrete representation of the continuum. The optimal material properties are given by the strain field at equilibrium (5), but in practice it is simpler to use an energetically equivalent isotropic material (see equivalent form of strain energies (6)). Standard procedures supported by a FEM analysis package were used to obtain the displacement field at equilibrium (internal min in (P2)). To solve the external max problem, an optimality criterion method, based on conditions (6)-(9), was applied. In order to predict the optimal *topology* of the structure, a stepwise procedure was developed. This procedure consists on solving a sequence of optimization problems (P2) for a given weighting function, which is updated at the end of each solution. The procedure is summarized as follows.

As a first step—to initialize the topology prediction—the optimal distribution of elastic material properties ρ_0 is computed for a *uniform* weighting function (i.e., with $w_0(x) \equiv 1$). Then, a cutoff value of material properties close to $\underline{\rho}$ is selected (i.e., $\rho_{th}^0 = \underline{\rho} + \Delta\rho_{th}^0$, where $\Delta\rho_{th}^0$ is a small positive increment). A new weighting function $w_1(x) = w_1(\rho_0(x))$ is obtained from (12) and (13) based on the optimal solution ρ_0 and the cutoff value ρ_{th}^0. Next, the optimization problem for this new weighting function w_1 is solved, resulting in a new optimal distribution of material properties ρ_1. The

distribution ρ_1 is characterized by a "shift" in ρ: the values of ρ_1 are *lower* in regions where initially $\rho_0 < \rho_{th}^0$ and *higher* where $\rho_0 > \rho_{th}^0$. In subsequent steps the cutoff value is increased, a new weight function is assigned, and the optimal design problem is solved again. This scheme is repeated until only the lower and upper bound values on material properties density remain in the final design. (The computational procedure terminates when the number of elements with ρ laying in-between bounds is lower than a user-specified number.) In other words, the solution procedure results in a gradual transformation of the initial optimal continuous structure to a discrete one, the latter obtained via a sequence of optimization subproblems. The solution of each subproblem becomes the initial design for the next optimization problem. The entire computational procedure is described in the form of a flow diagram (Fig. 1). In the diagram, the index n refers to the iterative procedure to find an optimal distribution of material properties for a given weight function (i.e., problem (P2)). The index i refers to an internal loop to satisfy the global resource constraint (7c). The optimality criterion method used to solve problem (P2) involves a local step size parameter for design variable change, denoted by α (a value between 0 and 1). The convergence tolerance for the objective function (compliance $l(u)$) is a given value δ, whereas the tolerance for the resource constraint is β. Finally, the index l refers to the sequence of optimization problems (P2). After each optimization problem l (for a fixed weighting function), the new cutoff value is obtained as $\rho_{th}^l = \rho_{th}^{l-1} + \Delta\rho_{th}^l$, where $\Delta\rho_{th}^l$ is the cutoff value increment.

Two parameters strongly affect the procedure and its result: the relative weight ratio $w_R = \overline{w} / \underline{w}$ and the cutoff value increment $\Delta\rho_{th}$. The first of them determines the dispersion of material properties ρ in a single step, while the other controls how fast the weighting function changes from step l to step $l+1$. Numerical experiments showed that usually for a given problem there exists a minimum value of the relative weight ratio $\tilde{w}_R$ that is satisfactory to obtain a discrete black and white design for an appropriate cutoff value increment. For weight ratios *lower* than $\tilde{w}_R$, a significant number of elements where ρ lies *between* the bounds may be present in the final design, regardless of $\Delta\rho_{th}$ (i.e., $\tilde{w}_R$ needs to be sufficiently large in order to reach a black/white design). On the

other hand, there is no unique criterion for the selection of the cutoff value increment $\Delta\rho_{th}$. The sensitivity of the design with respect to $\Delta\rho_{th}$ depends strongly on the cutoff value ρ_{th} at which this increment is applied. Therefore, the rate of adjustment of the weighting function is one of the keypoints of the algorithm since it affects the quality of the final design and the computational time. The method adopted here is as follows: let $V_S(\rho_{th}^l)$ be the volume of subdomain for which the trace ρ_l at step l is below the l-th cutoff value, i.e.,

$$V_S(\rho_{th}^l) = \int_{\Omega_{\rho_{th}^l}} dV \qquad \Omega_{\rho_{th}^l} = \left\{x : \rho_l(x) < \rho_{th}^l\right\} . \tag{15}$$

Recall that, from (12) and (13), $\Omega_{\rho_{th}^l}$ essentially correponds to the region where the weighting function is equal to its lower value $\underline{w}$. To adjust the cutoff value for the next optimization subproblem (step $l+1$), the basic idea is assume a value for $\Delta\rho_{th}^l$ and check that the volume $V_S(\rho_{th}^l + \Delta\rho_{th}^l)$ is bounded above and below as follows:

$$\underline{\xi} < \frac{V_S(\rho_{th}^l + \Delta\rho_{th}^l) - V_S(\rho_{th}^l)}{V_S(\overline{\rho}) - V_S(\rho_{th}^l)} < \overline{\xi} \tag{16}$$

where $\underline{\xi} < \overline{\xi}$, $\underline{\xi}, \overline{\xi} \in (0,1)$, are user-defined bounds. The cutoff value increment is calculated iteratively in order to satisfy (16). In (16), $V_S(\overline{\rho})$ refers to the volume of the domain occupied by the material that is not at the upper bound $\overline{\rho}$. The advantage of this volume criterion (to adjust the cutoff value) is that it is based on an a priori known quantity directly related to the topology of the final design.

4. Examples

A finite element discretization was used for the numerical solution of 2D and 3D problems of optimal material properties layout with a given weighting function. The finite element analysis package ANSYS was incorporated in the computational procedure described in the previous section. Standard linear, 4-node quadratic elements for plane

problems and 8-node brick elements for a three-dimensional example were applied. The material properties may vary from element to element, but they are assumed to be constant inside each element.

Example 1

The objective in the first example is to design the stiffest plane structure. The structure is restricted to a rectangular domain of medium aspect ratio (3x5) (see Fig. 2). A state of plane stress is assumed. Boundary conditions are specified at the left edge by zero vertical and horizontal displacements. On the opposite side, a concentrated load acts in the middle of the edge. The displacement field is approximated by a quadrilateral 4-node element and a 100x60 uniform mesh. The material properties are constant within each element. The upper bound of the trace of the elasticity tensor is assumed to be 10^5 times higher than the lower bound (i.e., $w_R = 10^5$). The volume fraction of the full material at the final design is specified to be 40%. Thus the total resource of material properties is

$$R = 0.4\overline{\rho}\int_{\Omega} dV .$$

Figure 1a shows the contour plot of the trace of the elasticity tensor ρ for the initial optimization problem with a uniform weighting function (i.e., $w(x) \equiv 1$). The black contours correspond to full material properties (i.e., $\rho = \overline{\rho}$). The lighter shades of gray indicate lower values of the elastic properties trace. Compared to the initial uniform material distribution, the total compliance was decreased by 1/3 in 31 iterations after which convergence of 10^{-6} was reached (10^{-3} after 5 iterations). Figures 1b and 1c show the evolution of the continuous design towards black and white for slow ($\overline{\xi} = 0.02$) and rapid ($\overline{\xi} = 0.05$) cutoff value adjustments. In the first case, the finer structure features a 22% increase in the objective function (compliance) relative to the optimal continuously varying material distribution design. (It is worth recalling that the black/white solution is sub-optimal compared to an optimal structure with continuously varying properties.) The second one is 28% less stiff than the continuous design. We note that despite using linear 4-nodes elements, no checkerboard pattern has occurred. However, for extremely low cutoff value adjustment, this feature was observed.

Example 2

The problem of a circular plate with a central hole compressed along a diagonal is now considered. The ratio of the external to the internal radius equals to 2. The load is distributed according to a sinusoidal function on 1/10 of the external edge. A state of plane stress is assumed. The structure and the loading have two axes of symmetry; hence the design domain can be restricted to one quarter of the original domain (see Fig. 3). Again, the 4-node elements were used to discretize ¼ of the structure. The mesh consisted of 5000 elements. As before, the same local bounds on the trace of the elasticity tensor were applied. To show the influence of the total resource available on the final result, four values corresponding to 20%, 30%, 40% and 50% of the volume fraction were applied (keeping the local constraints unchanged). Results are shown on Fig. 3. The values of the objective function for the optimal designs with a uniform cost function (i.e., $w(x) \equiv 1$) and increasing amount of available material (4 volume fractions stated above) are, in each case, 0.55, 0.58, 0.62 and 0.66 of the initial values corresponding to a uniform material distribution (i.e., ρ = constant). The compliance for black/white designs decreases respectively to 0.67, 0.70, 0.71 and 0.70 of the initial values for uniform material distribution.

The interesting feature observed here is that the light truss structure obtained for the least available material case (20% of volume fraction) evolves to a solid design for increasing total resource of material.

Example 3

This example is based on Lamé's problem in plane stress. The same design domain, as in example 2, is given. The load acting on the external edge is a uniform pressure. Thus the problem is axisymmetric for continuous distribution of material properties (i.e., it is essentially a 1D problem since it has radial symmetry). However, due to the specific choice of a weight function in this example, we expected a non-axisymmetric solution for the discrete design. Therefore, a quarter of the design domain was chosen for this analysis. The structure was discretized using quadrilateral 4-node elements. The total resource constraint was specified to satisfy 40% of the volume fraction. The solution for

the uniform weight function (i.e., $w(x) \equiv 1$) features a relatively uniform material properties distribution (see Fig. 4). The elements on the inner edge, having full material properties, form a strong reinforcing ring. However, the lower bound of the elasticity tensor trace is not reached anywhere in the design domain.

For the topology design problem, the procedure was very unstable for different choices of the design parameters. In this case, the uniform material properties distribution was apparently the reason that it failed to predict a discrete topology. One of the pathologies experienced was an axisymmetric checkerboard pattern. To avoid difficulties caused by the uniform material distribution, an initial user-defined weighting function was designated. This function, as shown in Fig. 4b, has three sectors where $w = \underline{w}$ (and $w = \overline{w}$ elsewhere). The final topology design was obtained using the same procedure as in the previous examples. Even though this topology depends on the initial choice of w, the introduction of arbitrary weighting functions in the design procedure may be used in practice to set preferences of the final topology. As shown in this example, if holes are required in each of the three sectors shown in Fig. 4b, this can be achieved simply by specifying a suitable weighting function.

Example 4

This example consists of a 3D-cantilever beam with a transverse force, similar to the 2D beam shown in example 1. The structure is required to support a concentrated load at the middle of the face opposite to the clamped face (see Fig. 5). The design domain has the shape of a 3x3x5 brick and the material is required to occupy at most 40% of its volume. The optimal topology is shown in Fig. 5 (the final design is shown in gray to see the mesh, however all visible elements are at the upper bound of the trace of the elasticity tensor).

Unlike its 2D analog, the resulting structure consists of two parallel "walls" separated by a long hole inside the beam. The objective function is 35.8% lower than the one given by a structure of uniformly distributed material properties. By comparison, the optimal structure with continuously varying material properties and same volume fraction provides a 38.5% reduction.

The same problem was subsequently solved for volume fractions of 20% and 10%. The resulting structure for a volume fraction of 20% is topologically similar to the one described above (see Fig. 6) and gives a 40% reduction in the objective function (compared to a 47% reduction for the structure of continuously distributed properties). For 10%, however, the supporting walls were broken and a structure close to the coarse 2D design was obtained (Fig. 7). The objective function in this case is much lower for the continuous structure (48.5%) than for the black/white structure (35%).

To test the capacity of a "common" small computer system to solve a relatively large scale problem, the 3D example was solved using 20-node brick elements (instead of 8-node bricks) which resulted in 50 000 degrees of freedom for the FE model. The solution took approximately 20 hours on a Pentium 150 PC machine. The results were topologically similar to those discussed before and the difference in objective function was less than 2%.

It has been observed that the computational procedure shows a small tendency to develop an unstable checkerboard pattern. However, checkerboarding occurs only for extremely low cutoff value adjustments. This feature was specifically visible when the discretization involved *linear* finite elements with constant material properties and can be eliminated by a more accurate approximation of the displacement field and the material properties distribution (Jog *et al.* (1993)).

5. Conclusions.

A method based on the arbitrary (free) elastic tensor formulation for the minimum compliance problem is used here to predict the optimal material layout and properties in the sense of structural topology design. The transformation of the continuously varying optimal material properties field to a discrete layout design is achieved by solving a series of optimization problems with weighted total resource (cost) constraint. Following this approach, the computational procedure was developed and implemented in the finite element analysis package ANSYS. The results of calculations performed on several two and three-dimensional examples showed that the present method is capable to solve

medium and large problems, being relatively more efficient than familiar schemes for topology design—based on the two-material composite model.

According to the formulation used here, the material from which the resulting structure is made has optimized pointwise properties. Thus, the measure of the objective function corresponds to a lower bound of the compliance of the design, relative to all linearly elastic material properties orientations, *including any possible configuration of a composite material.* In this respect, the free elastic tensor formulation produces a more general result than familiar methods founded on the two-material composite. On the other, hand we note that the same general formulation may be modified to provide modeling of materials with manufacturable microstructure by introducing additional constraints on the constitutive tensor. The form of such constraints should be appropriate to reflect restrictions on local geometry.

The external problem of optimal material distribution (P2) for given weighting function is solved by an iterative algorithm based on the optimality criterion (16), taking the first invariant of the elasticity tensor as the measure of material properties density. However, since the resulting design depends on the choice of this measure, the more general problem is of practical interest. A recently developed formulation (Taylor (1998)), where both objective and cost are expressed in the same basis, would be convenient for this purpose.

Acknowledgement

The authors are grateful for the support provided by the Ford Motor Company (SRL) under grant # 95-106R.

References

Bendsøe, M. P. (1995), "*Optimization of Structural Topology, Shape and Material*", Springer-Verlag, Berlin-Heilderberg.

Bendsøe, M. P., Mota Soares C. A., (Eds.) (1993), "*Topology Design of Structures*", Kluwer Academic Press, Dordrecht, The Netherlands.

Bendsøe, M. P., Guedes, J. M., Haber, R. B., Petersen, P., Taylor, J. E. (1994), "An Analytical Model to Predict Optimal Material Properties in the Context of Optimal Structural Design", *J. App. Mech.*, **61** (4) pp 930-937.

Bendsøe, M. P., Díaz, A., Lipton, R., Taylor, J. E. (1995), "Optimal Design of Material Properties and Material Distribution for Multiple Loading Conditions", *Int. J. Num. Meth. Eng.*, **38** pp 1149-1170.

Bendsøe, M. P., Guedes, J. M., Plaxton, S., Taylor J. E. (1996) "Optimization of Structure and Material Properties for Solids Composed of Softening Material", *Int. J. Sol. Struct.*, **33** (12) pp 1799-1813.

Guedes, J. M., Taylor, J. E. (1997), "On the Prediction of Material Properties and Topology for Optimal Continuum Structures", *Struct. Opt.* **14** (2-3) pp 193-199.

Díaz, A., Lipton, R. (1997), "Optimal Material Layout for 3D Elastic Structures", *Struct. Opt.*, **13** pp. 60-64.

Jog, C., Haber, R., Bendsøe, M. P. (1993), "A Displacement-Based Topology Design Method with Self Adaptive Layered Materials", In: cit. Bendsøe, M. P., Mota Soares C. A., (Eds.), pp. 219-238

Taylor, J. E., Washabaugh, P. D. (1995), "A Generalized Expression of Cost for Prediction of the Optimal Material Properties Tensor", In: Monteiro Marques, M. D. P., Rodrigues, J. F. (Eds.), "*Trends in Application of Mathematics and Mechanics*", Longman, Essex, England.

Taylor, J. E., Washabaugh, P. D. (1997), "On Structural Optimization Formulations with Generalized Cost Constraints", In: Godoy, L., Rysz, M., Suarez, L. (Eds.), Proceedings of the PACAM V, San Juan, Puerto Rico

Taylor, J. E. (1998), "An Energy Model for the Optimal Design of Linear Continuum Structures", To appear in: *Struct. Opt.*

Turteltaub, S., Washabaugh, P. D. (1998), "Optimal distribution of material properties for an elastic continuum with structure-dependent body force", To appear in: *Int. J. Sol. Struct.*

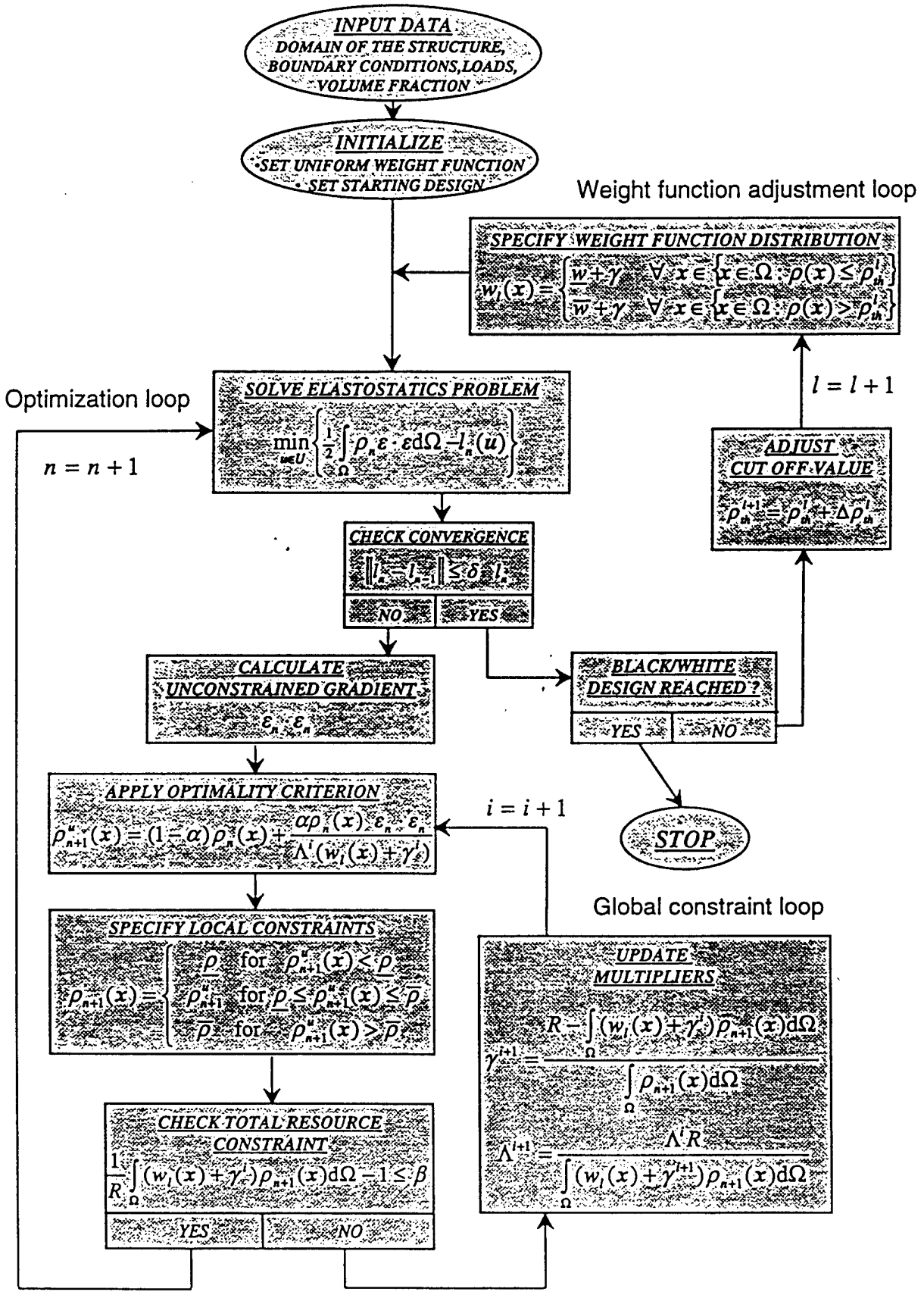

Fig.1. Flow diagram of the computational procedure

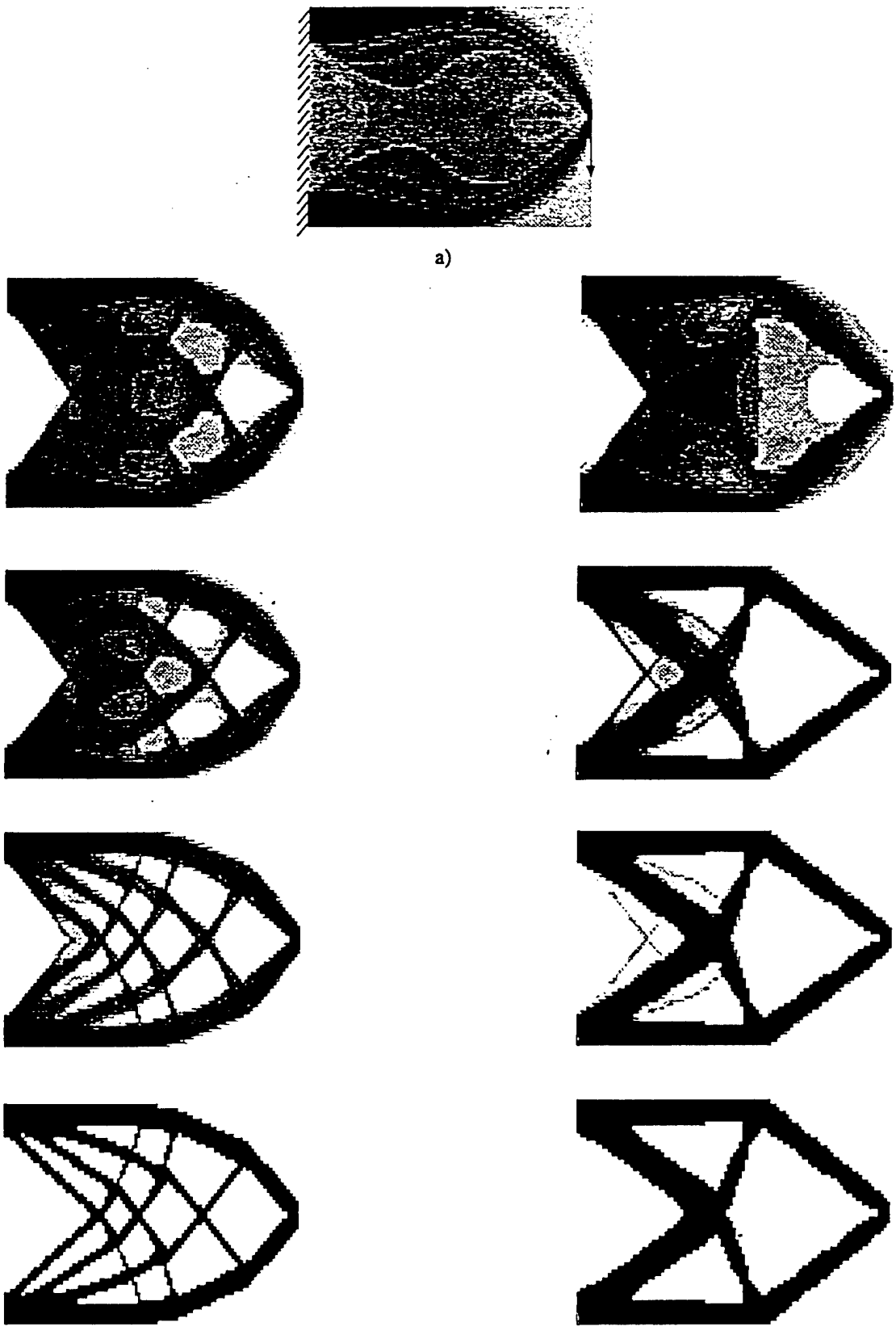

Fig.2. Cantilever beam subjected to transverse load: a) optimal distribution of the trace of elasticity tensor for continuously varying material properties, b)-c) transition to discrete design for slow(b) and rapid (c) cut off value adjustment rate.

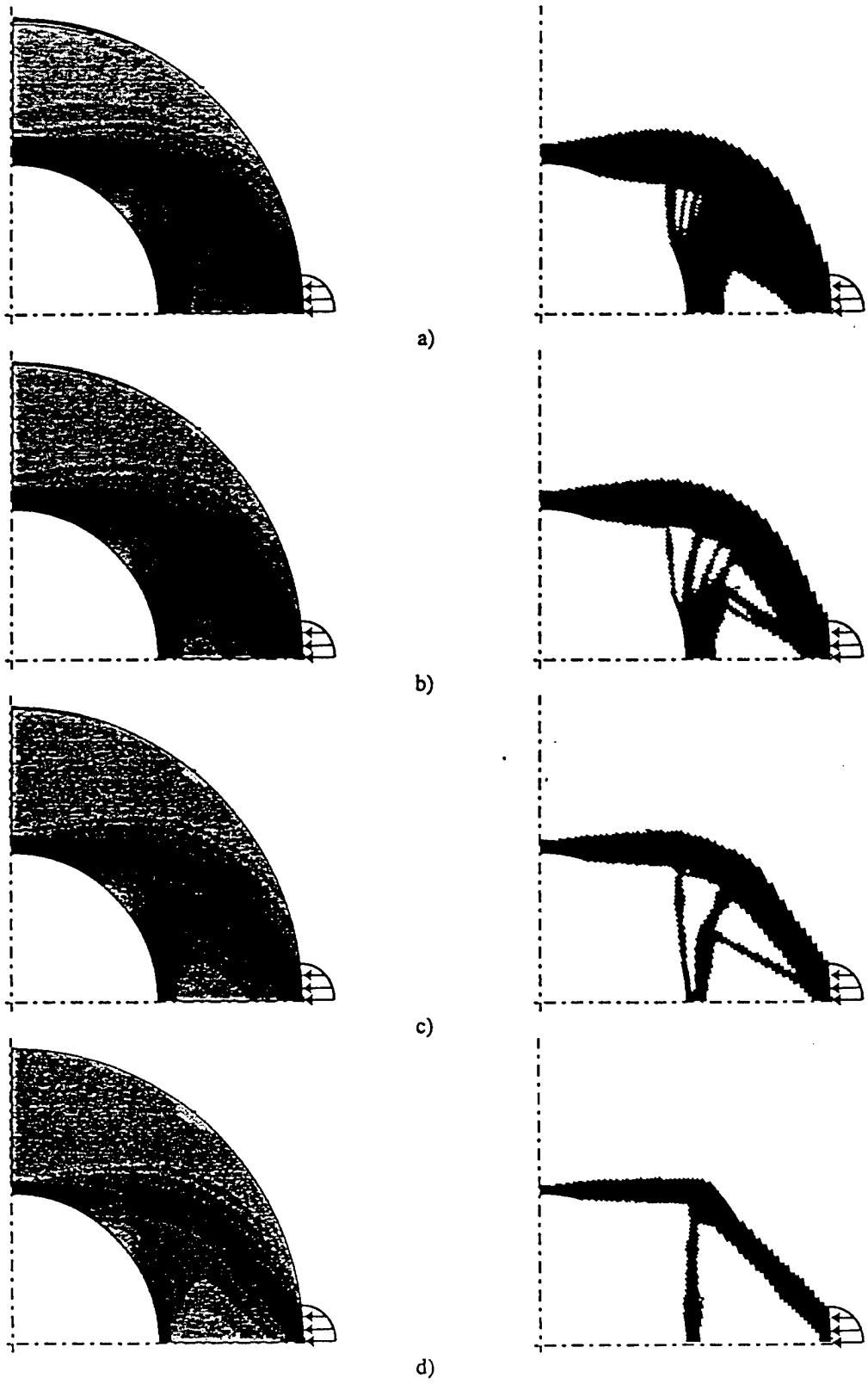

Fig.3. Prediction of optimal material field (left) and topology design (right) inside circular ring compressed along horizontal diameter for volume fraction equal to: a) 0.5 , b) 0.4, c) 0.3 ,d) 0.2.

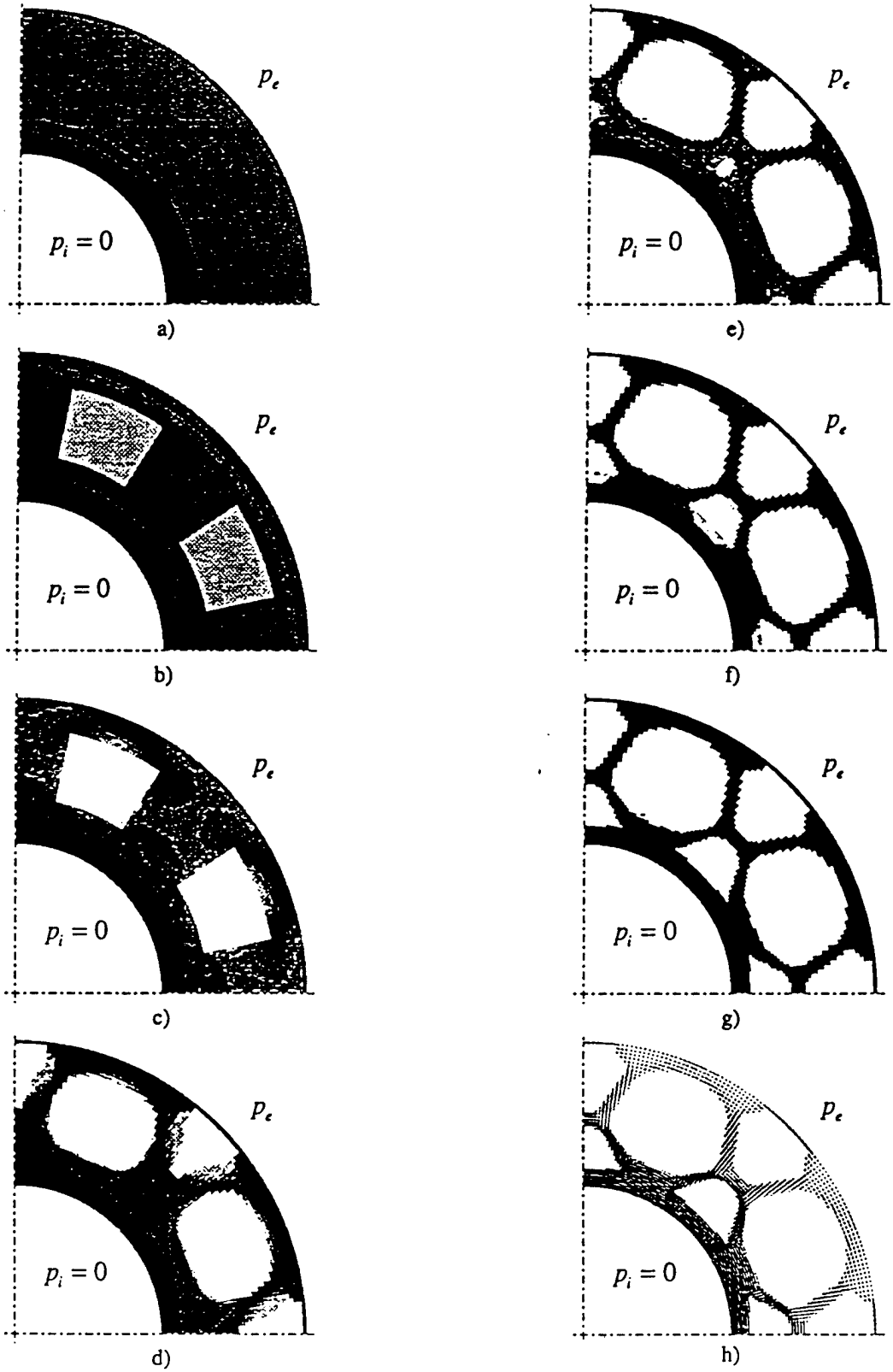

Fig.4. Circular plate with internal hole under uniform pressure on external edge: a) optimal solution for $w \equiv 1$, b) induced holes, c)-g) transition to discrete structure, h) magnitude and directions of principal strains at the final design.

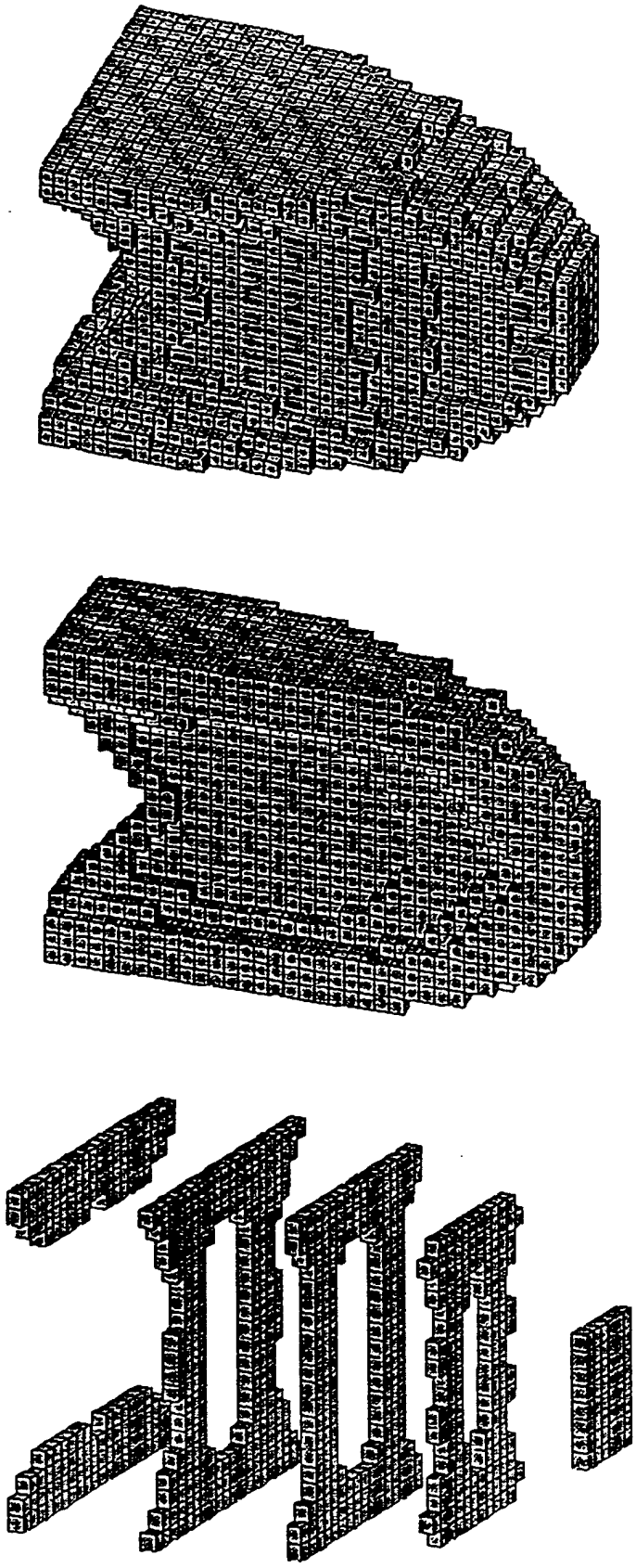

Fig.5. Final design of 3D cantilever beam for volume fraction of 0.4.

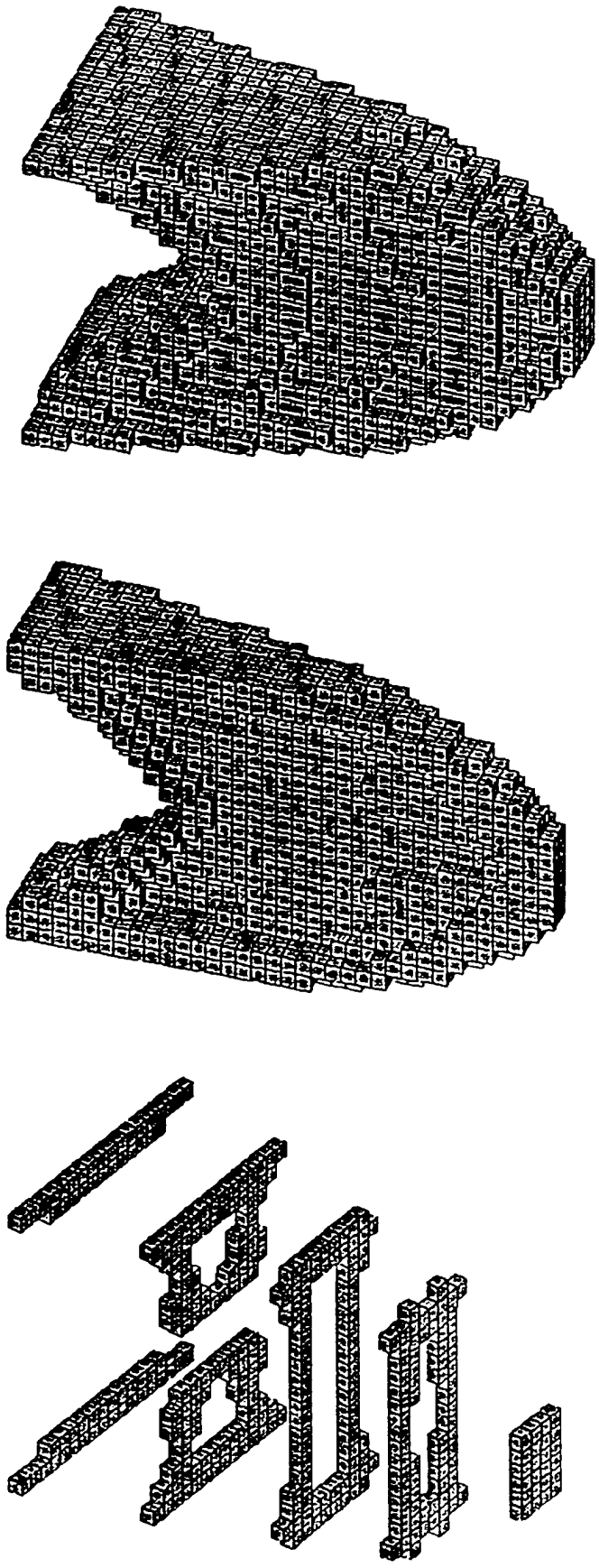

Fig.6. Final design of 3D cantilever beam for volume fraction of 0.2

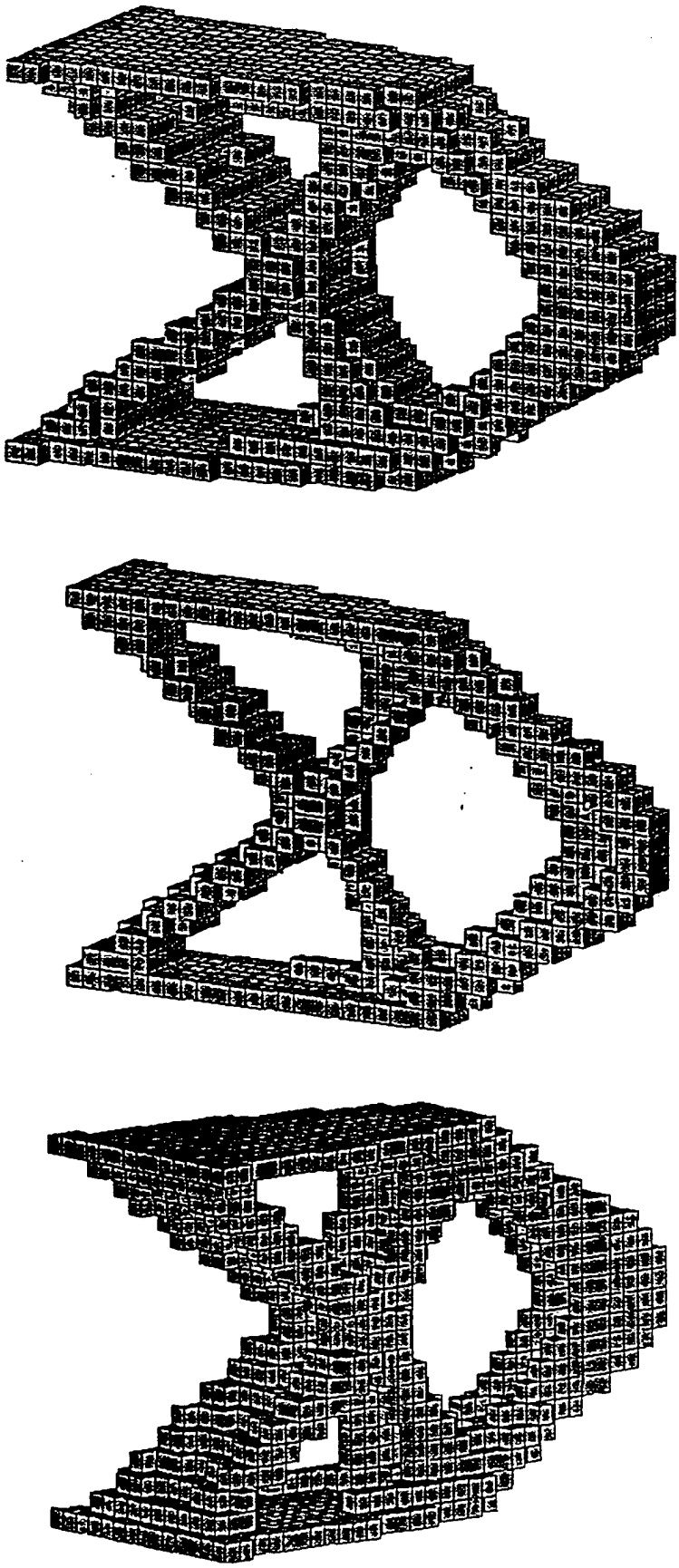

Fig.7. Final design of 3D cantilever beam for volume fraction of 0.1

Three-dimensional optimal design of structural topology, shape and material properties with design-dependent field force.

Sergio Turteltaub, Jakub Pawlicki*, John E. Taylor
and Peter Washabaugh

Department of Aerospace Engineering
The University of Michigan
Ann Arbor, MI 48109

Abstract

The optimization of material properties with the goal of achieving minimum structural compliance is analyzed in a three-dimensional setting. The formulation takes into account a design-dependent field force with the purpose of analyzing problems where self-weight or centrifugal forces have a non-negligible effect. With the introduction of

*Institute of Aeronautics and Applied Mechanics, Warsaw University of Technology, Warsaw, Poland.

an additional procedure, optimal topology design is predicted. An algorithm based on the optimality conditions is used to obtain numerical solutions to problems which illustrate relevant effects of the design-dependent field force.

1 Introduction.

The optimal design problem where the objective is to achieve minimum structural compliance for a linearly elastic continuum (or, equivalently, maximum structural stiffness) has been used extensively as the prototypical example for developing new optimization techniques and methods. Relatively recently, BENDSØE et. al [2] introduced a method where the elasticity tensor field is used as a variable for the design of a structure composed of a general inhomogenous and anisotropic material. Furthermore, their method predicts optimal material properties which vary *continuously* throughout the structure.

********* "black/white" or "0/1" layout **********

Hence, the formulation of the design problem must be modified in order to predict 0/1 solutions. However, the modification should be minimal so as to retain the pratical relevance of the original problem. This is precisely the motivation that led GUEDES and TAYLOR [4] to introduce a piecewise constant weight function w in an isoperimetric constraint of the optimal design problem. The idea was to introduce a weight function taking only two values, $\underline{w}$ and $\overline{w}$, such that the corresponding *solution* to the design problem would also take only two "values," even though the space of admissible design variables is not limited to such "values." A stepwise solution procedure

with appropriate adjustement of weighting leads to a result for 0/1 layout design. The same approach is considered here and the main purpose is to study the effect of a design-dependent field force in a three-dimensional setting. The design of a vibrating elastic structure for maximum fundamental frequency (see, e.g., PRAGER & TAYLOR [?]) or the prediction of shape for a rotating structure (DRUCKER & SHIELD [?]) are examples of problems in this category. Problems with a field force of this kind arise naturally, for example, in the context of the design of structures where the weight is taken into account or in the design of elements belonging to a rotating structure where a non-negligible inertial load is present (e.g., a turbine, a helicopter rotor blade, etc.). The fully dynamic problem is not addressed here; rather, the inertial loads are introduced as a time-independent field force so that, formally, the structure of an elastostatic problem is preserved.

Alternative methods to obtain a similar layout have been proposed (see, e.g., the survey ROZVANY et. al [?]). One of them is based on the use of an artificial constitutive power law that penalizes "intermediate" values of the design variable (see, e.g., PETERSSON and SIGMUND [7]). Only isotropic materials are used in this model and a (local) bound on the generalized derivative of the design variable is imposed to achieve closure. Another technique is to include a term in the objective functional that penalizes intermediate values of the design variable, but independently of the constitutive law, by using an explicit constraint (see, e.g., HABER at al. [5] and FERNANDES et. al [3]). This latter method also includes a (global) bound on the perimeter of the solid region to achieve closure. A comparative analysis of these different methods is beyond the scope of this work. Furthermore, the above mentioned

papers do not consider a design-dependent field force.

The basic optimization problem (maximum structural stiffness with design-dependent field force) is stated in Section 2. The optimality conditions for the design problem are presented in Section 3. Section 4 deals with a version of the design problem where the purpose is to generate a result for 0/1 layout (i.e., topology) design. The numerical implementation of both the basic design problem and the 0/1 layout problem is developed in Section 5 and some numerical examples are presented in Section 6. The last section includes a discussion and some conclusions regarding the effect of the design-dependent field force in the design of optimal structures.

2 Formulation of the problem.

2.1 Optimal design problem.

Let V be the set of kinematically admissible displacement fields and A the set of admissible design variables (fourth-order symmetric positive semi-definite tensor fields E_{ijkl}). Consider an elastic body occupying a region Ω, subject to a field force b_i which is assumed to depend on E_{ijkl}. In general, the field force is not necessarily a function of the material properties. However, this relation can be motivated in view of the form of the *optimized* structure which is composed of only two materials (i.e., 0/1 layout). In that case, the elasticity tensor field can be viewed as a characteristic function that describe the (disjoint) domains occupied by each material, thus a relation between b_i and E_{ijkl} can be established. In a sense, a functional relation between the field force and the elasticity tensor is similar to an artificial constitutive law

where the results are justified a posteriori only for the optimal solution.

Let W be the work done by the external forces, i.e.,

$$W(u_i, b_i(E_{ijkl})) = \int_\Omega b_i(E_{ijkl})u_i \mathrm{d}v + \int_{\partial\Omega_t} t_i u_i \mathrm{d}a \ , \tag{1}$$

where u_i is the displacement and t_i the prescribed surface traction (the prescribed displacement in $\partial\Omega_u$ is zero). The potential energy is given by $\Pi = U - W$, where $U = \frac{1}{2}\int_\Omega \varepsilon_{ij} E_{ijkl} \varepsilon_{kl} \mathrm{d}v$ is the total strain energy. Recall that the minimum value of the potential energy is $\Pi_* = -\frac{1}{2}W_*$ hence, the minimum structural compliance problem is stated as:

$$\begin{aligned} &\max_{E_{ijkl}\in A} \ \min_{u_i \in V} \Pi(E_{ijkl}, u_i) \\ &0 < \underline{\varphi} \le \varphi(E_{ijkl}) \le \overline{\varphi} \ , \\ &\int_\Omega \varphi(E_{ijkl}) \mathrm{d}v \le R \ , \end{aligned} \tag{P1}$$

where $\varphi(E_{ijkl})$ is a resource cost function, R is an upper bound on the total resource and $\underline{\varphi} = \underline{\varphi}(x)$ and $\overline{\varphi} = \overline{\varphi}(x)$ are given functions (independent of E_{ijkl}) satisfying $0 < \underline{\varphi} < \overline{\varphi}$. The second explicit restriction for E_{ijkl} is the resource constraint. GUEDES and TAYLOR [4] used a weighted cost function based on the trace of E_{ijkl}, i.e., $\varphi(E_{ijkl}) = wE_{ijij}$, where w is a weight function. The cost function considered here is similar, but based on the maximum eigenvalue of E_{ijkl}, i.e., let

$$\alpha = \max_{B_{ij}B_{ij}=1} B_{ij}E_{ijkl}B_{kl} \ , \tag{2}$$

and define

$$\varphi(E_{ijkl}) = w\alpha \ , \tag{3}$$

where $w = w(x)$ is a positive-valued weight function (an interpretation of the cost function is given in Section 2.2). Moreover, the functions $\underline{\varphi}$ and $\overline{\varphi}$ corresponding to the lower and upper bounds of the cost function are assumed to have the following form:

$$\underline{\varphi} = w\underline{\alpha} \ , \qquad \overline{\varphi} = w\overline{\alpha} \ ,$$

where $\underline{\alpha}$ and $\overline{\alpha}$ are given positive *constants* satisfying $0 < \underline{\alpha} < \overline{\alpha}$. Finally, it is also assumed that the field force b_i depends on α only, i.e.,

$$b_i = b_i(E_{ijkl}) = b_i(\alpha) \ . \tag{4}$$

It is useful to consider *discontinuous* weight functions (e.g., piecewise constant functions), hence one has to take into account possible discontinuities in the design and strain fields at points where w is discontinuous. However, the displacement field is assumed to be continuous everywhere.

2.2 Reformulation of the problem.

The design problem (P1) can be reformulated by using a saddle point theorem as proved in BENDSØE et al. [2]. This theorem can still be applied with a cost function (3) and field force (4). In this case, as shown in [8], the cost function (3) provides a positive definite optimal material of the form

$$E^0_{ijkl} = (\alpha - \underline{\alpha})\frac{\varepsilon_{ij}\varepsilon_{kl}}{\varepsilon_{mn}\varepsilon_{mn}} + \tfrac{1}{2}\underline{\alpha}\ (\delta_{ik}\delta_{jl} + \delta_{il}\delta_{jk}) \ . \tag{5}$$

The corresponding stress field is

$$\sigma_{ij} = E^0_{ijkl}\varepsilon_{kl} = \alpha\varepsilon_{ij} \ , \tag{6}$$

and the potential energy is

$$\Pi_0(\alpha, u_i) = \int_\Omega \tfrac{1}{2}\alpha\varepsilon_{ij}\varepsilon_{ij}dv - W_0(u_i, b_i(\alpha)) \ . \tag{7}$$

The optimal material characterized by (5) is an anisotropic (orthotropic) material. However, due to the coupling between the design and elastostatic problems and in view of (6), the optimal material, *restricted* to the optimal strain, behaves like an isotropic material with zero Poisson's ratio and Young modulus equal to α. The optimal material can be decomposed into an isotropic part characterized by a Young's modulus $E = \underline{\alpha}$ and zero Poisson's ratio and an anisotropic "reinforcement" aligned with the optimal strain field ε_{ij} and characterized by a unique non-zero value $\alpha - \underline{\alpha}$ (i.e., essentially it depends on the maximum eigenvalue α of E_{ijkl}). The isotropic part of E^0_{ijkl} is fixed and the problem reduces to identify the anisotropic reinforcement in order to optimize the structure. The cost function measures the (weighted) amount of reinforcement required for the optimal structure. Thus, the optimal design problem can be reformulated as

$$\begin{aligned} &\max_{\alpha} \quad \min_{u_i \in V} \ \Pi_0(\alpha, u_i) \ . \\ &0 < \underline{\alpha} \le \alpha \le \overline{\alpha} \ , \\ &\textstyle\int_\Omega w\alpha dv \le R \ , \end{aligned} \tag{P2}$$

At points where $\alpha = \underline{\alpha}$, the interpretation is that no reinforcement is required.

3 Optimality conditions.

Consider the Lagrangian L given by

$$L(\alpha, u_i; \underline{\lambda}, \overline{\lambda}, \Lambda) = \Pi_0(\alpha, u_i) + \int_\Omega \left[\underline{\lambda}(\underline{\alpha} - \alpha) - \overline{\lambda}(\alpha - \overline{\alpha})\right] \mathrm{d}v + \Lambda \left\{ \int_\Omega w\alpha \mathrm{d}v - R \right\} , \tag{8}$$

where $\underline{\lambda} = \underline{\lambda}(x), \overline{\lambda} = \overline{\lambda}(x)$ and Λ are Lagrange multipliers. The presence of a (possibly) discontinuous weight function needs to be taken into account since the design variable α and the strain field would also be discontinuous at the same points. Let S be the set of such points of discontinuity. Arbitrary variations of L with respect to u_i provide the equilibrium equations. Since u_i is continuous, then so is δu_i; in particular, $[\![\delta u_i]\!] = 0$ on the surface of discontinuity S, where, for any function f, $[\![f]\!] = f^+ - f^-$, $f^\pm$ being the values of f on each side of S. For given α, the local form of the elastostatic problem for the optimal strain ε_{ij} at points where α and ε_{ij} are smooth is

$$\left.\begin{aligned} (\alpha\varepsilon_{ij})_{,j} + b_i(\alpha) = 0 \quad & \text{in } \Omega - S , \\ \sigma_{ij} n_j = \alpha\varepsilon_{ij} n_j = t_i \quad & \text{on } \partial\Omega_t , \\ u_i = 0 \quad & \text{on } \partial\Omega_u , \end{aligned}\right\} \tag{9}$$

where n_j is the outward unit normal vector to the boundary $\partial\Omega$. At points where α and ε_{ij} are discontinuous, one has

$$\int_S [\![\alpha\varepsilon_{ij}\delta u_j]\!]\nu_i \mathrm{d}a = \int_S \left\{ [\![\alpha\varepsilon_{ij}]\!]\nu_i \langle \delta u_j \rangle + \langle \alpha\varepsilon_{ij} \rangle \nu_i [\![\delta u_j]\!] \right\} \mathrm{d}a = 0 ,$$

where ν_j is the normal vector pointing towards the "+" side of the surface of discontinuity S and, for any function f, $\langle f \rangle = \frac{1}{2}(f^+ + f^-)$. Moreover, since the integration by parts does not involve δb_i, possible discontinuities of b_i do

not affect the result. Therefore, since $[\![\delta u_j]\!] = 0$, the local form of the above equation is

$$[\![\alpha \varepsilon_{ij}]\!] \nu_j = 0 \qquad \text{on } S \,. \tag{10}$$

(This condition represents the continuity of the traction.) Let L' be the gradient of L with respect to α, i.e., $\delta L[\delta\alpha] = \int_\Omega L' \delta\alpha \mathrm{d}v$ and let b_i' be the gradient of b_i with respect to α; the gradient L' can be expressed, $\forall x \in \Omega - S$, by

$$L' = b_i' u_i - \tfrac{1}{2}\varepsilon_{ij}\varepsilon_{ij} - \underline{\lambda} + \overline{\lambda} + \Lambda w \,. \tag{11}$$

Therefore, the Karush-Kuhn-Tucker optimality conditions are, $\forall x \in \Omega - S$,

$$\left.\begin{aligned} L' &= 0 \,, & & \\ \underline{\lambda}(\underline{\alpha} - \alpha) &= 0 \,, & \underline{\lambda} &\geq 0 \,, \\ \overline{\lambda}(\alpha - \overline{\alpha}) &= 0 \,, & \overline{\lambda} &\geq 0 \,, \\ \Lambda \left\{ \textstyle\int_\Omega w\alpha \mathrm{d}v - R \right\} &= 0 \,, & \Lambda &\geq 0 \,. \end{aligned}\right\} \tag{12}$$

At points on S, the jump condition $[\![L']\!] = 0$ is trivially satisfied. For a more specific formulation of the optimality conditions one can use the following domains:

$$\begin{aligned} \underline{\Omega} &= \{ x \in \Omega \mid \alpha(x) = \underline{\alpha} \} \,, \\ \overline{\Omega} &= \{ x \in \Omega \mid \alpha(x) = \overline{\alpha} \} \,, \\ \Omega_i &= \{ x \in \Omega \mid \underline{\alpha} < \alpha(x) < \overline{\alpha} \} \,. \end{aligned} \tag{13}$$

Hence, since $\underline{\lambda} = 0$ for $x \in \overline{\Omega}$, $\overline{\lambda} = 0$ for $x \in \underline{\Omega}$ and $\underline{\lambda} = \overline{\lambda} = 0$ for $x \in \Omega_i$, the optimality conditions (12) become

$$\left.\begin{array}{lll} \Lambda w = \frac{1}{2}\varepsilon_{ij}\varepsilon_{ij} - b_i' u_i \,, & & x \in \Omega_i \,, \\ \Lambda w - \underline{\lambda} = \frac{1}{2}\varepsilon_{ij}\varepsilon_{ij} - b_i' u_i \,, & \underline{\lambda} > 0 \,, & x \in \underline{\Omega} \,, \\ \Lambda w + \overline{\lambda} = \frac{1}{2}\varepsilon_{ij}\varepsilon_{ij} - b_i' u_i \,, & \overline{\lambda} > 0 \,, & x \in \overline{\Omega} \,, \\ \Lambda \left\{ \int_\Omega w \alpha dv - R \right\} = 0 \,, & \Lambda \geq 0 \,, & x \in \Omega \,. \end{array}\right\} \tag{14}$$

In Section 4, a class of discontinuous functions w will be introduced such that the set of points of discontinuity S can lie either inside or on the boundary of Ω_i or on the boundaries between $\underline{\Omega}$ and $\overline{\Omega}$. In any case, for that class of functions, the jump condition is trivially satisfied, i.e., from (14),

$$\Lambda[\![w]\!] = [\![\tfrac{1}{2}\varepsilon_{ij}\varepsilon_{ij} - b_i' u_i + \underline{\lambda} - \overline{\lambda}]\!] \quad \text{on } S \,.$$

If w is continuous, then the jump conditions do not apply. Moreover, if $b_i' \equiv 0$ then one can prove that $\Lambda > 0$ (and hence that the resource constraint is satisfied as an equality, see [4]). However, this is not necessarily true if $b_i' \not\equiv 0$ (i.e., it is possible that $\Lambda = 0$ and the problem (P2) has a non-trivial solution). Before closing this section, it is interesting to observe that, from (14), the term $b_i' u_i + \Lambda w$ is necessarily non-negative in $\Omega_i \cup \underline{\Omega}$ (even if $\Lambda = 0$), but it could have any sign in $\overline{\Omega}$. Thus, if $b_i' u_i + \Lambda w < 0$, then, necessarily, this can only happen at a point where the material is at its *upper* bound. This fact will be used in Section 5.

4 Optimal design problem with discrete values.

As mentioned in the introduction, as an additional design requirement it is useful to identify solutions to the problem (P2) where the design variable is restricted to only two values: $\overline{\alpha}$ and $\underline{\alpha}$. The resulting structure is characterized by elasticity tensors $\frac{1}{2}\underline{\alpha}\,(\delta_{ik}\delta_{jl}+\delta_{il}\delta_{jk})$ and $(\overline{\alpha}-\underline{\alpha})\varepsilon_{ij}\varepsilon_{kl}/(\varepsilon_{mn}\varepsilon_{mn})+\frac{1}{2}\underline{\alpha}\,(\delta_{ik}\delta_{jl}+\delta_{il}\delta_{jk})$ respectively. The region occupied by the first material does not have "reinforcement," whereas the complementary region has a (reinforced) material with fixed magnitude $\overline{\alpha}$ and variable orientation (the magnitude of E_{ijkl} is measured here in terms of its maximum eigenvalue; its Frobenius norm is $\sqrt{E_{ijkl}E_{ijkl}} \doteq \sqrt{\overline{\alpha}\,(\overline{\alpha}-\underline{\alpha})+6\underline{\alpha}^2}$). For the specific case where $\underline{\alpha}$ and $\overline{\alpha}$ are chosen such that $\underline{\alpha} \ll \overline{\alpha}$, then the two materials are interpreted as "void" and "full material." In general, this corresponds to a suboptimal solution compared to one where α varies continuously (which can be obtained, e.g., with a weight function $w \equiv 1$). However, it is an optimal solution for some other weight function and satisfies the additional requirement of taking only two values.

The use of a weight function is intimately related to the resource constraint. In general, using only local bounds, one cannot rule out trivial solutions. The resource constraint is used to optimally distribute the material properties. However, the distribution of material properties that satisfy the resource constraint is accomplished via a single (constant) parameter, i.e., via the Lagrange multiplier Λ. In a sense, the use of a weight function w is an extension of this idea, except that w acts *locally* via the product Λw as

shown by (14). Hence, the effect of the Lagrange multiplier can be modified locally by a proper use of a weight function.

Let F be the class of piecewise constant weight functions defined as

$$w \in F \quad \Leftrightarrow \quad w = \begin{cases} \underline{w} & \text{in } \Omega_-^w \,, \\ \overline{w} & \text{in } \Omega_+^w \,, \end{cases} \tag{15}$$

where the domains Ω_-^w and Ω_+^w (to be defined later) satisfy $\Omega_-^w \cup \Omega_+^w = \Omega$ and $\Omega_-^w \cap \Omega_+^w = \emptyset$. The superscript reflects the fact that different domains correspond to different functions w. Suppose that for a given weight function the corresponding solution to (P2) is α (in general, not a piecewise constant function). Recall that the domain Ω_i, as defined by (13), represents the points where the design variable is between the lower and upper bounds $\underline{\alpha}$ and $\overline{\alpha}$. As an additional objective one looks for a function $w_* \in F$ in the following problem:

$$\inf_{w \in F} |\Omega_i| \,, \tag{P3}$$

where Ω_i is defined as an implicit function of w by $(13)_3$, (15) and the corresponding solution α to (P2). The functional dependence of Ω_i on w is somewhat complex but numerical experiments have shown that there are (numerical) approximations of a function w_* such that $|\Omega_i| \approx 0$. The resulting structure satisfies $\Omega = \underline{\Omega} \cup \overline{\Omega}$ and $\underline{\Omega} \cap \overline{\Omega} = \emptyset$. However, the uniqueness, and, in fact, the existence of w_* in the general case, have not been established. Nevertheless, the purpose here is to find at least one numerical approximation to such a function w_*. The domains Ω_-^w and Ω_+^w of (15) are now defined

as

$$\begin{aligned} \Omega_-^w &= \{x \in \Omega \mid \alpha(x) < \alpha_c\} , \\ \Omega_+^w &= \{x \in \Omega \mid \alpha(x) \geq \alpha_c\} , \end{aligned} \tag{16}$$

where the constant α_c, $\underline{\alpha} < \alpha_c < \overline{\alpha}$, is a prescribed "cutoff" value. The interpretation of the weight function w follows from this definition: the method assigns a weight $\underline{w}$ to regions of "weak" reinforcement ($\alpha < \alpha_c$) and a weight $\overline{w}$ otherwise.

In order to solve the problem (P3), an iterative procedure is used since, a priori, the domains Ω_-^w and Ω_+^w cannot be defined without knowledge of the optimal α which, in turn, depends on w. The details of the algorithm will be given in Section 5, but it is interesting to point out a few facts here: suppose that there exists a minimizer w_* of (P3) and assume that $\min_{w \in F} |\Omega_i| = 0$, then

$$\Omega_-^w = \underline{\Omega} , \qquad \Omega_+^w = \overline{\Omega} ,$$

hence Ω_-^w, the region of weight $\underline{w}$, coincides with the region without reinforcement and Ω_+^w, the region of weight $\overline{w}$, coincides with the reinforcement. From this point of view, the function w_* is related to the characteristic functions of $\underline{\Omega}$ and $\overline{\Omega}$. Moreover, recall that the resource constraint is viewed as a global bound on the "cost" of reinforcement. If the resource constraint is active for the weight function w_* (i.e., $\Lambda > 0$), one has, from $(14)_4$,

$$\underline{\alpha}\,\underline{w}\,|\underline{\Omega}| + \overline{\alpha}\,\overline{w}\,|\overline{\Omega}| = R ,$$

thus, for an appropriate interpretation of the regions with and without reinforcement, one should choose $\underline{w}$ and $\overline{w}$ such that

$$\underline{\alpha}\,\underline{w}\,|\underline{\Omega}| \ll \overline{\alpha}\,\overline{w}\,|\overline{\Omega}| .$$

If $\underline{\alpha}\,|\underline{\Omega}|\,/\overline{\alpha}\,|\overline{\Omega}|$ is bounded above and below, then a choice such as $\underline{w} \ll \overline{w}$ seems appropriate. However, based on the optimality condition $(14)_2$, this choice is *not* consistent with $\alpha = \underline{\alpha}$ in $\underline{\Omega}$. This can be seen by assuming $b_i' \equiv 0$, hence the multiplier $\underline{\lambda}$ would not be positive in $\underline{\Omega}$ if $\underline{w}$ is "small". Nonetheless, suppose that $\underline{\alpha} \ll \overline{\alpha}$ (which corresponds to the void/full material case) and assume that $|\underline{\Omega}|\,/\,|\overline{\Omega}|$ is bounded above and below, then $\underline{\alpha}, \overline{\alpha}, \underline{w}$ and $\overline{w}$ should satisfy

$$\underline{\alpha} \ll \overline{\alpha}\ ,\quad \underline{w} \gg \overline{w}\ ,\quad \underline{\alpha}\,\underline{w} \ll \overline{\alpha}\,\overline{w}\ ,$$

e.g., if $\underline{\alpha}/\overline{\alpha} = 10^{-p}$, $\overline{w}/\underline{w} = 10^{-q}$, $\underline{\alpha}\,\underline{w}/\overline{\alpha}\,\overline{w} = 10^{-(p-q)}$, then one should take $p > 0, q > 0$ and $p - q > 0$ sufficiently large, which gives $R \sim \overline{\alpha}\,|\overline{\Omega}|$ (with $\overline{w} = 1$). The above choice does not contradict the optimality conditions, therefore, the use of a weight function will be limited to the void/full material case. The resource cost function, which is the product of the weight function and the design variable α, would be small when $\alpha = \underline{\alpha}$ and large when $\alpha = \overline{\alpha}$. If $\underline{w}$ and $\overline{w}$ are of the same order of magnitude, then, in general, the corresponding structure would not be void/full material. The method does not require to set $\overline{w} = 1$, but this choice provides the same interpretation of the resource constraint as in the case when no weight function is used.

5 Numerical implementation.

5.1 Overview.

The algorithm has two main elements: the first one deals with the basic optimization problem (P2) for a given (fixed) weight function and the second

one corresponds to a sequence of basic optimization problems solved for different weight functions with the purpose of identifying a minimizer w_* in the problem (P3).

In order to obtain a numerical solution of the optimal design problem (P2), a method based on the optimality conditions (14) is used. One can compute a numerical sequence $\{\alpha_n\}$ of the design variable such that each α_n is chosen within the constraint space. This is enforced via the local and global Lagrange multipliers. In order to minimize W_0 in (P2), the corresponding displacement field u_i (for a given α) has to be obtained as the solution of (9). This can be achieved using a standard finite element code (in this case the program ANSYS was used).

For the problem (P3), the basic optimization problem (P2) is solved with a given weight function and a new weight function is defined from (15) and (16) using the new distribution of material properties α. A new optimization problem (P2) is solved with the updated weight function until a 0/1 layout is identified. Section 5.2 deals with the basic optimization problem (P2) while the 0/1 procedure for problem (P3) is described in Section 5.3.

5.2 Basic optimization problem.

The details of the algorithm are as follows (a concise version is given afterwards). Suppose that a given approximation α_n has been identified. To obtain α_{n+1}, first compute u_i^n (and hence ε_{ij}^n) by solving problem (9) with $\alpha = \alpha_n$. To remain in the constraint space at step $n+1$ while minimizing the objective functional, one needs to iterate in order to satisfy all constraints simultaneously. (The superindex k will be used in connection with this iter-

ative procedure.) The method proposed here is similar to the one used by BENDSØE et al. [1] except that it is not assumed that the global Lagrange multiplier is positive since the resource constraint might become active from step n to step $n+1$ or might not be active at all (this is due to the presence of a design-dependent field force). First, update α_n based on the optimality conditions without including the local constraints, i.e., from (14), define

$$\tilde{\alpha}_{n+1}^k = \alpha_n \left[\frac{\frac{1}{2}\varepsilon_{ij}^n \varepsilon_{ij}^n}{\max\{\gamma, (b_i^n)' u_i^n + \Lambda_{n+1}^k w\}} \right]^p , \tag{17}$$

where $\gamma > 0$ is a "small" number and p is an appropriately chosen value to improve convergence (usually $0 < p \leq 1$). For $k = 0$, one can take $\Lambda_{n+1}^0 = \Lambda_n$ which corresponds to the last value of Λ at step n. The form of the denominator follows from the remark at the end of Section 3: if $(b_i^n)' u_i^n + \Lambda_{n+1}^k w \leq 0$, then, setting it equal to a small number will force it to its proper value, i.e., the upper bound. The power p is used to avoid large fluctuations of the design variable. To complement the effect of p, and additional restriction can be implemented by imposing a "move limit" ζ as follows:

$$\tilde{\alpha}_{n+1}^k = \begin{cases} (1-\zeta)\alpha_n & \text{if } \tilde{\alpha}_{n+1}^k \leq (1-\zeta)\alpha_n , \\ \tilde{\alpha}_{n+1}^k & \text{if } (1-\zeta)\alpha_n < \tilde{\alpha}_{n+1}^k < (1+\zeta)\alpha_n , \\ (1+\zeta)\alpha_n & \text{if } \tilde{\alpha}_{n+1}^k \geq (1+\zeta)\alpha_n . \end{cases} \tag{18}$$

Now, impose the local constraints, i.e., for $k \geq 0$,

$$\alpha_{n+1}^k = \begin{cases} \underline{\alpha} & \text{if } \tilde{\alpha}_{n+1}^k \leq \underline{\alpha} , \\ \tilde{\alpha}_{n+1}^k & \text{if } \underline{\alpha} < \tilde{\alpha}_{n+1}^k < \overline{\alpha} , \\ \overline{\alpha} & \text{if } \tilde{\alpha}_{n+1}^k \geq \overline{\alpha} . \end{cases} \tag{19}$$

Observe that, without a denominator as the one used in (17), the value of α_{n+1}^k when $(b_i^n)' u_i^n + \Lambda_{n+1}^k w < 0$ would be $\underline{\alpha}$ instead of its correct value $\overline{\alpha}$.

If $0 \leq (b_i^n)' u_i^n + \Lambda_{n+1}^k w \leq \gamma$, then the denominator in (17) has the same effect, however, this does not preclude α_{n+1}^k to take values different than $\overline{\alpha}$ since the numerator could be small as well. In order to satisfy the resource constraint (either as an equality or an inequality), a penalty method is used. The Lagrangian is augmented by adding the term

$$\tfrac{1}{2}\eta \left(\int_\Omega w\alpha dv - R \right)^2 ,$$

where $\eta > 0$ is the penalty. Strictly speaking, the optimality conditions (14) should be modified to account for this term, however this is taken care of in the numerical procedure. Define

$$R_{n+1}^k = \int_\Omega w\alpha_{n+1}^k dv , \qquad \Delta_k = R_{n+1}^k - R , \tag{20}$$

and update the Lagrange multiplier as follows:

$$\Lambda_{n+1}^{k+1} = \max\left\{0, \ \Lambda_{n+1}^k + \eta\Delta_k\right\} . \tag{21}$$

Observe that this includes the case $\Lambda_{n+1} = 0$ if the resource constraint is not active. With this new multiplier, one can compute $\tilde{\alpha}_{n+1}^{k+1}$, from (17), then $\tilde{\alpha}_{n+1}^{k+1}$ from (18) and impose the local constraints (19) to obtain α_{n+1}^{k+1} as before. The process converges when $|\Lambda_{n+1}^{k+1} - \Lambda_{n+1}^k| \ll 1$, in which case $|R_{n+1}^k - R| \ll 1$ if the constraint is active. At the end of this iterative procedure one should have an appropriate approximation α_{n+1} which satisfies all constraints based on the previous step's strain field ε_{ij}^n. The procedure to obtain a numerical solution of (P2) can be summarized in the form of the following algorithm:

A. Initialization.

1: Set $\alpha_0 = \hat{\alpha}$ (Given initial guess).

2: Obtain u_i^0, ε_{ij}^0 from (9).

3: Set $\Lambda_0 = \hat{\Lambda}$ (Given initial guess; could be zero).

B. Update: $\alpha_n \to \alpha_{n+1}$.

1: Set $\Lambda_{n+1}^0 = \Lambda_n$ and compute $\tilde{\alpha}_{n+1}^0$, $\bar{\alpha}_{n+1}^0$ and α_{n+1}^0 from (17), (18) and (19).

2: For $k \geq 0$: compute R_{n+1}^k and Δ_k from (20) and update $\Lambda_{n+1}^k \to \Lambda_{n+1}^{k+1}$ from (21) and then $\alpha_{n+1}^k \to \alpha_{n+1}^{k+1}$ from (17), (18) and (19).

3: Check if $|\Lambda_{n+1}^{k+1} - \Lambda_{n+1}^k| \ll 1$, in which case take $\alpha_{n+1} = \alpha_{n+1}^{k+1}$, otherwise repeat step 3 until convergence.

C. Convergence (objective functional): check if $|W_0^{n+1} - W_0^n|/|W_0^n| \ll 1$, otherwise repeat B until convergence. Alternatively, one could check the optimality conditions (13) in some average sense (e.g., L_2-norm).

5.3 Discrete (0/1) layout.

The algorithm presented here is related to the problem (P3) as described in Section 4. Recall that in this case the values of $\underline{\alpha}, \overline{\alpha}, \underline{w}$ and $\overline{w}$ cannot be chosen arbitrarily. In order to obtain a discrete layout, a sequence of optimization problems (P2) are solved. For the first optimization problem, a uniform weight function is prescribed: the initial cutoff value is $\alpha_c^0 = 0$, hence, from (16),

$$w_0 = \overline{w} \quad \forall x \in \Omega \, .$$

At step l, solving the optimization problem with a weight function w_l, using the procedure described in Section 5.2, provides the corresponding optimal

design α_l. The weight function at step $l+1$ is obtained from step l as follows: the cutoff value is incremented by a (possibly constant) value $\Delta\alpha_c$,

$$\alpha_c^{l+1} = \alpha_c^l + \Delta\alpha_c \ ,$$

and new domains $\Omega_-^{w_{l+1}}$ and $\Omega_+^{w_{l+1}}$ are defined from (16) using α_l (hence w_{l+1} is determined from (15)). For practical purposes, one can choose a sufficiently large number of iteration steps, say n_l, and define a constant increment

$$\Delta\alpha_c = \frac{\overline{\alpha} - \underline{\alpha}}{n_l} \ ,$$

although a variable adjustment is sometimes more efficient. The process converges if $|\Omega_i^{l+1}|/|\Omega| \ll 1$. A proof of convergence is not available but numerical experiments show that it is possible to attain convergence with $\Delta\alpha_c$ small enough. If $\alpha_c^{l+1} > \overline{\alpha}$ but $|\Omega_i^{l+1}| \neq 0$, then the method fails. The procedure is summarized in the following algorithm:

A. Initialization.

1: Set $\alpha_c^0 = 0, w_0 \equiv \overline{w}$.

2: Solve optimization problem (P2) as described in Section 5.2 with, e.g., $\hat{\alpha} \equiv$ constant (initial guess for α), and obtain the corresponding solution α_0 (the subindex in α_0 refers to the solution of (P2) with $w = w_0$, not to the initial guess).

B. Update: $w_l \to w_{l+1}$.

1: Set $\alpha_c^{l+1} = \alpha_c^l + \Delta\alpha_c$.

2: Obtain w_{l+1} from (15) and (16) using α_l and α_c^{l+1}.

3: Solve optimization problem (P2) with $\hat{\alpha} = \alpha_l$ and obtain α_{l+1}.

C. Convergence (0/1 layout): check if $|\Omega_i^{l+1}|/|\Omega| \ll 1$, otherwise repeat B until convergence.

The application of this algorithm to an example problem is described in the next section.

6 Example applications: the optimal rotating structure.

As an illustrative three-dimensional example, consider the case of the (stiffest) design of a rotating structure occupying a design domain Ω and rotating at a constant angular velocity ω. Let $\{e_i^1, e_i^2, e_i^3\}$ be a cylindrical orthonormal basis where e_i^3 is aligned with the axis of rotation and e_i^1, e_i^2 are fixed with respect to Ω. The domain Ω is taken as a prismatic bar of unit lenght and rectangular cross section of area h^2. Suppose that the mass density ρ is related to the design variable α linearly, i.e.,

$$\rho = \kappa\alpha \ ,$$

where κ is a positive constants. In this case, the inertial force can be modeled as the body force

$$b_i(\alpha) = \omega^2 \kappa r \alpha e_i^1 \ , \tag{22}$$

where r is the orthogonal distance from a given point in Ω to the axis of rotation. The side attached to the axis of rotation is modeled as a clamped

end. The remaining sides of the structure are subjected to the following loads:

Case 1: shearing load:

$$t_i = \begin{cases} \tau_0 e_i^3 & \text{for } r = l \text{ (Uniform shear stress)} \\ 0 & \text{otherwise} \end{cases}$$

Case 2: torsional load:

$$t_i = \begin{cases} -\tau_0 e_i^3 & \text{for } r = 1 \ , \ x \in [-h, -h+\epsilon] \ , \\ \tau_0 e_i^3 & \text{for } r = 1 \ , \ x \in [h-\epsilon, h] \ , \\ 0 & \text{otherwise} \end{cases}$$

For the loading Case 2, ϵ is a small number, so that two opposite uniform shear loads are applied on strips of width ϵ. Recall that h is the width of the square cross-section and x is measured in the e_i^2 direction.

For illustration purposes, the corresponding optimal distribution of material properties (where $\alpha = \overline{\alpha}$) is shown, for Case 1, in Figures 1, 2 and 3 with and without a field force (i.e., with and without rotation). The design without a field force is symmetric with respect to the mid-plane e_i^1, e_i^2 but by taking into account the field force the structure is reinforced on the top (which is in compression) and is weakened on the bottom (which is in tension). Figures 4 and 5 correspond to the design for loading Case 2. Observe that the interior of the structure is essentially empty; in the case without a field force, it reproduces a well-known optimal design: a prismatic body with circular cross-section (within the limitations of a coarse mesh). However, the design with a field force is similar but it is not prismatic: it is tappered; thicker close to the axis of rotation and thinner towards the end where the load is applied.

7 Discussion and conclusions.

The differences between the optimal designs with and without a field force, as shown in the examples of Section 6, can be traced back to the same term in the optimality conditions (14): if $b_i' u_i < 0$, the design is locally stronger (compared to the case without a field force, i.e., $b_i = 0$). The converse is true when $b_i' u_i > 0$. In Case 1 (shearing load), the top (resp. bottom) of the structure is in compression (resp. tension), hence $b_i' u_i < 0$ (resp. $b_i' u_i > 0$) and this accounts for the features in the design. In Case 2 (torsional load) the situation is slightly different than in Case 1 since $b_i' u_i > 0$ everywhere, yet, compared to the case without field force, some sections are weaker but other are stronger. In this case, the term $b_i' u_i$ is greater towards the end of the structure where the surface loads are applied. Since in this case the (global) resource constraint is active, there is a fixed amount of material that is used, hence the structure becomes thicker closer to the axis of rotation where $b_i' u_i$ is smaller, as illustrated in Figure 5.

Although some technical issues remain open, the method shown here provides a practical way of identifying a 0/1 layout with an account of a design-dependent field force. Furthermore, the method is relatively easy to implement for three-dimensional problems since standard finite element programs can be used for this purpose. As a closing remark, it is worth noting that the use of a weight function is intimately related to the resource constraint since, if this constraint is not active ($\Lambda = 0$), the weight function does not affect the solution of the optimal design problem. Hence, in that case, one cannot expect to obtain a 0/1 layout using this method.

References

[1] BENDSØE, M., DÍAZ, A. and KIKUCHI, N.: Topology and generalized layout optimization of elastic structures, in: *Topology Design of Structures*, M. Bendsøe and C. A. Mota Soares (eds.), Kluwer, NATO ASI series, 227, pp 159–205, 1993.

[2] BENDSØE, M. P., GUEDES J. M., HABER R. B., PEDERSEN P. and TAYLOR, J. E.: An analytical model to predict optimal properties in the context of optimal structural design, *Journal of Applied Mechanics*, 61, pp 930–937, 1994.

[3] FERNANDES, P. R., GUEDES, J. M. and RODRIGUES, H., Topology optimisation of 3D linear elastic structures, Publication pending.

[4] GUEDES, J. M. and TAYLOR, J. E., xxx, xxx, xx, pp xxx–yyy, 19zz.

[5] HABER, R. B., JOG, C. S. and BENDSØE, M. P.: A new approach to variable-topology shape design using a constraint on perimeter, *Structural Optimization*, 11, pp 1–12, 1996

[6] JOG, C. S., HABER, R. B. and BENDSØE, M. P.: A displacement-based topology design method with self-adaptive layered materials, in: *Topology Design of Structures*, M. Bendsøe and C. A. Mota Soares (eds.), Kluwer, NATO ASI series, 227, pp 219–238, 1993.

[7] PETERSSON, J. and SIGMUND, O.: Slope constrained topology optimization, To appear in International Journal of Numerical Methods in Engineering.

[8] TURTELTAUB, S. and WASHABAUGH, P., xxx, *xxx*, Publication pending.

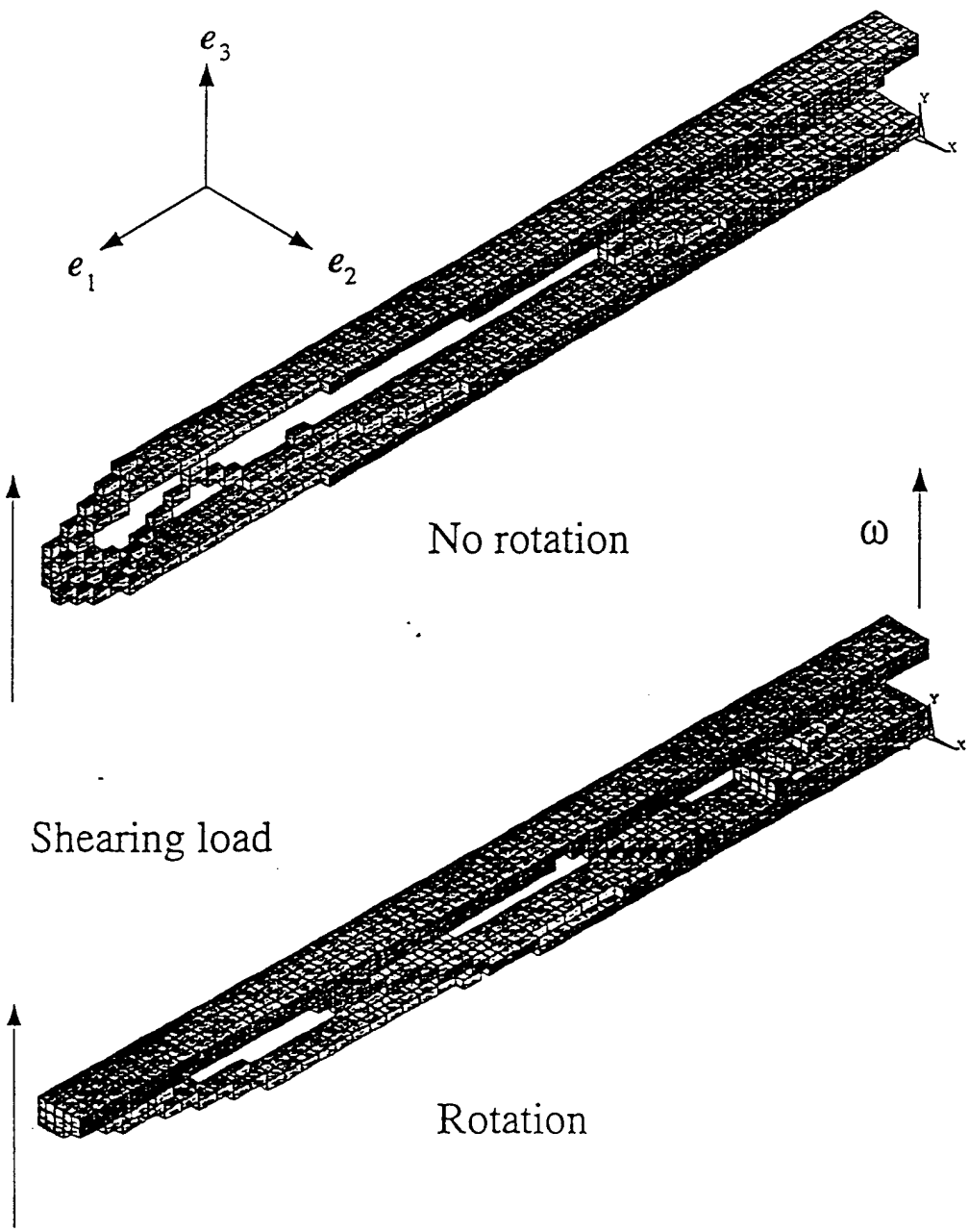

Figure 1: Case 1 (shear force): isometric plot of the optimal design *without* a field force (top) and *with* a field force (bottom). For clarity, only half of the design is shown (i.e., for $x \in [-h, 0]$).

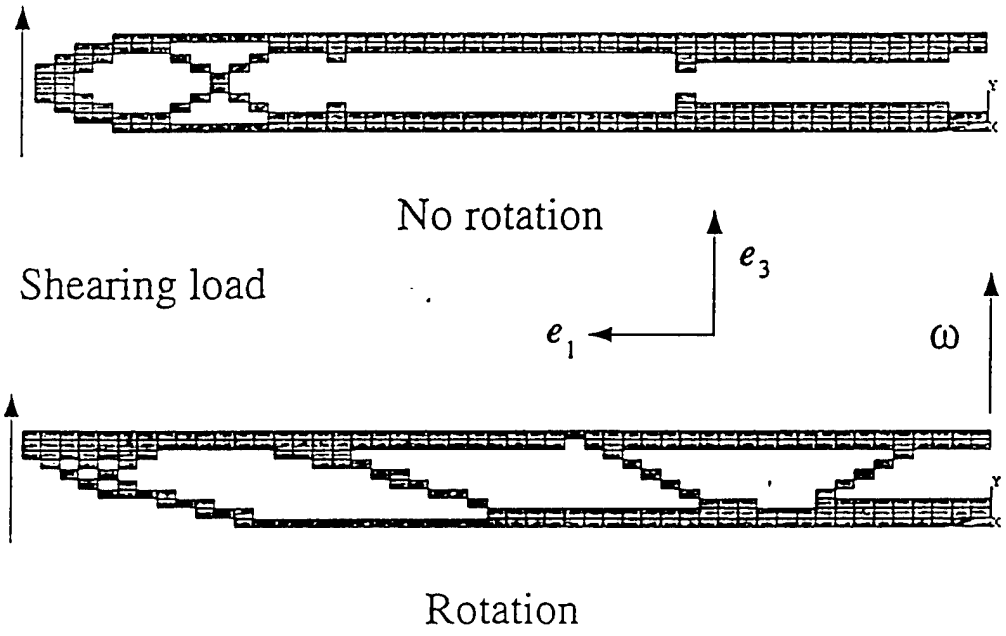

Figure 2: Case 1 (shear force): right view of the optimal design *without* a field force (top) and *with* a field force (bottom).

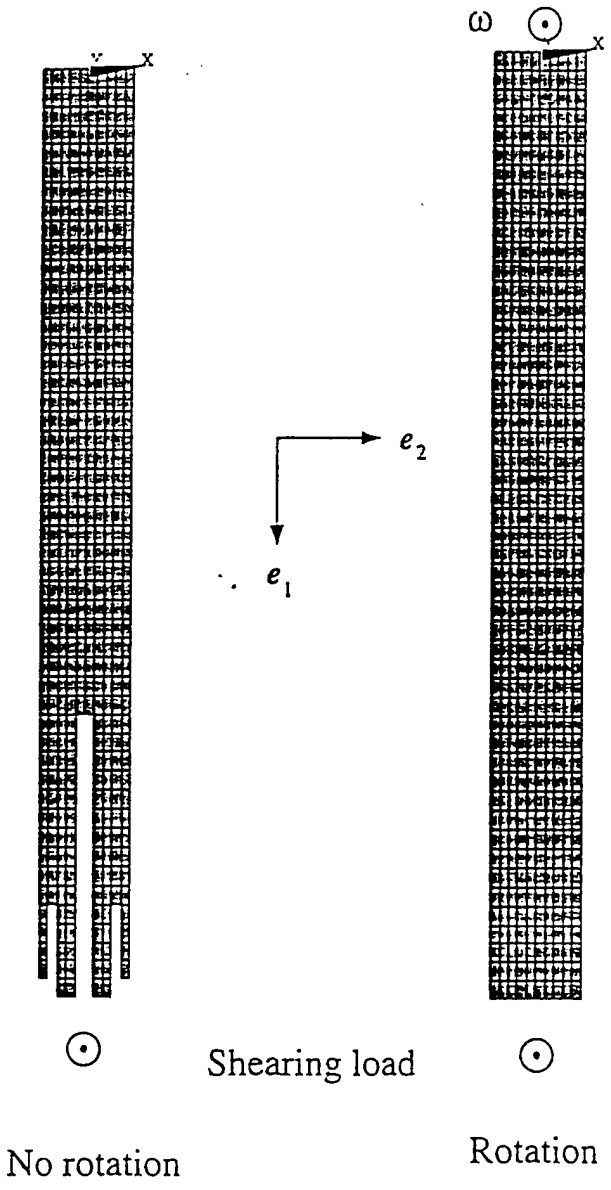

Figure 3: Case 1 (shear force): top view of the optimal design *without* a field force (left) and *with* a field force (right).

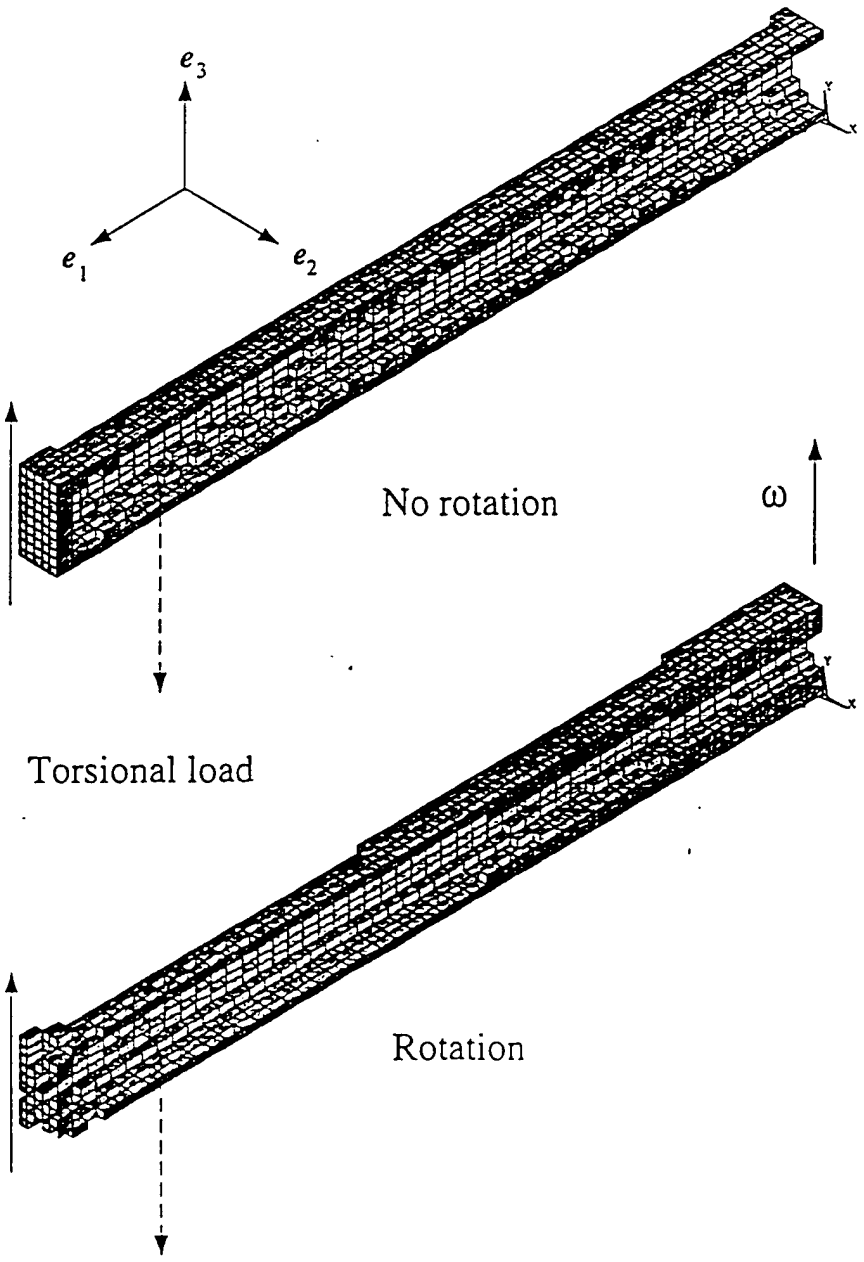

Figure 4: Case 2 (torsional force): isometric view of the optimal design *without* a field force (top) and *with* a field force (bottom). For clarity, only half of the design is shown (i.e., for $x \in [-h, 0]$).

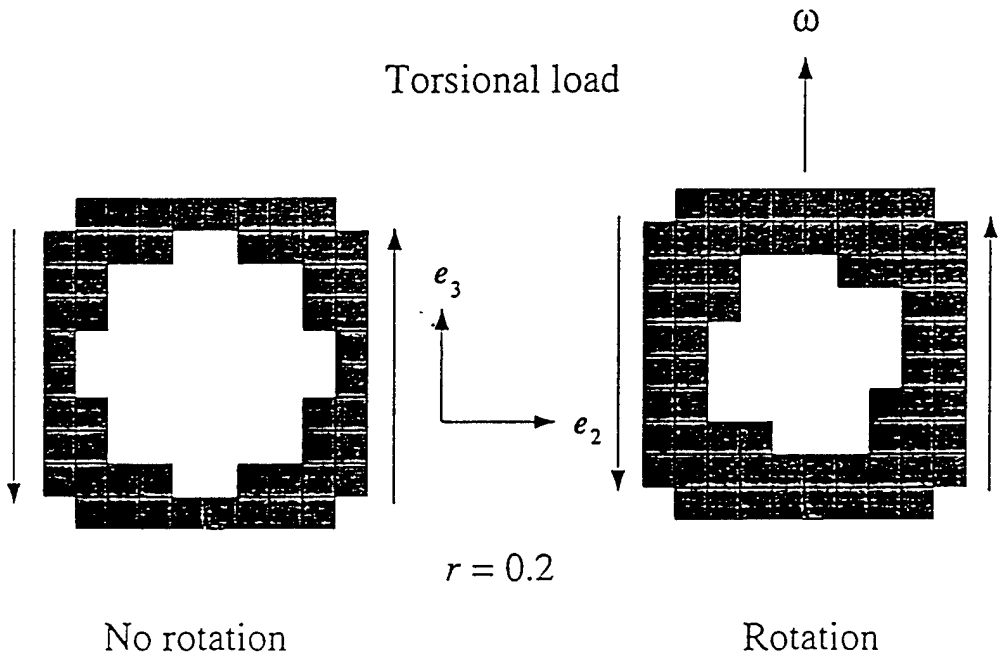

Figure 5: Case 2 (torsional force): cross-sectional view the of optimal design (for $r = 0.2$) *without* a field force (left) and *with* a field force (right).

A Design Model to Predict Optimal Two-Material Composite Structures

H. Rodrigues
IDMEC-Instituto Superior Técnico
Av Rovisco Pais, 1096 Lisboa Codex, Portugal
hcr@alfa.ist.utl.pt

Ciro A. Soto
Ford Research Laboratories
Dearborn, Michigan 48121-2053, USA
csoto@ford.com

J.E. Taylor
University of Michigan
Ann Arbor, Michigan 48109, USA
janos@engin.umich.edu

Abstract A method is presented for the prediction of optimal configurations for two-material composite continuum structures. In the model for this method, both local properties and topology for the stiffer of the two materials are to be predicted. The properties of the second, less stiff material are specified and remain fixed. At the start of the procedure for computational solution, material composition of the structure is represented as a pure mixture of the two materials. This design becomes modified in subsequent steps into a form comprised of a skeleton of concentrated stiffer material, together with a nonoverlapping distribution of the second material to fill the original domain. Computational solutions are presented for two example design problems. A comparison among solutions for different ratios of stiffness between the two materials gives an indication of how the distribution of concentrated stiffer material varies with this factor. An

example is presented as well to show how the method can be used to predict an efficient layout for rib-reinforcement of a stamped sheet metal panel.

1. Introduction

We address the problem of how to predict the optimal configuration of a continuum structure composed of two distinct, linearly elastic materials. The problem is cast in a form that has the stiffer of the component materials treated as 'designable', while properties of the second, less-stiff material are taken to be specified and fixed. The goal in the treatment of this design problem is twofold: i) to determine the local properties of the concentrated stiffer material and ii) to determine its the optimal topology, imbedded in the second material which occupies all the remainder of the original domain of the structure. The intention is that this result simulates an optimally reinforced two-material composite continuum structure. An interpretation of the model for computational solution is applied to produce example results in 2D and 3D showing the form of such designs. As another type of application, the modeling technique is applied to design the optimal layout for rib-reinforcement in a stamped sheet metal panel.

The analytical formulation for the composite design problem is based on the concept that has a designable continuum material represented (for linearly elastic material) by its constitutive tensor. The paper by Bendsøe et al. (1994) evidently is the first example where the arbitrary tensor-valued function representing material properties is treated directly as the design variable. [A quite different approach to represent variable material property within a design problem is described in Jacobs et al. (1997)]. In that presentation as well as subsequent other applications [see e.g. Bendsøe et al. (1995, 96); Bendsøe (1995)], the design objective was to minimize compliance and the global cost (isoperimetric) constraint was expressed in terms of the trace or the second order invariant of the modulus tensor. The present formulation is stated for the same objective, and for the cost constraint based on the trace measure of the modulus tensor.

Results from the cited earlier design formulations are comprised of a prediction of the local form of the optimal material (a zero-shear stiffness, orthotropic material in the case of single-purpose design), together with the (continuously varying) distribution of the trace of the modulus tensor, the latter representing a measure of merit of the material. In the present setting, the corresponding result has the form of an optimal distribution of a pure mixture of the two

constituent materials, having effective modulus equal to the sum of the constituent moduli. In order to be able to determine the design for a physically realistic composite material, i.e. a structural composite where the two materials are distinct, a recently described technique [Guedes and Taylor (1997a,b), Pawlicki et al. (1998) for example applications in 3D] for the computational prediction of optimal topology is applied. The technique, which differs sharply from the familiar approach [see e.g. Bendsøe (1995), Olhoff et al. [1997], amounts to a step by step computational procedure, making use of the above described continuously varying design as a starting point. A finite sequence of repeated solutions to the original design problem, each with stepwise, ordered modification to the 'unit cost distribution', leads to the final result in the form of a composite having the two materials appear as effectively distinct but mechanically combined. (A distinctly different example where 'overlap of materials' is addressed is reported in Rozvany et al. (1982).)

To summarize the contents of the paper, the model for prediction of the optimal composite continuum structure is described first in the form of an algorithm, where the elements described above are identified with steps in the algorithm, as are the means to manage the step-wise procedure itself. Implementation of the procedure into a form suitable for the production of computational results is described next. Example results are presented for the 'finite composite design' of a cantilevered beam under end load, and for a clamped beam subject to a distributed load. Sets of results are obtained for both examples to indicate how the layout of the stiffer material (reinforcement) is affected by varying the relative stiffness of the two materials. As indicated earlier, the model for composite design also is applied to predict optimal patterns for rib reinforcement of a sheet metal panel [the interpretation may be contrasted to the treatment of reinforcement of plates in Diaz et al. (1995)], and computational results for an example of this application are presented as well.

2. Model for the procedure

Let us consider the linear elastic structure occupying domain Ω, subjected to body forces $\mathbf{f}$, boundary tractions $\mathbf{t}$ and zero displacement on boundary Γ_u. The structure will be composed of two materials identified respectively by their elasticity tensors $\mathbf{E}^1$, for the weaker material and $\mathbf{E}^2$ for the stiffer material (see Figure 1 a). In a simple fiber-reinforced composite, for example, the two moduli might correspond to the matrix and the fiber materials, respectively.

The problem we address here is the following. Assuming that the domain Ω occupied by the complete composite structure is specified and fixed, and given an upper bound on the amount of available material `2` (stiffer material), we seek to identify optimal properties and topology of material `2` imbedded in material `1` , with no overlap of the less stiff material in the region of the stiffer one (see Figure 1 b). The objective for optimal design is to maximize a measure of the overall stiffness of the structure. The $\mathbf{E}^1$ material properties are taken to be specified and fixed, with $\mathbf{E}^1 > 0$. With Ω_2 to symbolize the part of the domain taken up by concentrated material '2' (to be optimally designed), it is required that in the final design $\Omega_1=\Omega - \Omega_2$. Since the structural domain Ω is fixed, this indicates that material '1' fills the part of the original domain not occupied by the optimal material '2' without overlap.

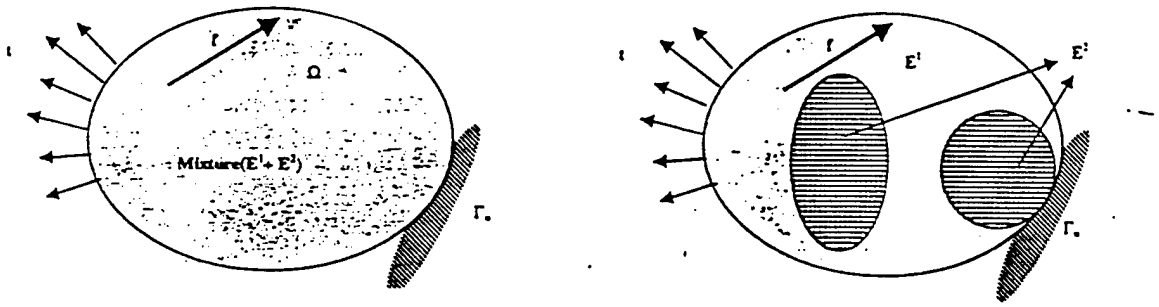

a) Initially as a perfect mixture. b) As a two material composite.

Figure 1- The structure subjected to body force f and boundary traction t.

In order to solve the problem described above, the following procedure is proposed:

Initial design

As a first step assume that one has a perfect mixture of the two materials (i.e. the effective material tensor of the mixture is given by $\mathbf{E}^{eff}=\mathbf{E}^1+\mathbf{E}^2$; note that for the 2D model to simulate laminated structure [see e.g. Pedersen (1993)] the 'mixture' provides an authentic model for the effective material modulus). Again, recall that at the final design the materials are to be effectively separated.

For this mixture and identifying the trace of the $\mathbf{E}^2$ tensor as the sensible measure of the material ($\rho = tr(\mathbf{E}^2)$), design material '2' to obtain its optimal local properties and distribution in Ω. Here the resulting design, obtained using the method described in Bendsøe et al. (1994), is

represented by continuously varying ρ (the plot of ρ is sometimes referred to as the 'shades of gray' diagram). Once this solution for the optimal material and its distribution over the structure are known, a finite number of optimization sub-problems are performed to predict a refinement of it into a design having total material separation and concentration of material '2' at its upper bound. The redesign of material '2' is accomplished using a method (Guedes and Taylor 1997 a) for the prediction of optimal topology. The method is applied stepwise, where in each step a gradually higher value of unit cost is ascribed to regions of relatively low value of ρ. Specific details are provided next, where the procedure is first described formally in the form of an algorithm, and is later expressed for computational treatment using a finite element interpretation of the continuum structure.

2.1. Algorithm

It is assumed that an initial design (the shades of gray results described above) has been obtained. Based on this result and recalling that 'design' is represented by the ρ field, the algorithm is described as follows:

Step 1: Define an increasing sequence of N evenly spaced cutoff values ρ_k^c, $k=1,2...N$ such that $\rho_k^c = \frac{\overline{\rho}}{\mathrm{N}}$ and $\rho_N^c = \overline{\rho}$; $\rho_k^c = k\left(\frac{\overline{\rho}}{\mathrm{N}}\right)$. An optimization sub-problem is to be solved for each value of ρ_k^c, where index k identifies steps in the procedure. The number N designates the number of steps to achieve the final design. Both N and the upper bound $\overline{\rho}$ are prescribed. Considerations of how properly to select values of these data are discussed below.

Step 2: For a given cut off value ρ_k^c, identify the following sub-domains of the structure:

$$\Omega_k^+ = \left\{x \in \Omega : \rho_k \geq \rho_k^c\right\}, \text{ sub-domain with higher value of material measure } \rho \qquad (1)$$

$$\Omega_k^- = \left\{x \in \Omega : \rho_k < \rho_k^c\right\}, \text{ sub-domain with lower value of material measure } \rho \qquad (2)$$

$\overline{\Omega}_k = \{x \in \Omega : \rho_k = \overline{\rho}\}$, sub-domain with material measure ρ at its upper bound. (3)

Recall that ρ is identified as the trace measure of the elasticity tensor $\mathbf{E}^2$, and note that $\overline{\Omega}_k \subset \Omega_k^+$ and $\Omega_k^+ \cup \Omega_k^- = \Omega$.

Step 3: With the objective of driving the designable material at each point to either its upper $(\overline{\rho})$ or lower $(\underline{\rho})$ bound value, a unit relative cost coefficient ω is modified stepwise in a manner to exaggerate the cost of material wherever ρ has value below the cutoff. Specifically, the relative unit cost function based on the results at step k is set equal to the constant value one or $\overline{\omega}$ according to

$$\omega_k = \begin{cases} 1 \ for \ x \in \Omega_k^+ \\ \overline{\omega} \ for \ x \in \Omega_k^- \end{cases} \tag{4}$$

with value of the constant $\overline{\omega} >> 1$.

Total cost at the $(k+1)st$ step is evaluated according to:

$$\int_\Omega \omega_k \rho_{k+1} \, d\Omega \ . \tag{5}$$

Step 4: Once the relative unit cost is defined, optimize the material '2' elasticity tensor $\mathbf{E}^2$, *i.e.*, determine the measure ρ_{k+1} and the remaining attributes of $\mathbf{E}^2$ using the cost distribution determined in step 3. This is accomplished by solving the (shades of gray) problem:

$$\underset{\substack{\mathbf{E}^2 \\ 0<\underline{\rho} \le \rho_{k+1} = tr(\mathbf{E}^2) \le \overline{\rho}}}{Min} \left\{ \int_\Omega f_i u_i d\Omega + \int_\Gamma t_i u_i d\Gamma \right\} \tag{6}$$

subjected to the following constraints:

$$\int_\Omega \left(1 - \chi(\overline{\Omega}_k)\right) E^1_{ijkl} \, e_{ij}(\mathbf{u}) \, e_{kl}(\mathbf{v}) d\Omega + \int_\Omega E^2_{ijkl} \, e_{ij}(\mathbf{u}) \, e_{kl}(\mathbf{v}) d\Omega -$$
$$- \int_\Omega f_i v_i \, d\Omega - \int_{\Gamma_t} t_i v_i \, d\Gamma = 0 \quad \forall \, \mathbf{v} \in \mathbf{V} \tag{7}$$

$$\int_{\Omega_1^-} \rho_{k-1}\, d\Omega + \int_{\Omega_2^-} \overline{\omega}\, \rho_{k-1}\, d\Omega \le R. \tag{8}$$

where V represents the set of admissible displacements and where $\chi\left(\overline{\Omega}_k\right)$ is the characteristic function defined in terms of the set $\overline{\Omega}_k$ as:

$$\chi\left(\overline{\Omega}_k\right) = \begin{Bmatrix} 1 \;\; for \;\; x \in \overline{\Omega}_k \\ 0 \;\; for \;\; x \notin \overline{\Omega}_k \end{Bmatrix} \tag{9}$$

Note that u and $\mathbf{E}^2$ in (7) are intended to stand for the solution of the current step.

An alternative, equivalent statement of the equilibrium condition (7) is:

$$\int_{\Omega-\overline{\Omega}_k} \left(E^1_{ijkl} + E^2_{ijkl}\right) e_{ij}(\mathbf{u})\; e_{kl}(\mathbf{v})\, d\Omega + \int_{\overline{\Omega}_k} E^2_{ijkl}\, e_{ij}(\mathbf{u})\; e_{kl}(\mathbf{v})\, d\Omega -$$
$$- \int_{\Omega} f_i v_i\, d\Omega - \int_{\Gamma_t} t_i v_i\, d\Gamma = 0 \quad \forall\, \mathbf{v} \in \mathbf{V} \tag{10}$$

Note that in form (10) for the problem, separation of the structure in Ω into the domain $\overline{\Omega}_k$ where $\rho(\mathbf{x}) = \overline{\rho}$ and the remaining $\Omega - \overline{\Omega}_k$ is reflected explicitly in the integrals.

The lower bound $\underline{\rho}$ is set to have the value on the order $10^{-7}\,\overline{\rho}$.

For the equilibrium constraint (7) note that the fixed material '1' exists (mixed with material '2') only where the measure of material '2' is not its upper bound *i.e.* material '1' is removed from the region with full material '2'. As the procedure converges this will provide full pointwise separation of the two materials. Also in the resource constraint we assume, as previously stated, that the material unit cost for higher value of the material measure ρ is equal to one, and for the lower value of the measure is $\overline{\omega} >> 1$. The distribution of material '1' is fixed during this step, and the solution obtained provides the description ρ_{k+1} of the trace of $(\mathbf{E}^2)_{k+1}$ as well as the current local material properties $\left(\mathbf{E}^2_{ijkl}\right)_{k+1}$.

Step 5: Set the cut off value to ρ^c_{k+1}

Go to step 2 and repeat the procedure until the limiting cutoff value $\overline{\rho}$ is reached.

2.2. Optimal distribution of the designable material

We will analyze in more detail the optimization subproblem to be solved in step 4 of the previous section. The aim of this step is to solve the following problem: For a prescribed material unit cost function $\omega(\mathbf{x})$ and fixed sets $\overline{\Omega}_k$, Ω_k^+ and Ω_k^-, find the optimal distribution of designable material as the one that minimizes the structural compliance (maximizes the stiffness) of the structure, as stated in the optimization problem (6-8).

Following the presentation in the cited Bendsøe et al. (1994) paper for the treatment of this problem, the optimization problem can be equivalently stated as,

$$\underset{\substack{\mathbf{E}^2 \geq 0 \\ \underline{\rho} \leq \rho = tr(\mathbf{E}^2) \leq \bar{\rho}}}{\text{Max}} \; \underset{v \in V}{\text{Min}} \left\{ \begin{array}{l} \dfrac{1}{2}\left[\displaystyle\int_\Omega \left(1 - \chi(\overline{\Omega}_k)\right) \mathbf{E}^1_{ijkl}\, e_{ij}(\mathbf{v})\, e_{kl}(\mathbf{v})\, d\Omega + \int_\Omega \mathbf{E}^2_{ijkl}\, e_{ij}(\mathbf{v})\, e_{kl}(\mathbf{v})\, d\Omega \right] - \\ - \displaystyle\int_\Omega f_i v_i \, d\Omega - \int_{\Gamma_t} t_i v_i \, d\Gamma \end{array} \right\} \tag{11}$$

subjected to the resource constraint ,

$$\int_{\Omega_k^+} tr(\mathbf{E}^2)\, d\Omega + \int_{\Omega_k^-} \overline{\omega}\, tr(\mathbf{E}^2)\, d\Omega \leq R\,. \tag{12}$$

Note that in this statement of the structural compliance optimization problem, the equilibrium constraint is interpreted in the form of a minimum potential energy statement.

The design variable $\mathbf{E}^2$ is characterized by the field $\rho(\mathbf{x})$ which identifies global distribution of the trace measure of $\mathbf{E}^2$, and by its local tensorial structure. The maximization problem in (11) can be split into two successive maximization problems (see Bendsøe et al. 1994), associated respectively with these 'field' and 'local structure' attributes of $\mathbf{E}^2$.

Thus (11) is rewritten as:

$$\underset{\underline{\rho} \leq \rho \leq \bar{\rho}}{Max} \; \underset{\substack{\mathbf{E}^2 \geq 0 \\ tr(\mathbf{E}^2) = \rho}}{Max} \; \underset{v \in V}{Min} \left\{ \begin{array}{l} \dfrac{1}{2}\left[\displaystyle\int_\Omega \left(1 - \chi(\overline{\Omega}_k)\right) E^1_{ijkl}\, e_{ij}(\mathbf{v})\, e_{kl}(\mathbf{v})\, d\Omega + \int_\Omega E^2_{ijkl}\, e_{ij}(\mathbf{v})\, e_{kl}(\mathbf{v})\, d\Omega \right] - \\ - \displaystyle\int_\Omega f_i v_i \, d\Omega - \int_{\Gamma_t} t_i v_i \, d\Gamma \end{array} \right\} \tag{13}$$

where the inner maximization identifies the optimal elasticity tensor within a prescribed value of the trace ρ (optimal relative values among tensor components) and the outer max establishes the

optimal distribution of the trace of the elasticity tensor within the prescribed upper and lower bounds (optimal material distribution).

From the fact that the resource constraint is only dependent on the design variable ρ, *i.e.*, on a norm of the tensor E^2 (the trace in our case) and not on its individual components, consider, for now, only the inner max min problem in (13). Following the same argument as presented in Bendsøe et al. (1994), the inner max and min can be interchanged as,

$$\underset{v\in V}{Min}\ \underset{\substack{E^2\geq 0\\ tr(E^2)=\rho}}{Max}\left\{\begin{array}{l}\dfrac{1}{2}\left[\displaystyle\int_\Omega \left(1-\chi(\overline{\Omega}_k)\right)E^1_{ijkl}\,e_{ij}(v)\;e_{kl}(v)\,d\Omega+\int_\Omega E^2_{ijkl}\,e_{ij}(v)\;e_{kl}(v)\,d\Omega\right]-\\ -\displaystyle\int_\Omega f_i v_i\,d\Omega-\int_{\Gamma_t} t_i v_i\,d\Gamma\end{array}\right\} \tag{14}$$

Following this transformation, the maximum can be solved analytically for the design variable E^2 and has the solution,

$$E^{2^*}_{ijkl}=\rho\,\frac{e_{ij}(v)e_{kl}(v)}{\left\|e_{ij}(v)\right\|^2} \tag{15}$$

with the optimal strain energy density equal to,

$$\frac{1}{2}E^{2^*}_{ijkl}\;e_{ij}(v)\;e_{kl}(v)=\frac{1}{2}\rho\,e_{ij}(v)\;e_{ij}(v)\;. \tag{16}$$

Substituting (16) into problem (13) one obtains,

$$\underset{0\leq\rho\leq\bar{\rho}}{Max}\ \underset{v\in V}{Min}\left\{\begin{array}{l}\dfrac{1}{2}\left[\displaystyle\int_\Omega \left(1-\chi(\overline{\Omega}_k)\right)E^1_{ijkl}\,e_{ij}(v)\;e_{kl}(v)\,d\Omega+\int_\Omega \rho\,\delta_{ik}\delta_{jl}\,e_{ij}(v)\;e_{kl}(v)\,d\Omega\right]-\\ -\displaystyle\int_\Omega f_i v_i\,d\Omega-\int_{\Gamma_t} t_i v_i\,d\Gamma\end{array}\right\} \tag{17}$$

subjected to the resource constraint ,

$$\int_{\Omega_t^-}\rho\,d\Omega+\int_{\Omega_t^-}\overline{\omega}\,\rho\,d\Omega\leq R\,. \tag{18}$$

(Note: Result (15) is valid only for one load condition).

The previous problem is a maxmin problem where the inner minimization has a unique solution. Thus the problem is differentiable and the necessary conditions for a maximum are,

$$\frac{1}{2}e_{ij}(\mathbf{u})e_{ij}(\mathbf{u}) - \Lambda - \eta_u = 0 \quad \forall x \in \Omega_k^- \tag{19}$$

$$\frac{1}{2}e_{ij}(\mathbf{u})e_{ij}(\mathbf{u}) - \overline{\omega}\Lambda + \eta_l = 0 \quad \forall x \in \Omega_k^- \tag{20}$$

where $\mathbf{u}(\mathbf{x})$ is the unique solution of the inner minimization *i.e.* the displacement of the structure at equilibrium. Note that these conditions are to be satisfied at the optimum.

In the previous conditions Λ is the Lagrange multiplier for the resource constraint and η_u and η_l are the multipliers for the upper and lower bound constraints respectively.

Complementarity conditions for the problem are:

$$\eta_u(\rho - \overline{\rho}) = 0, \eta_u \geq 0, \rho \leq \overline{\rho} \quad \forall \mathbf{x} \in \Omega \tag{21}$$

$$\eta_l(\underline{\rho} - \rho) = 0, \eta_l \geq 0, \rho \geq \underline{\rho} \quad \forall \mathbf{x} \in \Omega \tag{22}$$

$$\Lambda\left(\int_{\Omega_i^-} \rho \, d\Omega + \int_{\Omega_i^-} \overline{\omega}\,\rho \, d\Omega - R\right) = 0, \ \Lambda \geq 0 \tag{23}$$

It follows from (21, 22) that

$$\eta_u \eta_l = 0 \quad \forall \mathbf{x} \in \Omega \tag{24}$$

From the preceding conditions it can be shown that $\Lambda > 0$, implying that the resource constraint will be active.

2.3. Optimal distribution of the designable material (alternative formulation)

As an alternative to the part of the procedure of section 2.1 where the fixed material is removed, it is possible to reformulate the problem of optimal distribution of material so that the fixed material is gradually removed within the process of optimizing the material distribution.

With this purpose in mind, it is assumed that within the material distribution optimization, the domain occupied by the fixed material '1' is the complement of the domain $\overline{\Omega}(\rho) = \{\mathbf{x} : \rho = \overline{\rho}\}$, and consequently a function of ρ. Thus problem (13) is restated has,

$$\underset{0\le\rho\le\bar{\rho}}{Max}\ \underset{tr(E^2)=\rho}{\underset{E^2\ge 0}{Max}}\ \underset{v\in V}{Min}\left\{\begin{array}{l}\dfrac{1}{2}\left[\displaystyle\int_\Omega\left(1-\chi_\varepsilon\left(\overline{\Omega}(\rho)\right)\right)E^1_{ijkl}e_{ij}(v)\ e_{kl}(v)\,d\Omega+\int_\Omega E^2_{ijkl}\ e_{ij}(v)\ e_{kl}(v)\,d\Omega\right]-\\ -\displaystyle\int_\Omega f_i v_i\,d\Omega-\int_{\Gamma_t} t_i v_i\,d\Gamma\end{array}\right\} \tag{25}$$

where the $\chi_\varepsilon\left(\overline{\Omega}(\rho)\right)$ is an ε differentiable regularization of the characteristic function of the set $\overline{\Omega}(\rho)=\left\{x\in\Omega:\rho\ =\bar{\rho}\right\}$, having the properties (see Figure 2):

$$\chi_\varepsilon(\rho)=\begin{cases}1 & \text{if}\quad \rho=\bar{\rho}\\ \dfrac{(\rho+\varepsilon\bar{\rho}-\bar{\rho})^2(\varepsilon\bar{\rho}+2\bar{\rho}-2\rho)}{(\bar{\rho}\varepsilon)^3} & \text{if } (1-\varepsilon)\bar{\rho}<\rho<\bar{\rho}\\ 0 & \text{if } \rho\le(1-\varepsilon)\bar{\rho}\end{cases} \tag{26}$$

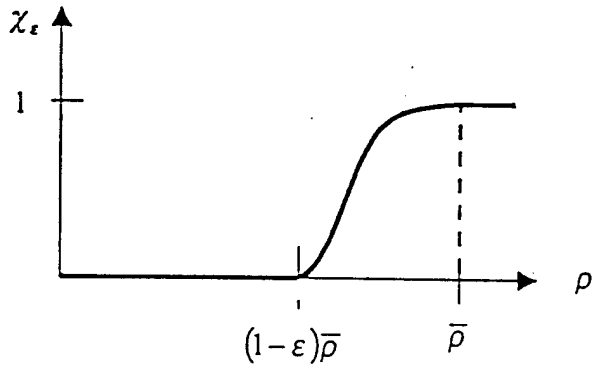

Figure 2- Regularization of the characteristic function.

Note that this regularization is non-symmetric in the ε neighborhood of $\bar{\rho}$ and thus imposes the effective separation of the two materials on the region $\overline{\Omega}(\rho)$ (*i.e.*, at all the points where $\rho=\bar{\rho}$).

Following the rationale of the previous section we will have the same characterization of the optimal material E^2 (15), but the necessary conditions on ρ (written for the entire domain) are,

$$-\left.\frac{d\chi_\varepsilon(\rho)}{d\rho}\right|_{\rho=\rho^*}E^1_{ijkl}e_{ij}(u)e_{kl}(u)+e_{ij}(u)e_{ij}(u)-\Lambda-\eta_u+\eta_l=0\quad\forall x\in\Omega \tag{27}$$

where, Λ, η_u and η_l satisfy the orthogonality conditions (21-24) and

$$\frac{d\chi_\varepsilon(\rho)}{d\rho} = \begin{cases} 0 & \text{if} \quad \rho = \bar{\rho} \\ \dfrac{6(\rho - \bar{\rho} + \varepsilon\bar{\rho})(\bar{\rho} - \rho)}{(\bar{\rho}\varepsilon)^3} & \text{if } (1-\varepsilon)\bar{\rho} < \rho < \bar{\rho} \\ 0 & \text{if } \rho \le (1-\varepsilon)\bar{\rho} \end{cases} \tag{28}$$

The purpose of this a regularization is to implicitly remove the fixed material $\mathbf{E}^l$ in regions within Ω where the designable material is at its upper bound. Note that for every $\varepsilon \neq 0$ the problem as stated in (25) is a meaningful design problem. However, the limit case (*i.e.*, when $\varepsilon=0$) is not a well posed problem, in the sense that one can get as close as one wants to the designable material upper bound and still have fixed material coexisting with the designable material.

3. Method for computational solution

As described above, the final structural topology is predicted through an iterative procedure where the designable material is concentrated at its upper bound $\bar{\rho}$ (remember that the trace of elastic tensor is identified as such a measure). This is attained through the solution of a series of material optimization sub-problems (defined in section 2.2) where the material unit cost is iteratively adjusted so that lower trace measures impose a higher cost on the resource distribution.

In the following, the implementation of these steps for computation is discussed.

3.1. Material unit cost

The basic idea behind a non-uniform material unit cost imposed on the resource constraint is to induce a concentration of the designable material at its upper bound (full material). As the first step, the optimization problem is solved initially assuming a uniform material unit cost. Based on results for this optimal solution, the structural domain is divided into two regions, the part Ω^- (below cutoff value ρ^c) and Ω^+ (the part above ρ^c), as defined earlier. Once these sets are

defined, one computes the new optimal material distribution imposing a higher unit cost on material in Ω^-, *i.e.* the resource constraint is now changed to,

$$\int_{\Omega^-} \rho \, d\Omega + \int_{\Omega^-} \overline{\omega} \, \rho \, d\Omega \leq R, \quad \overline{\omega} >> 1 \tag{29}$$

In figure 2 this process is simulated in a one-dimensional sketch for initial, intermediate and final distributions. Assuming that the material distribution is known for the initial design, the resulting distribution $\rho(\mathbf{x})$ for the subsequent steps (general step k and final step N) reflects a relative increase value in regions $(\Omega - \Omega^-)$. The increase for the k^{th} step, and the concentration of material at the upper bound for the final design are shown in separate curves.

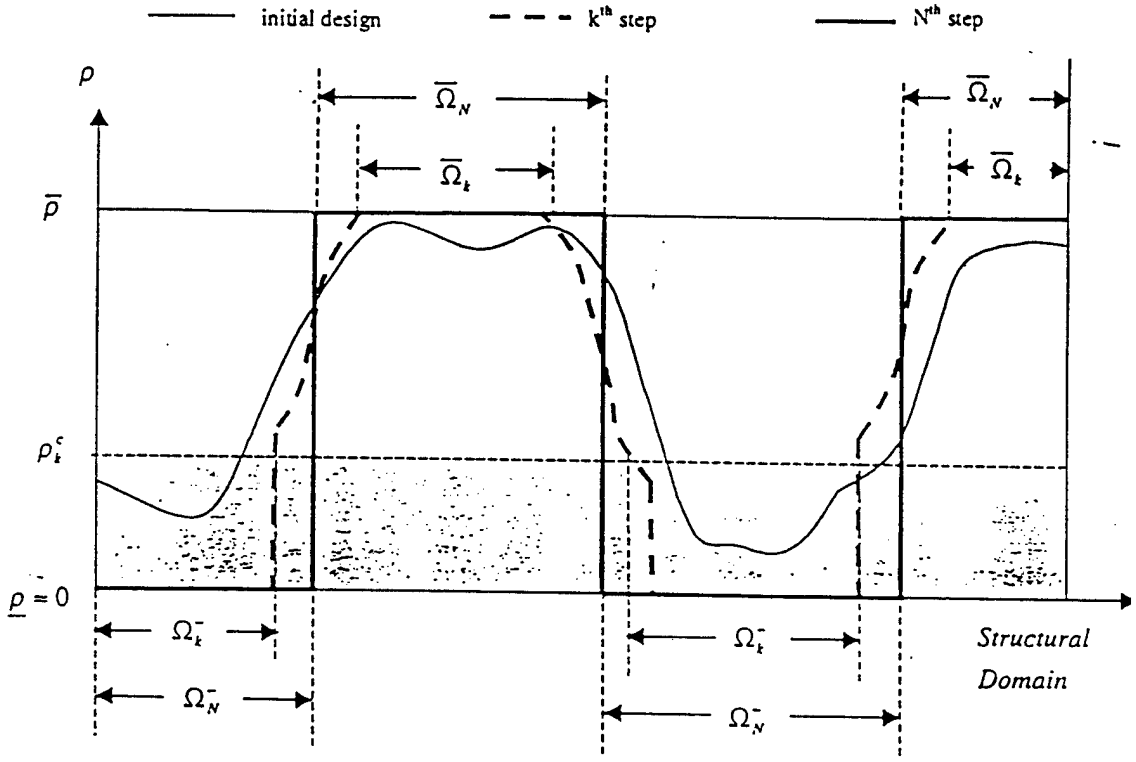

Figure 3- Sketch of material measure $\rho(x)$ for initial, intermediate and final designs (typical).

The idea behind this approach is simple, but one major feature of the method needs to be addressed. It follows from the fact that the procedure attributes higher unit costs according to regions occupied by low material measure ρ, rather than to the material itself. As a consequence, once a region is included in the Ω^- sub-domain it tends to remain there. To deal with such a feature, care should be taken in the selection of the number of cutoff values.

3.2. Optimal material distribution

Once the material unit cost function (ω_k at the k^{th} step of the topology design procedure) is defined, one can calculate the new optimal material distribution. Note that the domain occupied by the fixed material is known and fixed during this step.

The methodology adopted is based on a sequential solution of the optimality conditions (19, 20) with the strain field calculated using a finite element approximation of the elastostatic problem, characterized by the equilibrium statement (7) (the commercial program ANSYS was exploited for this purpose).

So based on the material unit cost for the procedure step k (ω_k) and assuming the design variable ρ^e constant at each finite element, one can write the optimality conditions separately for each element. From the discrete interpretation of the these conditions, and introducing the upper and lower bound constraint thickness parameter ζ (defined by the user), the solution is obtained by the fixed point method,

$$\left(\rho^e\right)_{i+1} = \begin{cases} \max\left[(1-\zeta)\left(\rho^e\right)_i, \underline{\rho}\right] & \text{if } \alpha^e\left(\rho^e\right)_i \le \max\left[(1-\zeta)\left(\rho^e\right)_i, \underline{\rho}\right] \\ \alpha^e\left(\rho^e\right)_i & \text{if } \max\left[(1-\zeta)\left(\rho^e\right)_i, \underline{\rho}\right] \le \alpha^e\left(\rho^e\right)_i \le \min\left[(1+\zeta)\left(\rho^e\right)_i, \overline{\rho}\right], \\ \min\left[(1+\zeta)\left(\rho^e\right)_i, \overline{\rho}\right] & \text{if } \min\left[(1+\zeta)\left(\rho^e\right)_i, \overline{\rho}\right] \le \alpha^e\left(\rho^e\right)_i \end{cases} \tag{30}$$

with the multiplier α^e given by,

$$\alpha^e = \frac{\left\langle e_{ij}(u) e_{ij}(u) \right\rangle_e}{2\omega_k \Lambda}. \tag{31}$$

for each finite element.

In the previous algorithm, the index 'e' ranges over all the finite elements, 'i' is the iteration counter and $< >_e$ identifies the average operator applied to the e^{th} element strain field.

The calculation of the Lagrange multipliers Λ is determined, within each iteration, through a updating scheme that imposes the resource constraint,

$$\left(\int_{\Omega_\varepsilon^-} \overline{\omega}\rho \, d\Omega + \int_{\Omega_\varepsilon^-} \rho \, d\Omega \right) = R \,. \tag{32}$$

In the case of the alternative formulation described in section 2.3, where the domain occupied with fixed material is gradually removed, the fixed point algorithm is as previously stated in (30) with the α^e factor given by,

$$\alpha^e = \frac{\left\langle e_{ij}(u) e_{ij}(u) \right\rangle_e}{2\left(\omega_k \Lambda + \frac{d\chi_\varepsilon}{d\rho} E^1_{ijkl} \left\langle e_{ij}(u) e_{ij}(u) \right\rangle_e \right)} \,. \tag{33}$$

4. Examples

The examples presented below, try to demonstrate the applicability of the developments described within the context of three-dimensional structural applications. The first two examples are discretized, for computational purpose with eight node isoparametric brick elements, an uniform finite element mesh and the computational procedure is programmed within the Ansys finite element software.

4.1. Example 1

The first example considered is the problem of finding the optimal topology of material '2' in an end loaded cantilever beam made of an isotropic material with Young Modulus E^1 and Poisson coefficient 0.2 (material '1'). The design domain has dimensions 20x12x1 (see Figure 4) and the resource constraint upper bound equals 40% of the volume of the design domain.

Material two has Young modulus upper bound of 10^9 Pa and a lower bound of 10^1 Pa. The black and white procedure takes N=40 steps and the shades of gray optimization (step 4 of the procedure) is limited to 5 iterations.

This example is the 3D equivalent of the 2D example described in Guedes and Taylor (1997). Even though three dimensional, the model would behave like a two-dimensional one due to the small design domain thickness. This fact will permit the comparison of the results obtained with

the ones presented for 2D solutions in the case of non-existent material '1' (see e.g. Guedes and Taylor (1997)).

The solutions obtained are shown for various ratios between the maximum Young modulus for material '2' (max E^2, attained at $\rho = \overline{\rho}$) and the Young modulus for the fixed material, E^1.

The first solution has a small value of this ratio (10^{-7}) and consequently is equivalent to the optimal topology design problem restricted to one material. The subsequent results consider higher material ratios.

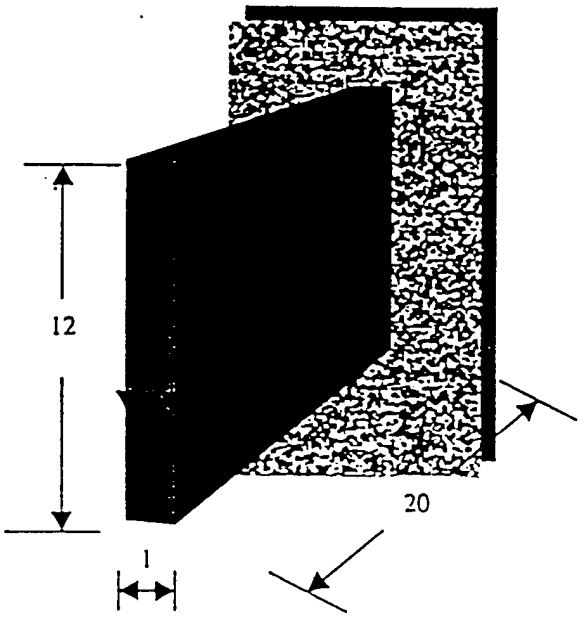

Figure 4- Design domain and boundary conditions.

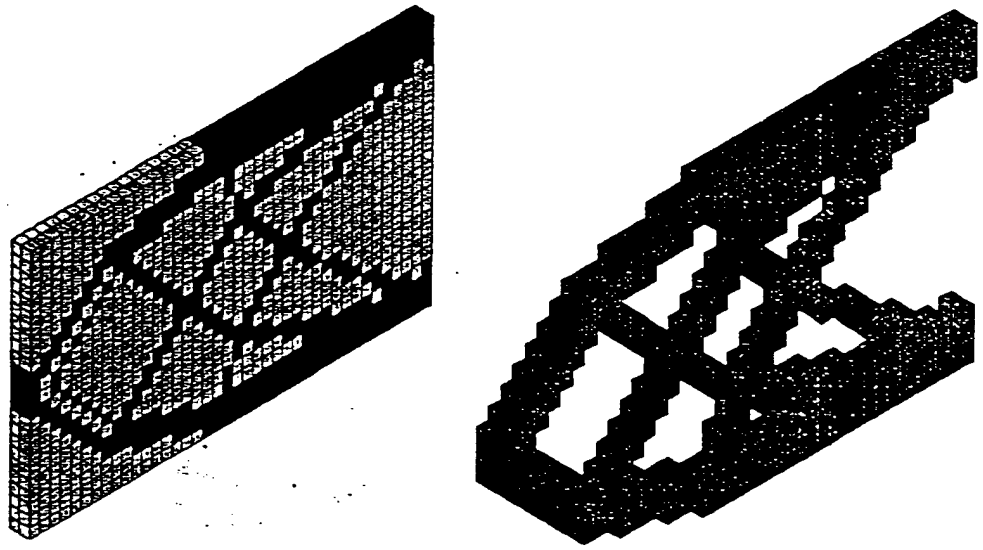

a) b)

Figure 5- Optimal topology for $E^1/(\max E^2)=10^{-7}$.

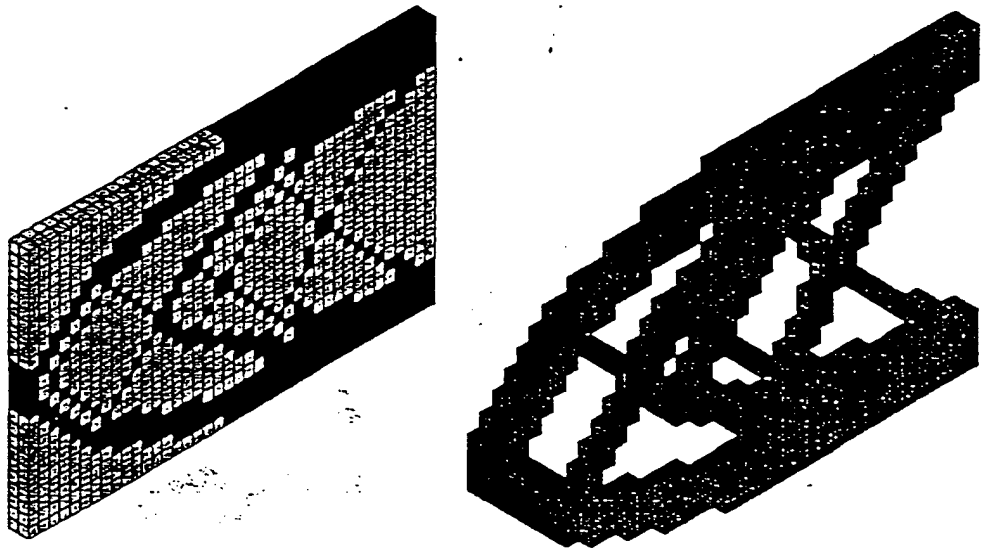

a) b)

Figure 6- Optimal topology for $E^1/(\max E^2)=1/50$.

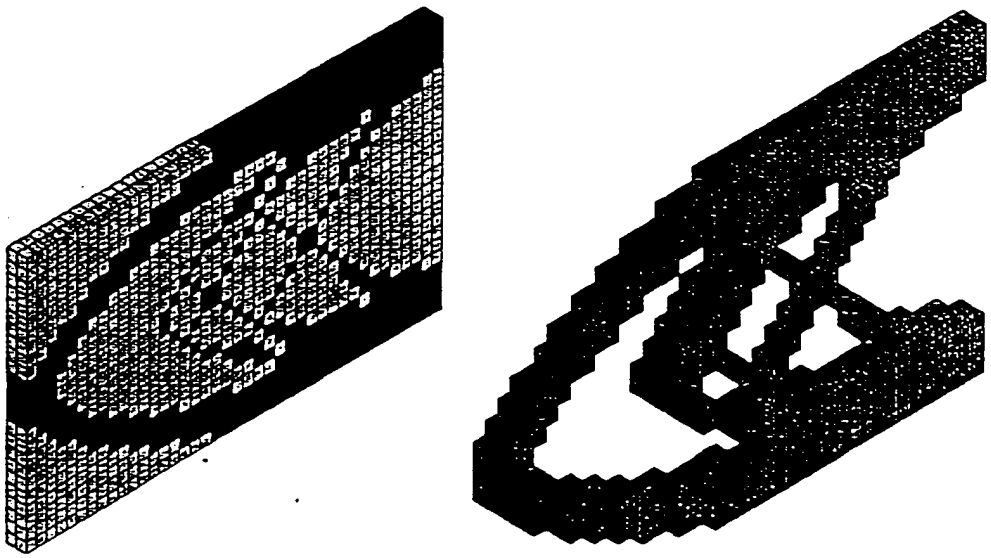

a) b)

Figure 7- Optimal topology for $E^1/(\max E^2)=1/10$.

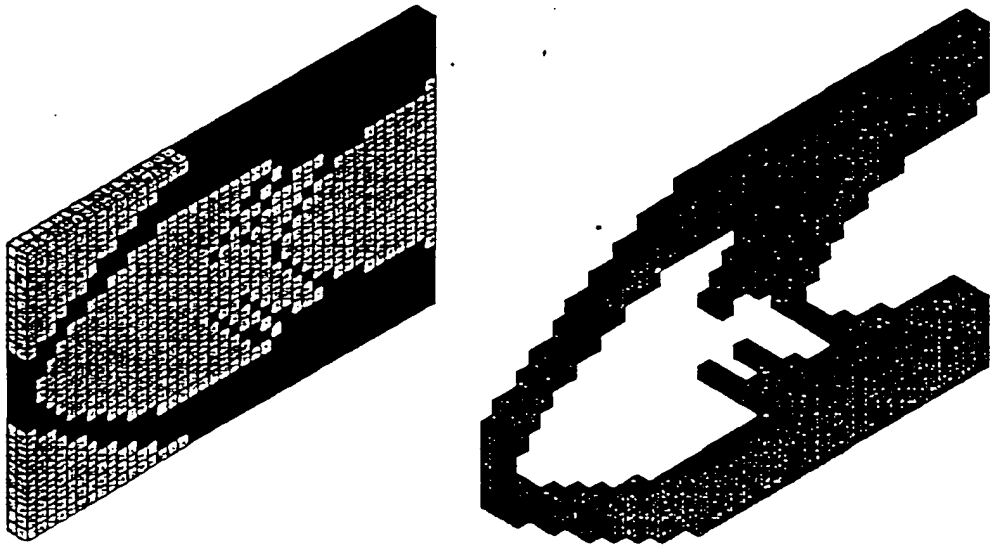

a) b)

Figure 8- Optimal topology for $E^1/(\max E^2)=1/3$.

Figures on the left show the designable material imbedded within the fixed material. In the right, and to better portray the final topology of the designable material, the fixed material is not shown. Note also that for representation purposes the designable material (material '2') is

identified in black color when the two materials are present and in lighter gray when material '1' is removed from the figure.

From the results obtained one can observe that the truss like structure inside the domain weakens as the material ratio increases. This is attributed to the fact that as material '1' is stiffened, it has an higher contribution in carrying the shear load present, thus freeing material '2' to support the bending load.

4.2. Example 2

This example considers the topology optimization of material '2' for the cantilever beam presented in Figure 9. The design domain has dimensions 8x8x20 and is discretized with 10264, eight node isoparametric brick elements. The applied force is restricted to a shear force distributed as shown below. The resource constraint upper bound is equal to 40% of the design domain volume. Material '2' has a Young modulus upper bound of 10^9 and a lower bound of 10^1. The black and white procedure was done in N=20 steps and the shades of gray optimization (step 4 of the procedure) is limited to 5 iterations.

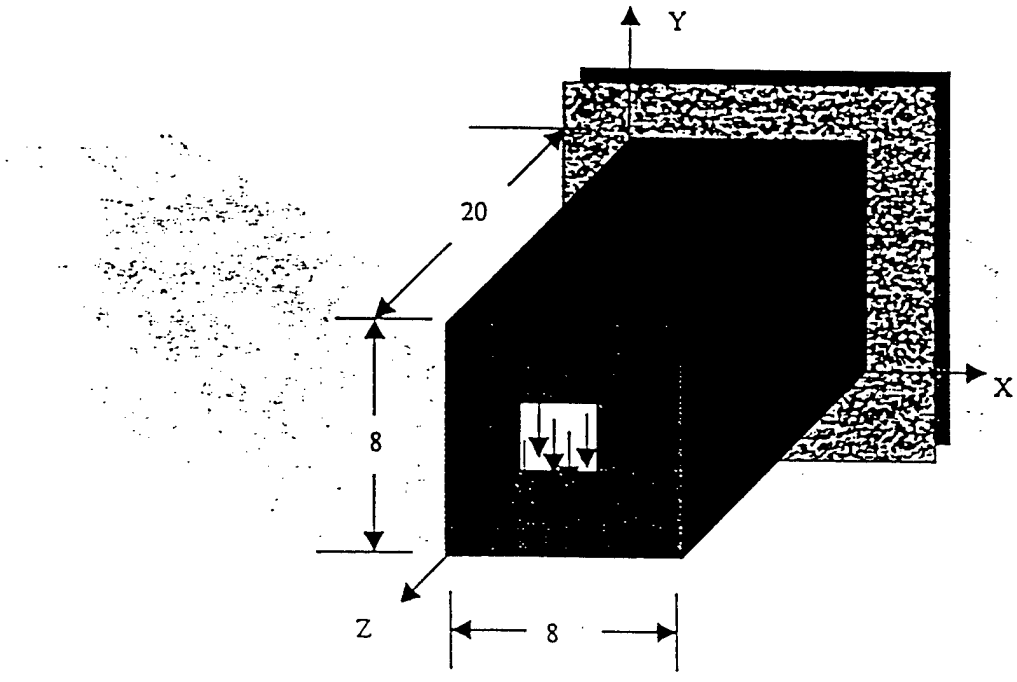

Figure 9 - Design domain and boundary conditions.

The figures below display the results obtained for different ratios of $E^1/(\max E^2)$. For this example, the fixed material ('1') is assumed isotropic. For each material ratio, the final result internal structure can be visualized in the various transversal and longitudinal cuts shown.

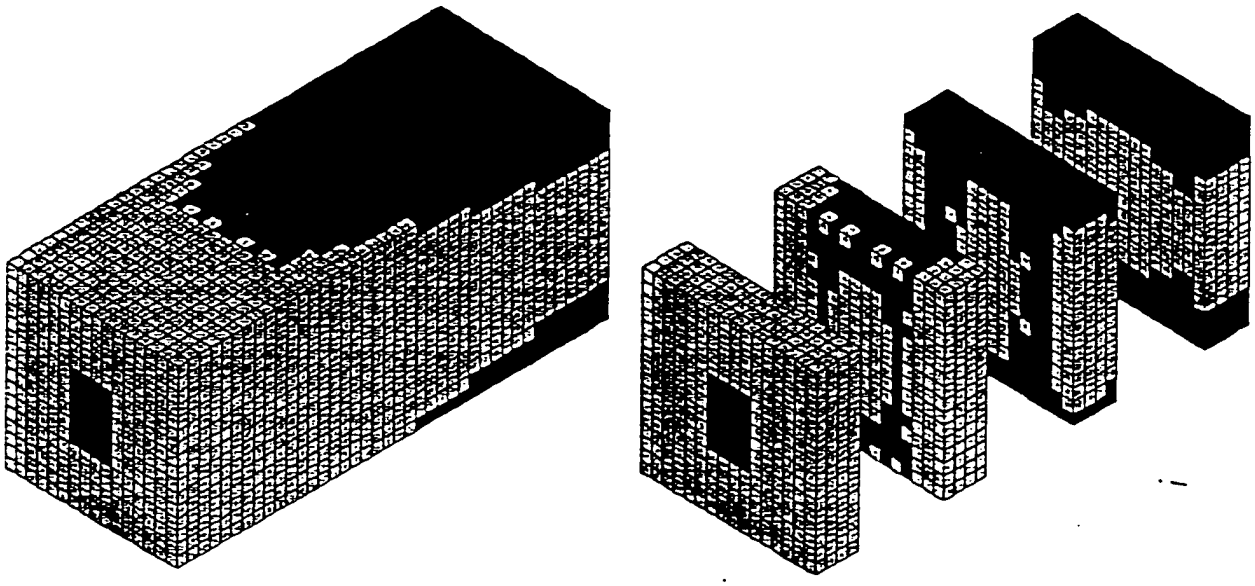

Figure 10 - Final topology for $E^1/(\max E^2)=10^{-7}$.

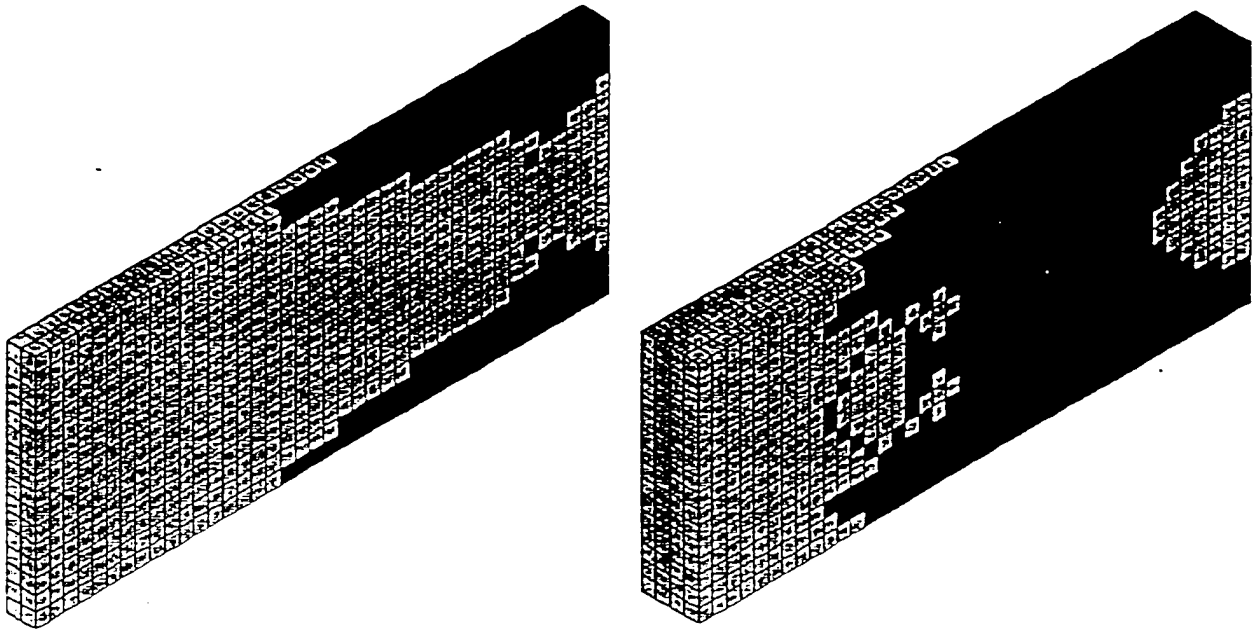

X=1

X=2

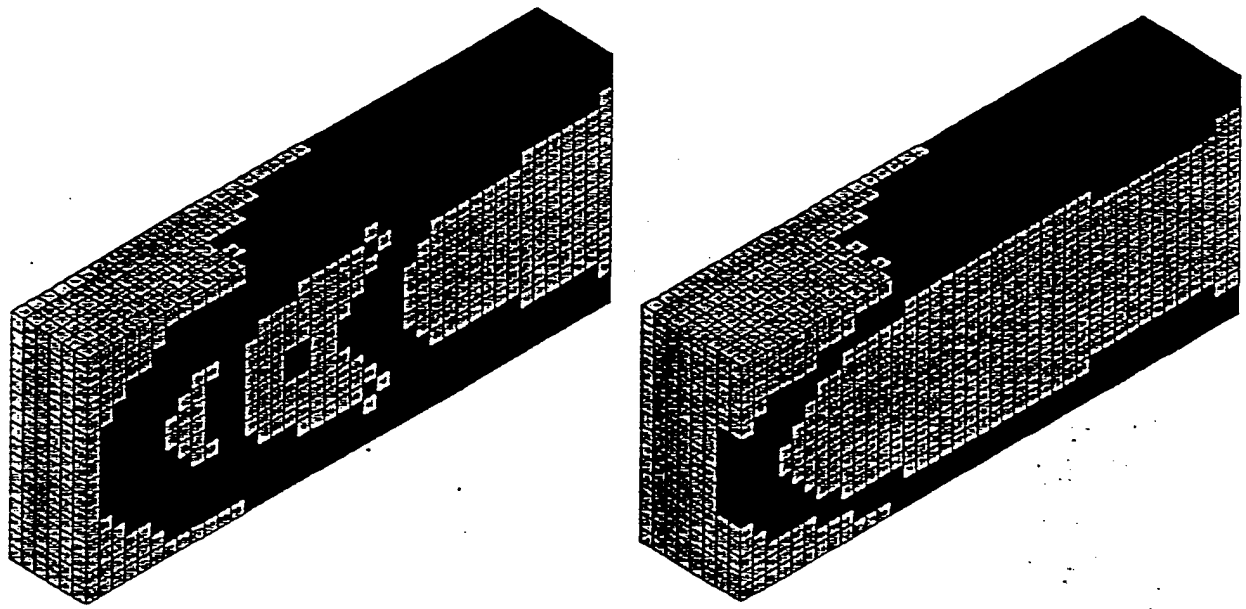

X=3 X=4

Figure 11- Final topology for $E^1/(\max E^2)=10^{-7}$ (longitudinal cuts).

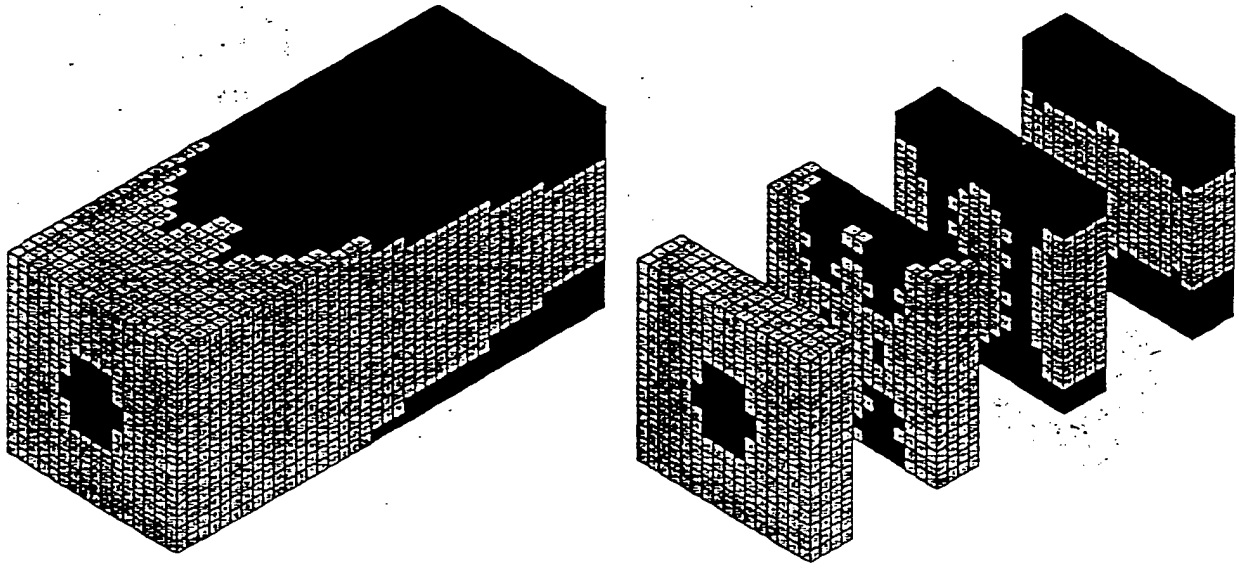

Figure12- Final topology for $E^1/(\max E^2)=1/10$.

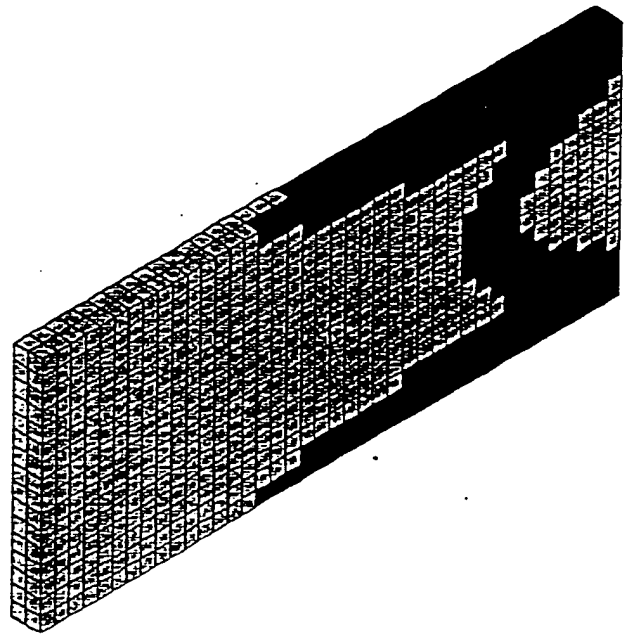

X=1

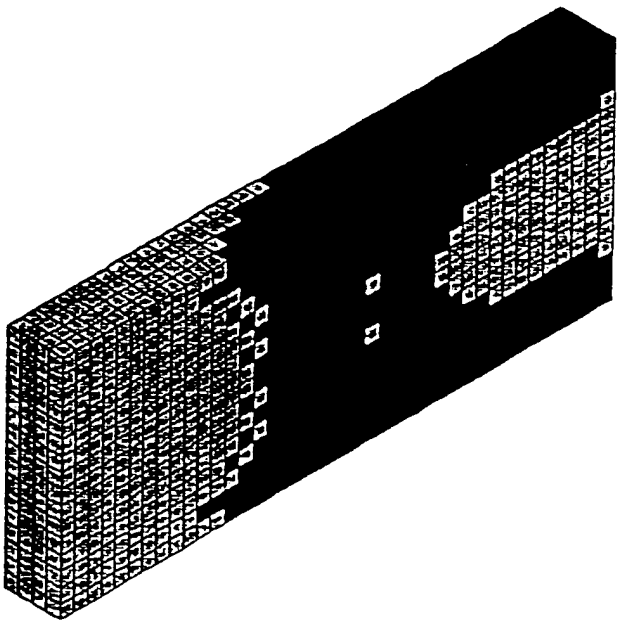

X=2

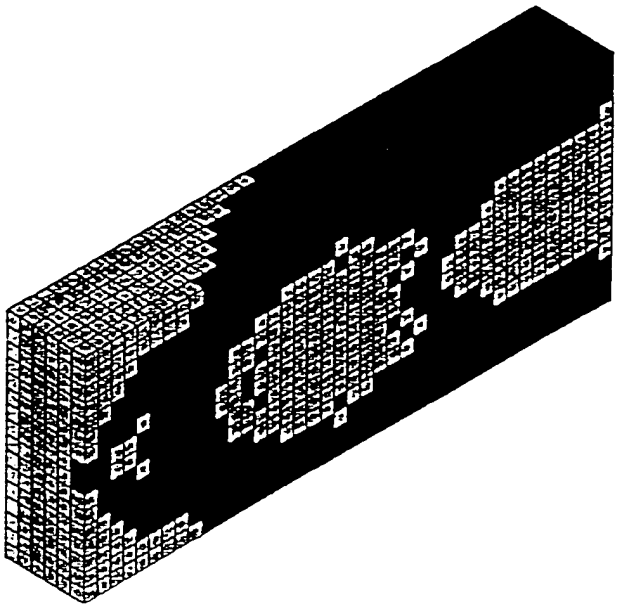

X=3

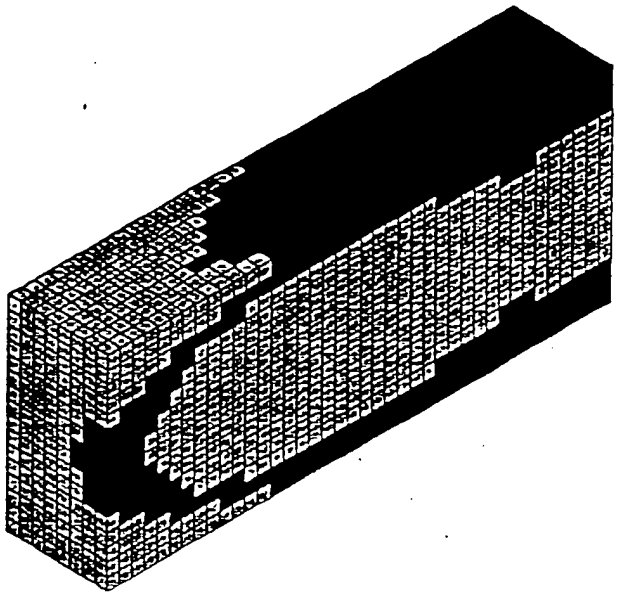

X=4

Figure 13- Final topology for $E^1/(\max E^2)=1/10$ (longitudinal cuts).

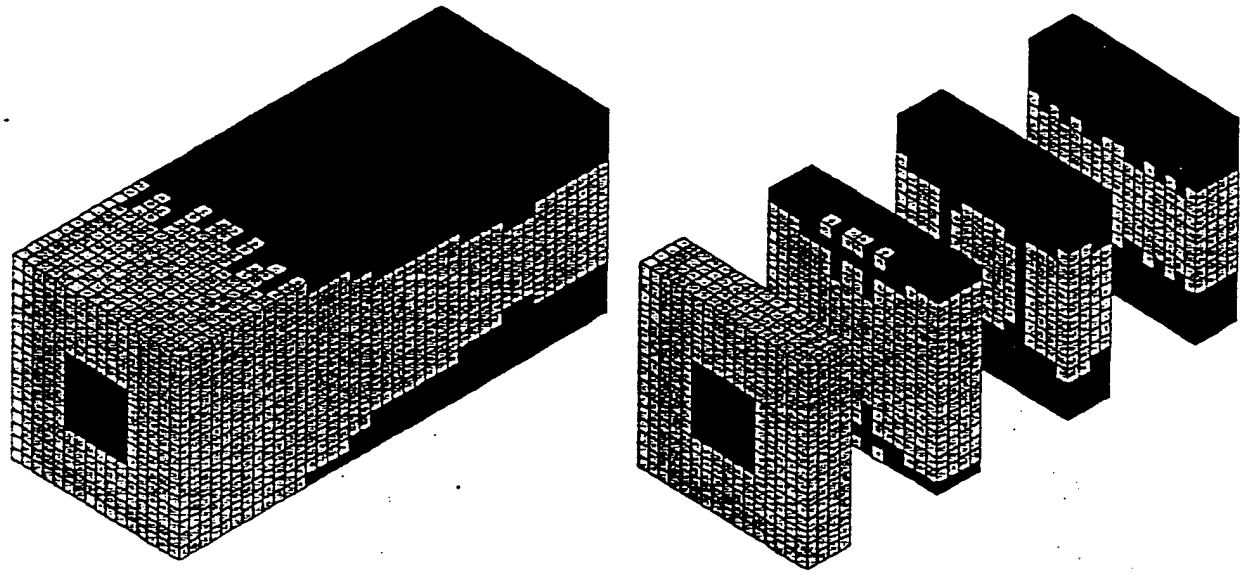

Figure 14- Final topology for $E^1/(\max E^2)=1/3$.

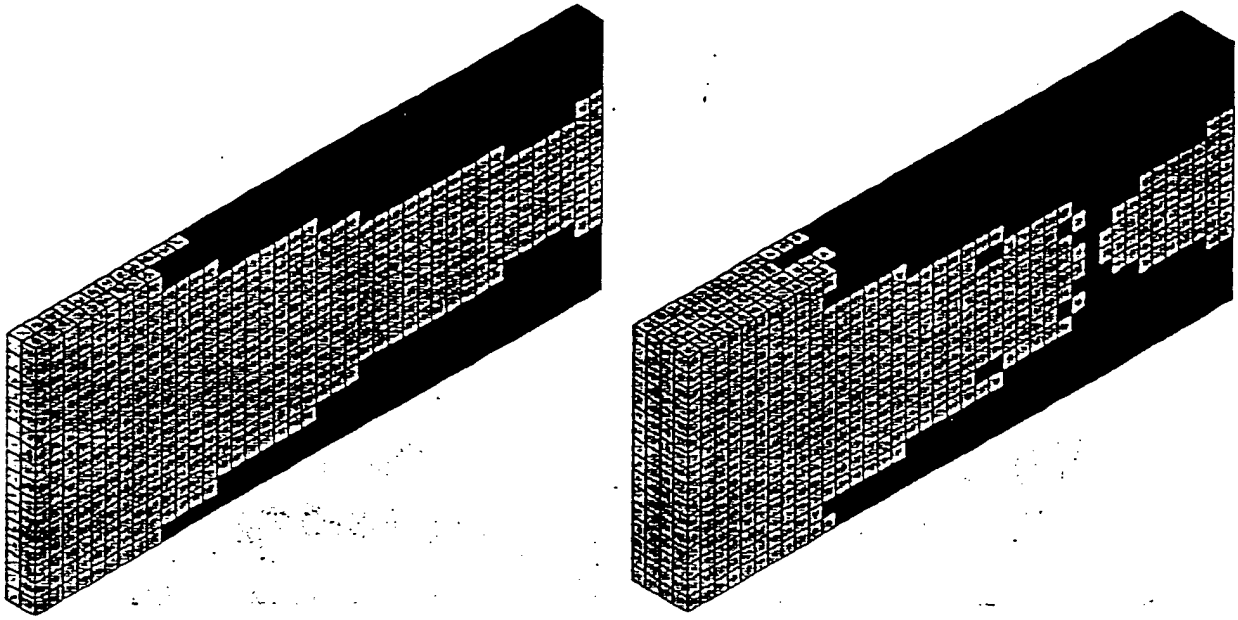

X=1

X=2

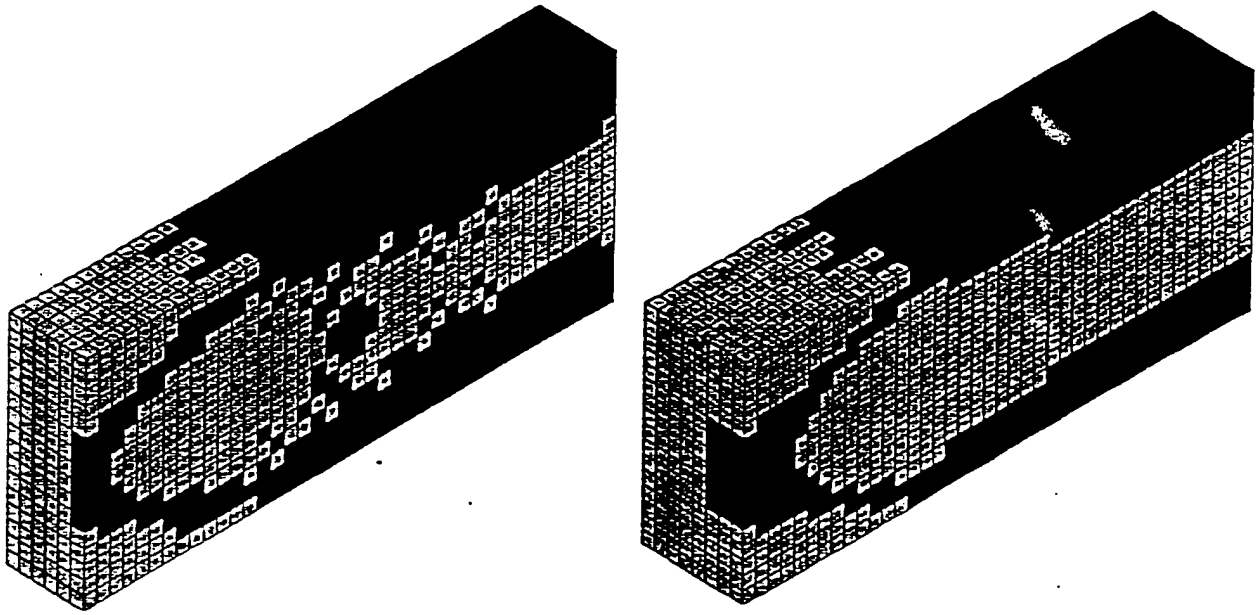

X=3 X=4

Figure 15- Final topology for $E^1/(\max E^2)=1/3$ (longitudinal cuts).

For this last material ratio, the next figure shows the final topology of material '2' with material '1' removed.

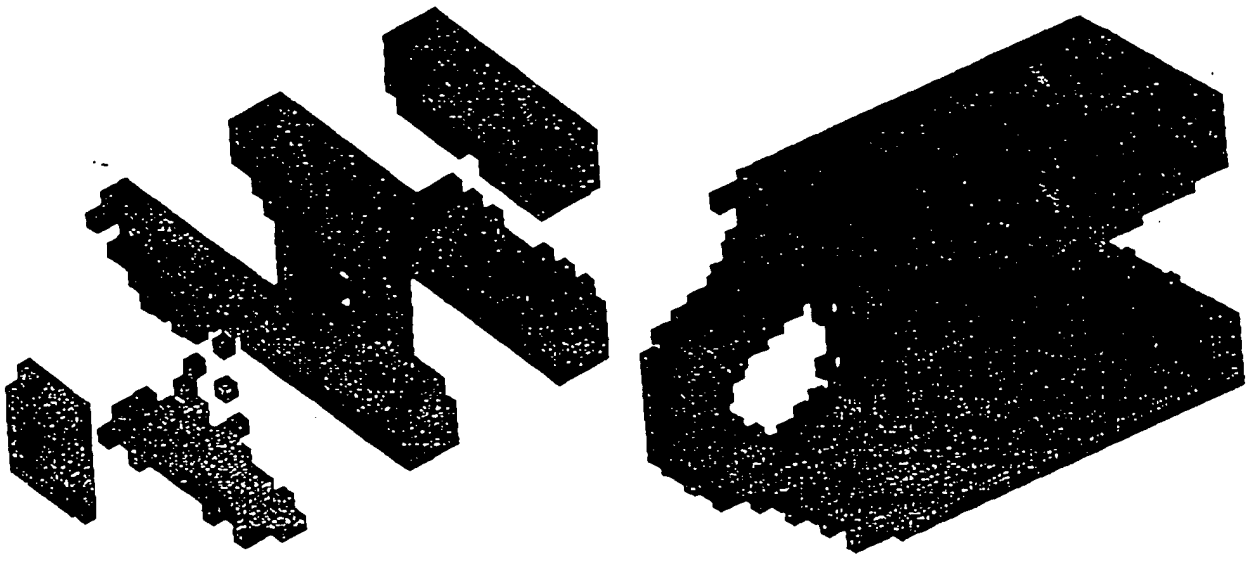

Figure 16- Final topology for $E^1/(\max E^2)=1/3$ (material one not shown).

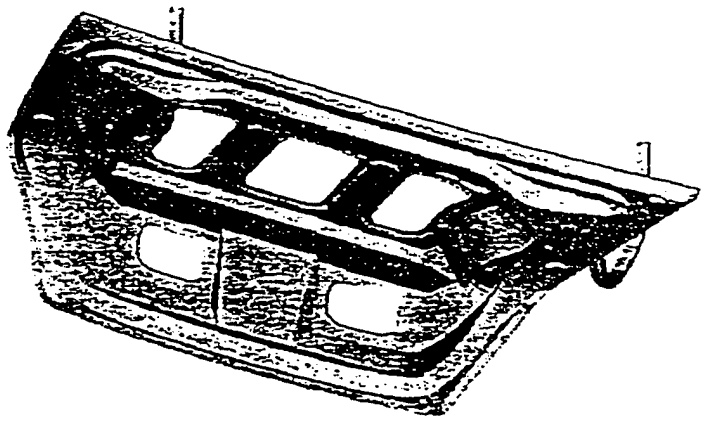

Figure 17- Computer model of the car decklid.

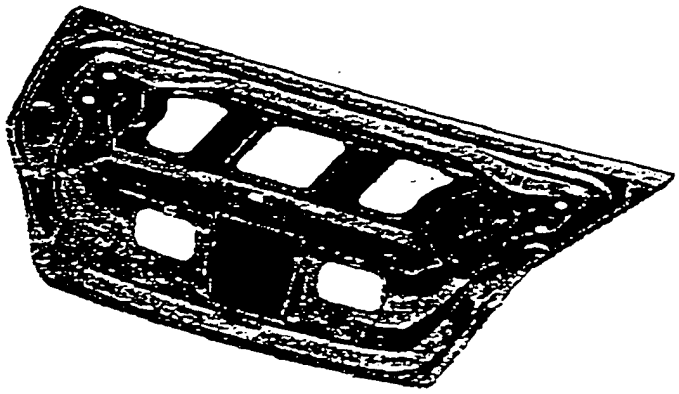

Figure 18- Optimum topology of embossed ribs using 30% of the area.

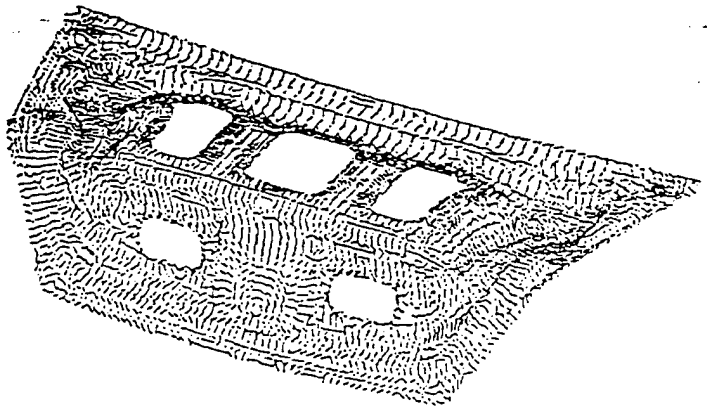

Figure 19- Optimum orientation of embossed beads.

Note: For representation purposes the designable material (material '2') is identified in black color when the two materials are shown and in lighter gray when material '1' is removed from the figure.

We note here the big gap between the first (10^{-7}) and second material ratio (10^{-1}) used in the examples. This is due to the fact that the changes in topology as function of the material ratio are only easily detectable for ratios above 10^{-2}.

4.3. Example 3 Embossed Ribs in Stamped Plates

The design model described in this work has many applications, among them, the optimum design of reinforcing embossed ribs (also known as beads) in stamped plates. A particular case of the optimization problem (13) is obtained when the local structure of the material '2' is fixed and orthotropic, and when material '1' is isotropic. In such cases it is possible to determine the optimum layout of embossed ribs (material '2') within the flat plate (material '1'). In order to solve this particular optimization problem the only modification required is to fix the form of E^2 in the most inner maximization problem in (13).

Due to the geometric complexity of this real life example it was solved using software developed at Ford for this particular application of optimum layout of embossed ribs of constant properties. The structure in question is the decklid of a sedan vehicle (see Figure 17) subject to a vertical load at the key switch. The objective of the problem is to maximize the stiffness for such load condition by embossing ribs in the decklid inner panel. The resource constraint metric is the area allowed to be covered by embossed ribs. For this example, embossed areas are limited to 30% of the total decklid area. Figures 18 and 19 show the 'optimum topology' and the 'optimum orientation of the principal directions' of the embossed ribs, respectively.

The stiffness of the decklid was increased 100% with the resulting topology/orientation of ribs.

5. Discussion

To contrast the present treatment of two-component composite design with common models for the design of continuum structures based on homogenization interpretation of a two-phase materials [the subject is surveyed in Bendsøe (1995); see also Cherkaev and Gibiansky (1997); Lipton (1988)], note that in the latter the local properties are designated to have specific form, e.g. isotropic, rather than to be represented by a free modulus tensor. Also, the 'zero-one' interpretation for the prediction of optimal topology from the latter models [Rozvany (1995) et al. provides a survey on methods for topology design] results in a ill-posed problem, whereas in the present approach topology is predicted on the basis of an ordered sequence of solutions to a well-posed optimization problem.

For simplicity, the model for two-component composite design is described in this paper in a relatively narrow form. However, the same method may be applied equally well in other contexts- for structural design with non-linear materials as represented in Bendsøe et al. (1996), for example, or for problems where the local measure of material cost is expressed by an invariant other than the trace of the modulus tensor [see e.g. Taylor and Washabaugh (1995), Taylor (1998) for expressions of generalized cost].

Acknowledgement The first and third authors express their appreciation for support received from the Ford Motor Company – Scientific Research Laboratories under grant #95-106R.

The first author expresses also appreciation for partial support received from INVOTAN through the Nato Science Fellowships Programme.

References

Bendsøe, M.P.; Guedes J.M.; Haber, R.B.; Pedersen, P.; Taylor, J.E. (1994) "An Analytical Model to Predict Optimal Material Properties in the Context of Optimal Structural Design" J. Applied Mech., Vol. 61, No.4, pp. 930-937.

Bendsøe, Martin Philip (1995), Optimization of Structural Topology, Shape and Material, Springer-Verlag, Berlin-Heidelberg.

Bendsøe, M.P.: Diaz, A.; Lipton, R.; Taylor, J.E. (1995), "Optimal Design of Material Properties and Material Distribution for Multiple Loading Conditions", Int. J. Num. Methods in Engrg., Vol.38, pp. 1149-1170.

Bendsøe, M.P.: Guedes, J.M.; Plaxton, Sheldon; Taylor, J.E. (1996) "Optimization of Structure and Material Properties for Solids Composed of Softening Materials", Int.J. Solids & Structures, Vol. 33, No 12, pp. 1799-1813.

Cherkaev, Andre and Leonid Gibiansky (1993) "Coupled Estimates for the Bulk and Shear Moduli of a Two Dimensional Isotropic Elastic Composite", J.Mech. & Physics of Solids 41, pp. 937-980.

Diaz, Alejandro; Robert Lipton and Ciro A. Soto (1995) "A New Formulation of the Problem of Optimum Reinforcement of Reissner-Mindlin Plates", Comput. Methods Appl. Mechn. Engng. 123, pp. 121-139.

Guedes, J.M. and J.E. Taylor (1997a) "On the Prediction of Material Properties and Topology for Optimal Continuum Structures", Structural Optimization, to appear.

Guedes, J.M. and J.E. Taylor (1997b) "An Alternative Approach for the Prediction of Optimal Structural Topology", Proc. McNU'97 Joint ASME, ASCE, SES Summer Mtg, June 29-July 2, 1997 Northwestern University, to appear.

Jacobs, Christopher, Juan C. Simo, Gary S. Beaupre and Dennis R. Carter (1997), "Adaptative Bone Remodeling Incorporating Simultaneous Density and Anisotropy Conditions", J. Biomechanics , 30,6, pp. 603-613

Lipton, Robert P. (1988) "On the Effective Elasticity of a Two-Dimensional, Homogenized Incompressible Elastic Composite", Proceedings Royal Society of Edinburgh, Vol. 109A.

Olhoff, N.; J.B. Jacobsen and E. Ronholt (1997) "Three-dimensional Structural Topology and Layout Optimization Based on Optimum Microstructures", extended abstracts of the ISSMO 2nd World Congress, May 26-30, 1997, Zakopane, Poland.

Pawlicki, J. R.; J.E. Taylor; S. Turteltaub and P.P. Washabaugh (1998) "The Prediction of Optimal Material Layout and Properties for Elastic Continuum Structures", in manuscript.

Pedersen, P. (1993) "Optimal Orientation of Anisotropic Materials/Optimal Distribution of Anisotropic Materials, Optimal Shape Design With Anisotropic Materials", in G.I.N. Rozvany (ed.) Optimization of Large Structural Systems, Kluwer Academic Publishers, Dordrecht, The Netherlands.

Rozvany, G.I.N.; N. Olhoff; G. Cheng and J.E. Taylor(1982) "On The Solid Plate Paradox in Structural Optimization", J. Struct. Mech., 10, pp.1-32.

Rozvany, G.I.N.; M.P. Bendsøe and U. Kirsch (1995) "Layout Optimization of Structures", Appl. Mech. Rev., Vol. 48, No 2, pp. 41-119.

Taylor, J.E. and P.D. Washabaugh (1995) "A Generalized Expression of Cost for Prediction of the Optimal Material Properties Tensor", in Trends in Application of Mathematics of Mechanics, Manuel D.P. Monteiro Marques and José Francisco Rodrigues, eds., Longman, Essex, England.

Taylor, J.E. (1998) "An Energy Modal for the Optimal Design of Continuum Structures", Structural Optimization, (to appear).